ALMA MATER STUDIORUM - UNIVERSITA' DI BOLOGNA

Corso di laurea in

Ingegneria chimica e di processo- Curriculum sustainable technologies and biotechnologies for energy and materials

TITOLO DELLA TESI

Bioplastics filled with nut shells particles: valorization of agro-wastes for the development of sustainable materials.

Tesi di laurea in

Composite Materials And Technology

Relatore Prof: Paola Fabbri

Presentata da: Pietro Bianca

Anno accademico

2020-2021

Dedicated to Gianfranco Borin

Summary

INTRODUCTION

During the last century, plastics have offered many innovative solutions for social needs and challenges, improving the quality of life for millions of people across the globe. Nowadays, plastic is present everywhere in our life, from drinking clean water to fashion, until virtual connection (Europe, 2020)

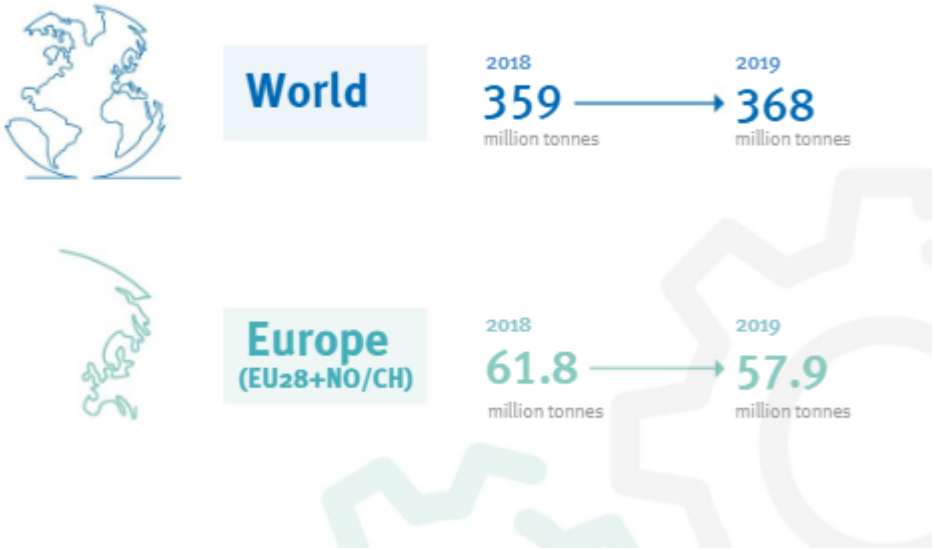

Figure 1 Plastic Production (Europe, 2020)

The production and use of plastic have many drawbacks that are becoming worser and worser in the last years like GHG's production and high waste amounts that is currently present everywhere in the global environment from the heart to the sea.

That is why governments have pushed the industrial and consumer markets towards "green" and to develop materials that are more environmentally friendly and derive from renewable materials. The focus has shifted to the total "carbon footprint" and the bio-based polymers in order to replace the existing polymers in different sectors and provide new combinations of properties.

Biopolymers are particularly good both for their practical side and their economic advantage for industries and municipalities that consist in savings of raw materials and the reduction of

costs in the end life-cycle of the products. Renewable biologically degradable products also contribute to circular economy. This means that the agricultural sector obtains the possibility to get a rising percentage of its additional turnover from non-food products and, when it is disposed, the recover material can be taken back to the agriculture as compost with economics and ecological advantages (E. Bugnicourt, 2014). A 2014 report published by BCC Research has estimated in 2014 the global bioplastic demand at more than 1400 kt (metric kilo tonnes)

The two main biopolymers commercially produced are polylactic acid and polyhydroxyalkanoate, that derive from renewable feedstocks and show properties of conventional material like polypropylene, polyethylene, polystyrene, and PET. PLA and PHA are being used in many applications including food packaging, disposable cups, grocery bags, and biomedical applications (Conrad, 2009).

PLA CHARACTERISTICS

Poly lactic acid, or polylactide, is a thermoplastic aliphatic polyester produced from renewable natural resources by fermentation of polysaccharides or sugar, that can be extracted from:

- Corn
- Potato
- Cane molasses
- Sugar-beet
- Non-food cellulosic biomass
- Non-food crops

PLA is industrially obtained from the polymerization of lactic acid (LA) or from the ring opening polymerization of the lactide that is the cyclic dimer of lactic acid.

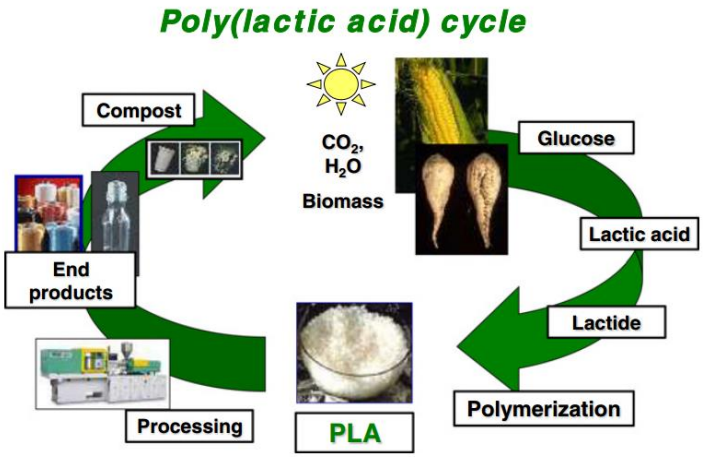

Figure 2 PLA life cycle (Marius Murariu, 2016)

The nomenclature of PLA depends on which production routes is used or on the content of L- and D- enantiomers. Polymers that derive from the lactic acid obtained with the polycondensation, are referred as Polylactic acid, while the ones prepared from lactide ring opening polymerization are named polylactide.

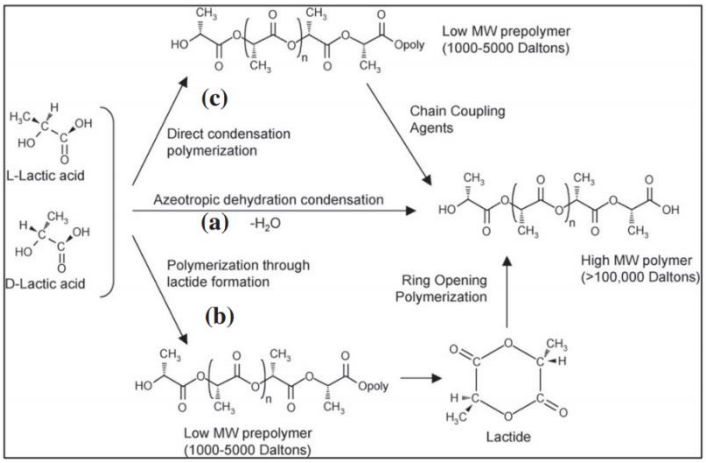

Figure 3 Polymerization of PLA (Marius Murariu, 2016)

The thermal, mechanical and biodegradation characteristics of PLA depend on the choice and distribution of the stereoisomers in the polymer chains.

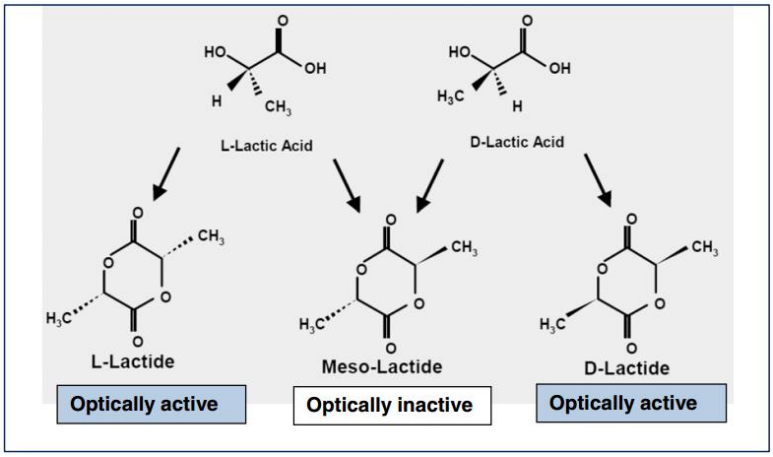

Figure 4 Starting stereoisomers (Marius Murariu, 2016)

The optical purity of PLA has strong effects on the structural, thermal, and mechanical properties of the polymer. With high content of L-isomers, greater than 90%, our polymer tends to be semi crystalline, while with lower optical purity it is amorphous. The melting temperature (T_m) and glass transition temperature (T_g) of PLA decrease with the increasing of the D-isomers content.

So, it is stated that PLAs with low D-isomer content are mostly indicated in applications that require semi crystalline polymers, while with higher percentage of D-isomer they are generally used where amorphous polymers with low activation temperature are required.

PLA has good mechanical properties that are even higher than those of PS, PP, PE. The tensile strength and elastic modulus are comparable to those of PET, but it is very brittle with an elongation that is less than 10% and low toughness. The polylactic acid is mainly used for packaging application, whereas the low glass transition temperature is a disadvantage in application where high temperature resistance is required. (Marius Murariu, 2016)

PHA CHARACTERISTICS

Polyhydroxycalkanoates (PHAs) are biogenic polyesters that can be naturally accumulated in microbial cultures cultivated on agricultural raw material. These biodegradable polymers can be processed in order to make useful products, particularly for packaging and agriculture.

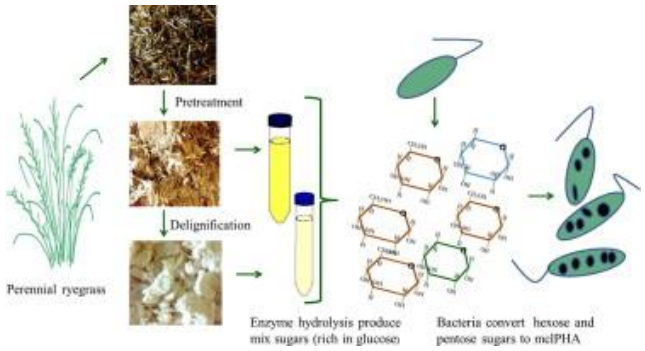

Figure 5 PHA's by Bacteria conversion (Davis, 2013)

Poly(3-hydroxybutyrate) (PHB) is the member with the most widespread and the best properties of the polyhydroxyalkanoate family. This linear polyester is accumulated in intracellular granules by a wide variety of Gram-positive and Gram-negative organism under conditions of nutrient limitation other than the carbon source. The molecular weight of PHB goes from 50 000 to over a million, and it depends on the organism, the growth's conditions and the methods of extraction.

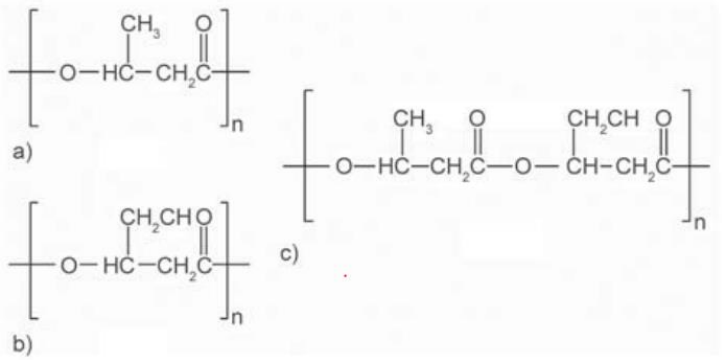

Figure 6 Chemical structure of: a)PH3B b)PHV c) PHBV (E. Bugnicourt, 2014)

As said before, PHB is produced by microorganisms in response to stress conditions of pure or mixed bacteria. This polymer is a product of carbon assimilation, from glucose or starch, employed as a form of energy storage molecule when other forms of energy are not available.

The microbial condensation of acetyl-CoA, that gives acetoacetyl-CoA, which is subsequently reduced to hydroxybutyryl-CoA, is used as a monomer to polymerize PHB.

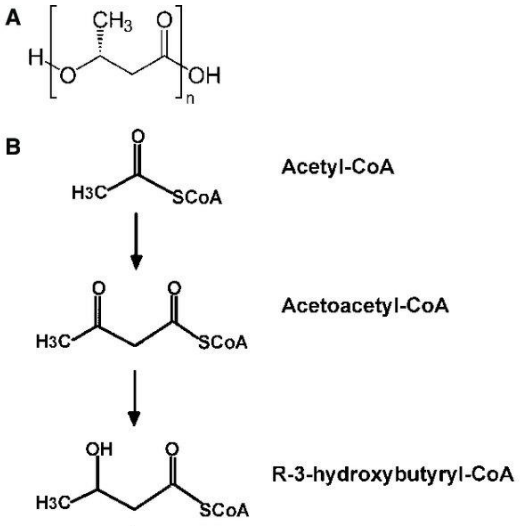

Figure 7 PHB monomers formation (Reusch, 2012)

Biologically produced, polyhydroxybutyrate (PHB) is a semicrystalline isotactic stereo regular polymer with 100% R configuration that allows high level of degradability. The properties of the polyhydroxyalkanoates depend on their chemical composition. Generally, it does present good resistance to moisture and aroma barrier properties, it is relatively brittle, as the elongation at break is below 15% and stiff. PHB is a fragile material due to re-crystallization with ageing at room temperature. For these reasons, efforts in compounding PHB are mainly focused on the search of plasticizers and nucleating agents capable of reducing the crystallization process and improving flexibility and elongation in the final product. The general characteristics of PHAs are:

- Water insoluble and relatively resistant to hydrolytic degradation.
- Good ultra-violet resistance but poor resistance to acids and bases.
- Soluble in chloroform and other chlorinated hydrocarbons.
- Biocompatible and hence suitable for medical applications.
- Sinks in water, facilitating its anaerobic biodegradation in sediments.
- Nontoxic.
- Less ‘sticky’ than traditional polymers when melted.

It does also have high melting temperature and relatively high tensile stress. (E. Bugnicourt, 2014)

FILLER

The combination between renewable-based biodegradable biopolymer with the intercalation of natural filler permits to obtain a biocomposite that could become a sustainable and a technically alternative to the common plastic used for packaging. The use of natural filler opens the way for the enhance of agro-based residues, reducing the overall impact of the food production cycle. This kind of bio composite allows a more sustainable packaging by favouring a cradle-to-cradle concept and promoting circular economy (Estefanía Lidón Sánchez-Safonta, 2018). Another k-aspects are their natural abundance, low density, high specific stiffness and biodegradability.

The use of shells coming from the food production of nuts as filler for the creation of a biocomposite with biopolymer matrix is completely coherent with the characteristics outlined before, due to the fact that nuts have a high worldwide market and shells are more or less the 60-80% of the total weight of the fruit (S. Ferrándiz-Bou, 2020). Shells does also have peculiar properties that could be very interesting for the creation of biocomposites, like:

- Inertness
- Hardness
- Stiffness
- Thermal resistance

In the next section it will be analysed how the market production developed in the last years. The aim of the analysis is that of stressing the usefulness of the introduction of this kind of filler in biopolymer in terms of availability and waste reduction.

Walnut's shell

During the last decade, the production of Walnuts has shown a constant increase of around the 4%/year. During 2019-2020 the worldwide production of walnuts was of 2'279 thousand tons. The main producers are China, USA and Chile, while Italy is in the 11th place with a production of 18 tons (Calcagni G. , 2019). While the consume pro capite per year of walnuts is shown in the graph below:

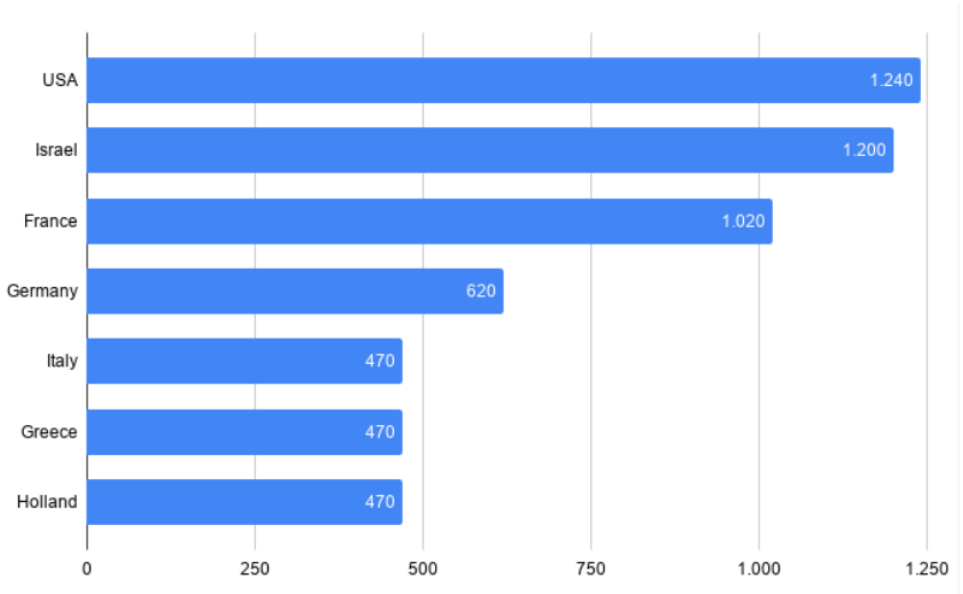

Figure 8 Pro capite consume of walnuts in g/yr. (https://www.landini.it/produzione-mondiale-noci/)

Hazelnut's shell

Italy does cover the second place in terms of production of hazelnuts worldwide with the production of 165'000 tons/year, the first producer is Turkey with 710'000 ton (Calcagni R. , 2020)

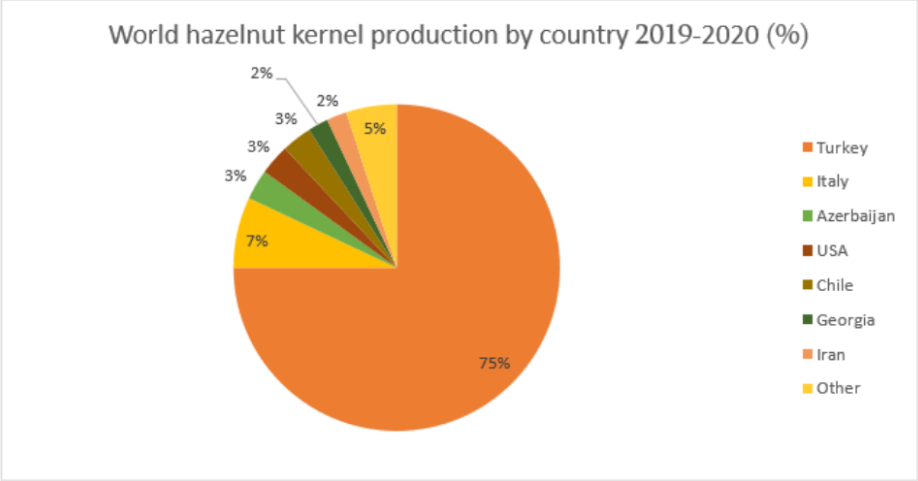

Figure 9 Hazelnut's production percentage

Almond shell

The Almond production is stated at around 8.5 thousand of tons per year (Soressi, 2020), while the production of Almonds in Italy during the 2020 was at around 80'516 ton (Pelegalli, 2021).

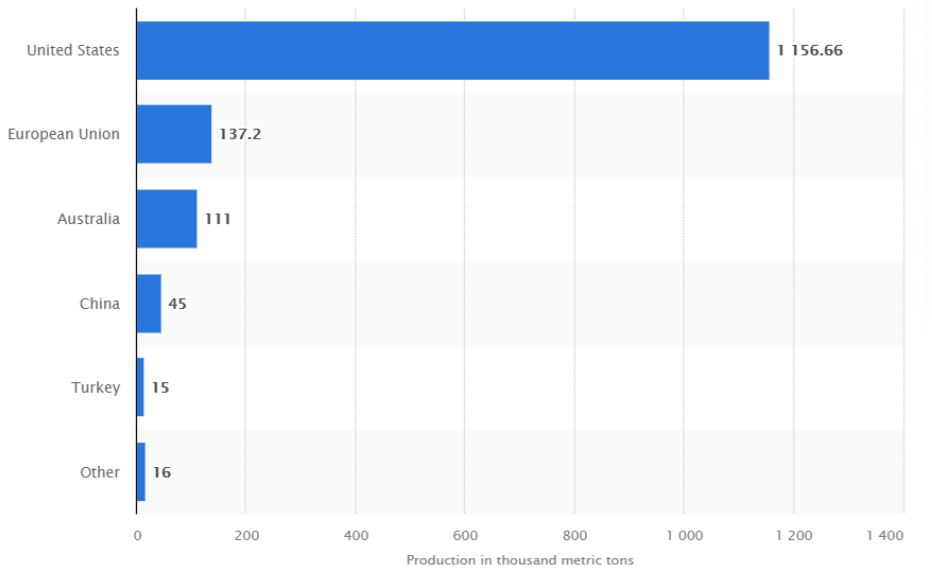

Figure 10 Almond production in 2019-2020 (Soressi, 2020)

MATERIAL AND METHODS

MATERIALS

For the matrix it has been used Polylactide (PLA) Ingeo™ Biopolymer 4060D by NatureWorks (specific gravity 1.24, glass transition temperature 55-60°C) (Universal Sector, 2021), while for the Polyhydroxyalkanoate it was used PHBV from TianAn Biopolymer ENMAT (specific gravity 1.25, DSC Melting Point 170-176°C) (Technical Data Sheet & Processing Guide, 2011). The shells were supplied by Arianna Fibers srl with two different grain size: a smaller one between 0-200 µm and a larger one from 200 to 1000 µm. In the table below are summarized the characteristics of the shell fillers:

Table 1 Specific characteristics of the filler given by Arianna Fibers

CODE	LOTTO	TYPE	Grain Size (µm)	Apparent density (g/cm^3)	Water content (%)
KERN WM200	WB073	Walnuts	0-200	0.26	9.0
KERN WO210	WB074	Walnuts	200-1000	0.29	9.0
KERN AO210	AB047	Almonds	200-100	0.58	9.3
KERN AM200	AB048	Almonds	0-200	0.37	9.0
KERN HM200	HB069	Hazelnuts	0-200	0.29	11.4
KERN HO210	HB045	Hazelnuts	200-1000	0.46	10.4

WETTABILITY

The first test required was the detection of wettability of the shell's powders in order to understand if the interphase between the biopolymer matrix and the filler could be good.

These measurements are done with the use of a tensiometer (Sigma700/701, Biolin Scientific) that's is able to measure the direct contact angle.

Figure 11 Tensiometer Sigma700/7001 by BIolin Scientific

The powder holder is a silica glass with a small hole in the bottom that is almost completely filled with the filler.

Figure 12 Sample holder for the powder

The powder holder is immersed into the liquid and the amount of liquid absorbed into the powder bed is measured against time.

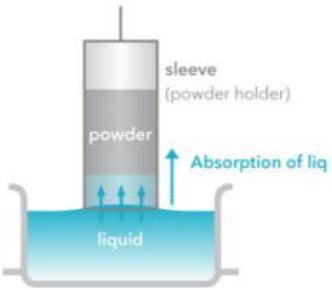

Figure 13 Scheme of the test

Theory

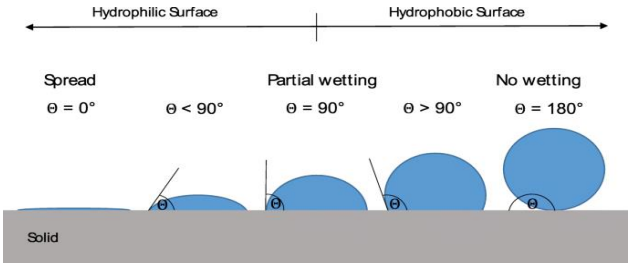

Figure 14 Range of wettability angle

The calculation is done by the Capillary rise or Washburn method based on the Poiseuille law related to the liquid flow through a capillary:

$$v = \frac{R_D^2}{8\eta}\frac{\Delta P}{l}$$

[1. 1]

Where v is the kinetics of flow, R_D the hydrodynamic radius of the capillary, η the viscosity of the liquid, l the length of the capillary and ΔP the pressure difference that can be expressed as the sum of a capillary pressure and hydrostatic pressure. So, the expression can become:

$$\frac{dh}{dt} = \frac{R_D^2}{8\eta h}\left[\frac{2\gamma_l cos\theta}{R_s} \pm \rho g h\right]$$

[1. 2]

h is the liquid front height, g is the gravitation constant, R_s the mean static radius of the capillary and ρ the liquid density. The hydrostatic pressure is neglected and by substituting $r = \frac{R_D^2}{R_s}$ the equation can be integrated by assuming $h = 0$ when $t = 0$

$$h^2 = \frac{r\gamma_l cos\theta}{2\eta}t$$

[1. 3]

Known as the Washburn equation. Due to the fact that the observation of the front of liquid is very difficult, it is possible to relate the height with the weight:

$$w = \varepsilon\rho\pi^2 h$$

[1. 4]

Where ε is the porosity of the packed column, by combining the two equation ([1. 3][1. 4]) is possible to write:

$$w^2 = (r\varepsilon^2(\pi R^2)^2)\frac{\rho^2\gamma_l cos\theta}{2\eta}t$$

[1. 5]

Where R is the inner radius of the tube. That leads to:

$$w^2 = c\ \frac{\rho^2\gamma_l cos\theta}{2\eta}t$$

[1. 6]

The term c is a geometric factor and is constant as long as packing and the particle size remains similar. This constant has to be experimentally determined, to solve it we need to do the measurement firstly with a completely wetting liquid, in our case Hexane (puriss. p.a. acs reagent, reag. Ph. Eur., $\geq 99\%$ GC by SIGMA-ALDRICH,CO. St. Louis), in order to assume that the contact angle can be zero ($\cos(0) = 1$) . By knowing the properties of the liquid (present in the programme database) it is possible to calculate the geometric factor. After the definition of "c", the evaluation of the contact angle with the liquid of interested can be done, in this case water (demineralized water). This kind of experiment has to be repeatable and carefully controlled since it is not possible to re-use the same powder for the two measurements. (Sigma700/701 Operation Manual Force Tensiometer Revision 2.7)

Measurement

As said before, two measurements must be done: firstly, the measurement for the material constant c in liquid hexane; secondly, for the contact angle in water. It is crucial that the

powder size and packing must be as identical as possible. In order to measure the contact angle we need the surface tension, density and viscosity that can be automatically inserted by the programme. The sample holder is filled with the powder at a fixed weight of $0.455 \pm 0.001g$. Later it is hanged on the balance hook and then the vessel containing the liquid is placed right below with the help of the Manual Membrane Keyboard.

After that, we need to set the experiment name, type (Round Rod) and heavy phase: firstly Hexane than Water. Now it is possible to start the test.

During the test the weight and the square of weight are plotted over time, the test is runed till the plateau is reached.

Then the powder is removed from the container, the container is cleaned and the powder is put again. The same procedure is done, and a new test has started.

Analysis of the powder wettability data

For defining the material constant, the measurement done with Hexane is open. A linear part of the curve is selected by pressing the button “Mark range”, then “Calculate Slope” followed by “Calculate C”

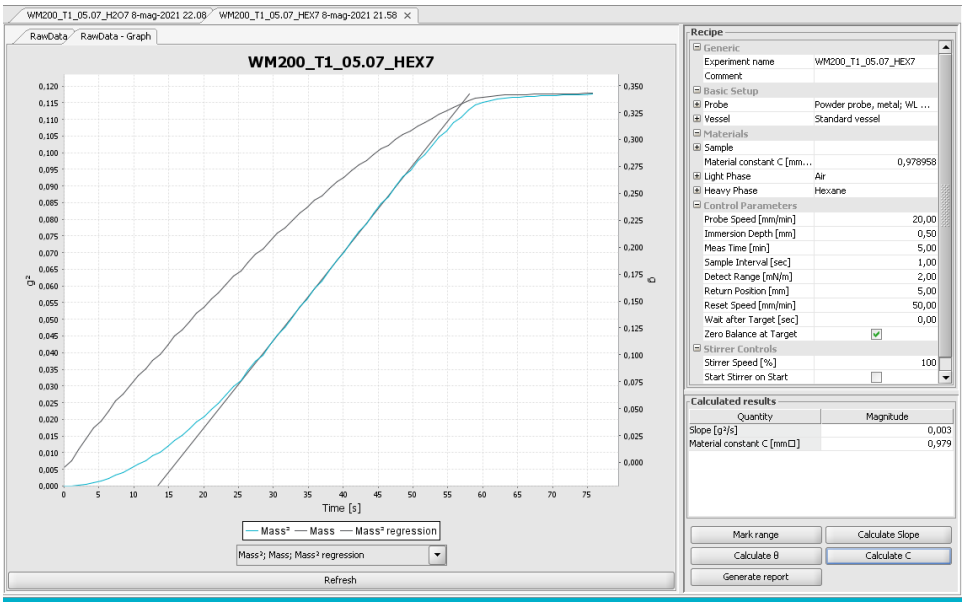

Figure 15 Graph with Hexane and evaluation of C

After that, the measurement with the other liquid (water) is open, the material constant is inserted in the recipe. The graph is open, and the range is selected like above; the slope is calculated followed by “Calculate Θ”. Contact angle is now calculated. (Sigma700/701 Operation Manual Force Tensiometer Revision 2.7)

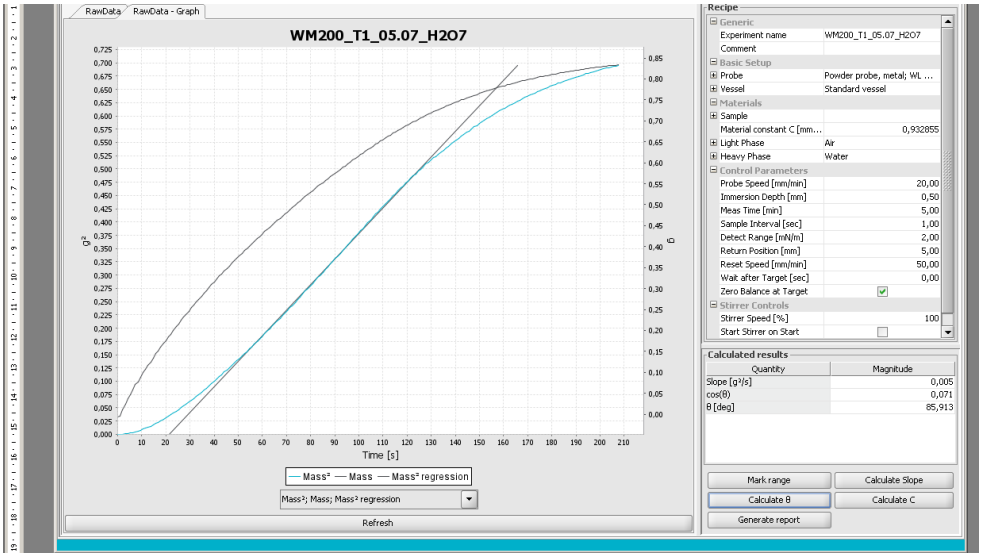

Figure 16 Evaluation of the contact angle

Excel file preparation

In order to have a precise evaluation of the wettability angle, the experiment is done at least ten times (1 test with Hexane and one with water). The result is inserted in an Excel file where we calculate the average of the material constant and the angle ($\theta[deg]$) than we evaluate the Gaussian distribution function:

$$\sigma = \sqrt{\sum \frac{(R_m - R_i)^2}{n-1}}$$

$$N = \frac{1}{\sigma\sqrt{2}} e^{-\frac{(R_n - R_m)^2}{2\sigma^2}}$$

Where σ is the standard deviation and N is the frequency, then we select the values that are inside the standard deviation and we calculate a new average.

PHB-PLA/FILLER COMPOSITES PREPARATION

Prior to the blending step, the filler and the biopolymer pellets (PHA and PLA) were dried in an oven (INCOFAR APP.-SCIENTIFICI, Modena) at 70°C for at least 24 h.

Figure 17 Oven for drying

For the creation of the composites , blending is done with an internal mixer (BRABENDER® OHG, Duisburg). Due to the fact that the chamber has a volume of $50\ cm^3$, we need to calculate the right weight of the pellets and fillers in order to have biocomposites with the 10, 25, 40 %w/w. We set the machine has follow:

- PHA: Temperature 175°C, rotor speed 50 rpm, time 8 minutes
- PLA: Temperature 185°C, rotor speed 50 rpm, time 8 minutes

In order to have an evaluation of the possible rheological response we look at the equilibration Torque at the 6^{th} minute of mixing.

Figure 18 Internal mixer used

Biocomposite created

The presence of two different types of biopolymer matrix, three different types of shell's filler with two different granulometry, induce the cataloguing of the composite as follow:

- Neat PLA as "PLA ref" and neat PHA as "PHA ref."
- Almond:

Table 2 Almond ID

NAME	MATRIX	FILLER CONCENTRATION [%w/w]	GRAIN SIZE [µm]
PHA AM200 10	PHA	10	0-200
PHA AM200 25	PHA	25	0-200
PHA AM200 40	PHA	40	0-200
PHA AO210 10	PHA	10	200-1000
PHA AO210 25	PHA	25	200-1000
PHA AO210 40	PHA	40	200-1000

-Hazelnuts

Table 3 Hazelnut ID

NAME	MATRIX	FILLER CONCENTRATION [%w/w]	GRAIN SIZE
PHA HM200 10	PHA	10	0-200
PHA HM200 25	PHA	25	0-200
PHA HM200 40	PHA	40	0-200
PHA HO210 10	PHA	10	200-1000
PHA HO210 25	PHA	25	200-1000
PHA HO210 40	PHA	40	200-1000

- Walnuts:

Table 4 Walnut ID

NAME	MATRIX	FILLER CONCENTRATION [%w/w]	GRAIN SIZE
PHA WM200 10	PHA	10	0-200
PHA WM200 25	PHA	25	0-200
PHA WM200 40	PHA	40	0-200
PHA WO210 10	PHA	10	200-1000
PHA WO210 25	PHA	25	200-1000
PHA WO210 40	PHA	40	200-1000

Figure 19 Example of biocomposites post melt blending

DIFFERENTIAL SCANNING CALORIMETER (DSC)

Thermal analysis is done with a DSC Q10 (TA Instrument Q Series™, New Castle, DE) in order to find how the filler content, type and granulometry is going to change the thermal properties like:

- PHB : Melting Temperature ($T_m, °C$) , Enthalpy of melting ($\Delta H_{m,T}, J/g$) , Crystallization Temperature ($T_c, °C$), Enthalpy of crystallization ($\Delta H_{c,T}, J/g$) and the degree of crystallization ($X_c, \%$)
- PLA: Glass Transition Temperature ($T_g, °C$) and Entropy ($\Delta S_{Tg}, J/\ g°C$)

Theory

The DSC technique analyses the difference in heat flow between a pan containing the sample and an empty one used as reference. The two pans are subjected to the same thermal cycle. When the detecting material undergoes a thermal transition, chemical or physical change that result in an emission or absorption of heat, thermal energy is added or removed to the sample in order to maintain the two pans at the same temperature. Pans are inserted inside a heating chamber where a thermocouple is placed near the pan in order to have a temperature as close

as possible to the one of the samples. So, two loops are present in order to control the temperature:

- First loop is for maintaining sample and reference at the same temperature accordingly to the set thermal cycle
- Second loop is able to compensate the heat in order to keep both pans at the same temperature when a transition occurs

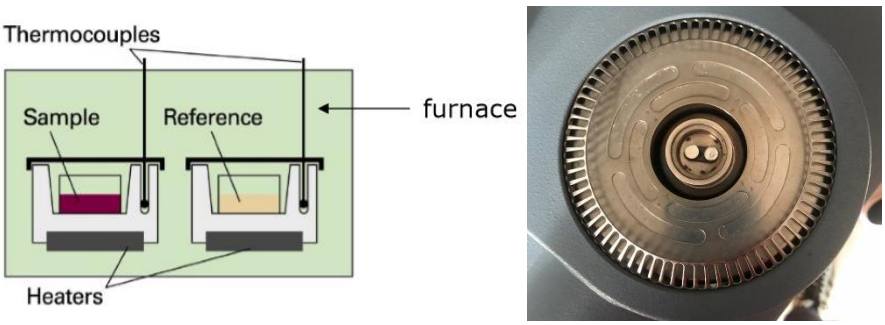

Figure 20 Furnace and pan disposition in DSC

The phenomena observed by DSC are:

- Phase transitions as melting and crystallization, they can be exothermal or endothermal processes observed as graphical peaks
- Glass transitions observed as inflection points
- Chemical reaction like oxidation, decomposition and curing that are seen as peaks

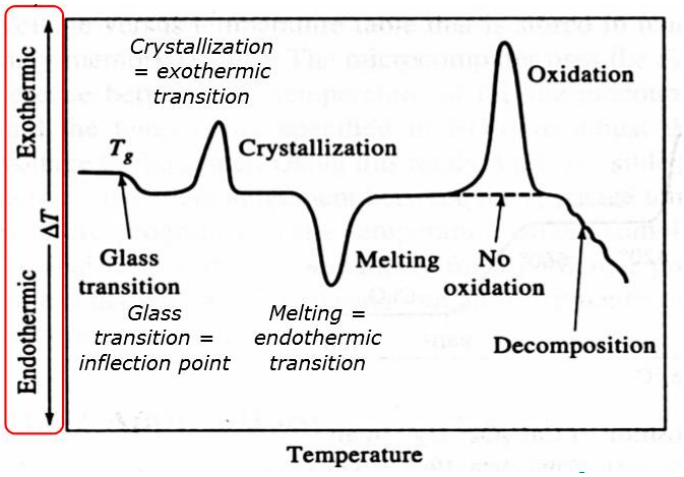

Figure 21 Thermal Transition in polymers

For a good detection of the thermal analysis, the heating rate must be not too low in order to have more intense peak, but also not too high for detecting every transition that may take place. Also, the mass of the sample affects the DSC curve; small masses lead to sharp peaks so it is possible to lose information about the transition related to phase contained in small amount, while big masses will lead to a not uniform heating of the sample. (Esposti, THERMAL ANALYSIS: TGA DSC, 2021)

Method

The first thing to do is the preparation of the sample, which is then inserted in a pan made of aluminium. The mass of the sample is always between 8-15 mg. Finally, the pan is closed with a pin.

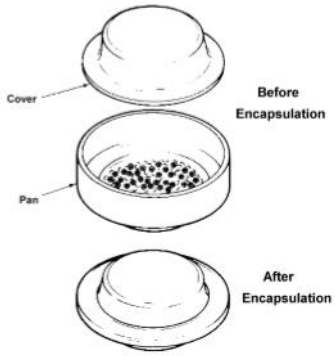

Figure 22 preparation of the test

Firstly, the DSC furnace need a Proscan; only the reference pan is inserted, then the programme is open, wait until the flange temperature reaches the value of -70°C, the name and weight of the test is inserted (when the Proscan is done, no weight is required). The nitrogen flux is at 50 ml/min in order to have an inert atmosphere. The Proscan analysis follows those steps:

1) Ramp 20°C/min till 150°C
2) Isothermal for 2 min
3) Ramp from 150°C to 20°C

4) Isothermal for 10 min

After that, it is possible to start the tests; the sample pan is placed, and a different thermal cycle is required. This is called “Granuli fino a 195°C” and it has to:

1) Ramp 30°C/min to -40°C
2) Equilibrate at -40°C
3) Mark end cycle 1
4) Ramp 20°C/min to 195°C
5) Mark end cycle 2
6) Isothermal for 4 min
7) Mark cycle 3
8) Ramp 10°C/min to -40°C
9) Mark cycle 4
10) Isothermal for 6 min
11) Mark end cycle 5
12) Ramp 20 °C/min 195°C
13) Mark end cycle 6
14) Ramp 20°C/min to 25 °C
15) Isothermal for 30 min useful for change the sample

The result is plotted as a graph where it is possible to evaluate the transition temperature and heat absorbed/emitted by using a linear integral calculation.

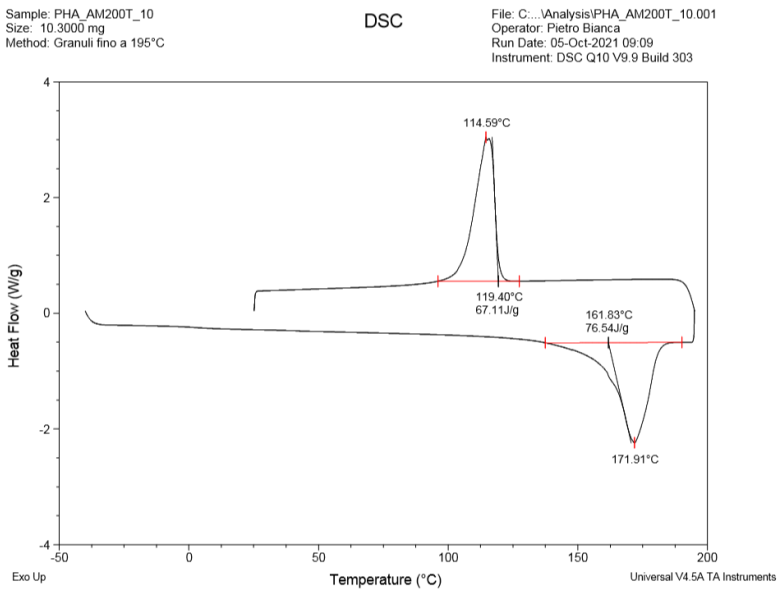

Figure 23 Example of Result by DSC

PHB DETECTION

There are some unknown characteristics of the PHBV used, like:

- Molecular weight
- Valerate content
- Presence of additives or plasticizer

Some specific analyses are required; a separation process in order to detects the Valerate content and a GPC test to understand the Molecular weight.

Separation Procedure

The separation procedure is fundamental in order to understand the presence of Valerate inside our PHBV pellets and also to make the right sample for the GPC test; two separations where done:

- Qualitative for the detection of the Valerate content
- Quantitative that is necessary for the molecular weight detection

Qualitative

Inside, a reaction balloon it is placed:

- PHBV : 10.07 g
- Chloroform : 130 ml

In order to recondense the evaporated phase during heating and to avoid the leakage of dispersed component inside the solvent, a cold-water flux at low speed is used. The balloon was placed inside a silicon bath heated at 60°C; the solution (PHBV+ Chloroform) is stirred at 500 rpm. This condition was kept till the two phases are completely dispersed.

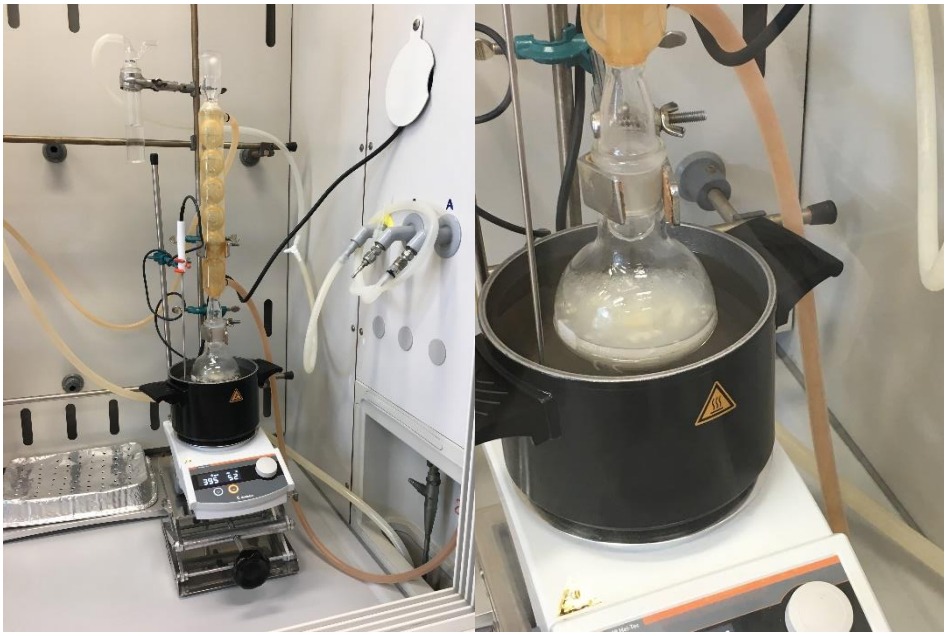

Figure 25 Experiment configuration for the Dispersion of PHBV inside Chloroform

The obtain solution (10.07g of PHBV inside 130ml of CHCl3) is taken out inside the silicon bath. Another 125 ml of chloroform is taken, and it will be used to wet the filter and to clean the reaction balloon. A flask for precipitation is used and it is inserted above a filter “pores 2” with a CELITE Standard Super Cell fine (Diatomaceous earth, calcinated by SIGMA-ALDRICH), the salt is wetted with chloroform to compact it. With the help of a PE pipe the obtained solution is inserted to the filter and by taking the vacuum with a vacuum pump the filtration starts. In order to help the filtration, chloroform is added in the solution inside the balloon, also to clean it completely.

Figure 24 PHBV + chloroform solution filtration

After this filtration, a cooled methanol (-20°C) is put inside a baker; the amount of it must be of at least three times the volume of the solution, so, around 400 ml. Furthermore, some more chloroform is added in order to reduce the viscosity. The methanol is stirred at 450 rpm and, with the help of a PE pipe, the solution of PHBV in chloroform is added inside the methanol, little by little, in order to avoid the intercalation of any contaminant in the polymer. The obtained suspension is filtered in a filter with lower porosity (porosity 4) with a paper filter above it, than it is wetted with methanol to help the filtration. Vacuum is imposed with the vacuum pump and the filtration is started.

Figure 25 Polymer + Methanol filtration; there's the presence of a Polymer layer above the filter

The layer of polymer above the filter is called “cake”, that is taken out from it and broken in smaller pieces, put inside a glass dish and covered with aluminium. The dish is placed inside an oven for 24h at 70°C. After that, the polymer is detected and a really small amount of Valerate is present inside our Polymer.

Quantitative

Quantitative analysis is done in order to detect the amount of additives or plasticizer present inside the pellets so a much more smaller amounts of pellets is required:

- PHB : 1.0474 g
- Chloroform : 50 ml

The separation procedure is the same described before with smaller amount of Methanol also:

- Methanol : 50 ml

After the drying the final weight of the polymer is measured:

- PHB final : 0.9818 g

So, the lost in weight is calculated as:

$$\Delta w\% = \frac{|PHA_F - PHA_I|}{PHA_I} * 100 = 6.26\%$$

This loss in weight may be related to the additive’s presence in our detecting Polymer; so, we may assume that the content of additives is between 5-10%.

GPC Analysis

Working principle of GPC

Gel Permeation Chromatography is a liquid chromatographic technique used to detect the molecular weight and molecular weight distribution in polymers. Those characteristics of polymers are fundamental to predict the final properties of them.

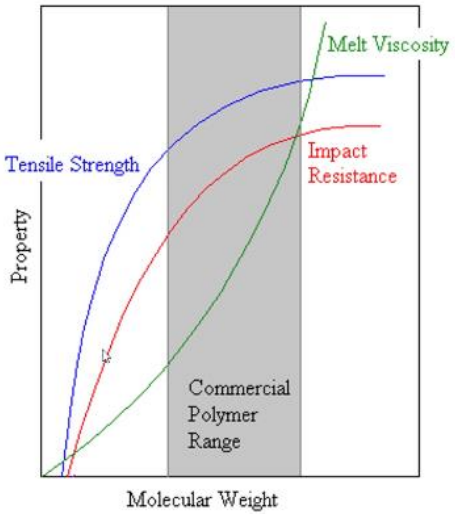

Figure 26 Relation between molecular weight and properties in polymers

This test works with the passing through of a mobile phase (polymer + solvent) in a stationary phase (porous column) and by detecting the resident time or volume. It is possible to detect the weight and distribution of a given molecule.

Instrumentation

The main component of a size exclusion chromatography is:

- Computer with a specific software to control and detect the experiment
- Solvent at high purity (chloroform or acetonitrile) that will be the mobile phase and needs also a filter in order to avoid the introduction of solid matters in our testing machine
- Degasser formed by a set of membranes able to remove air bubbles that may occlude the solvent flow

- Pump for delivering the solvent inside the GPC system; this pump must guarantee a constant flow to the whole process in order to have an accurate and reproducible analysis. This pump must be made of an inert material in order to avoid the reaction with the solvent and must be able to withstand high pressure
- Injector that is where the solution is insert inside the testing machine. It does have two positions:
    a) Load Position: sample goes into the loop
    b) Inject Position: the solvent is forced to pass through the loop and the sample will enter the column
- Column compartment that is where the chromatographic separation takes place. This compartment must be at constant temperature (35°C) in order to avoid changes in viscosity of the mobile phase. Columns are stainless steel hollow tubes with a solid porous bed. In order to increase the accuracy of the analysis many columns are put in series at increasing Length and decreasing diameter of the pores in order to have a better distribution of the different molecular weight of the sample.
- Detectors have the fundamental role of detecting the change in the mobile phase due to the presence of the sample. They must be very sensitive; generally we use many detectors in series. They could be UV-VIS detector that can see the presence of chromophores or refractive index

Test setting

When polymer chain is immerged and transported by an eluent flow, they form coils that have different dimensions depending on the length of the chains. Due to this fact every coil can diffuse in and out of a specific size of pores; bigger coils will have a lower resident times because it can go inside only big pores, while smaller coils can stay in both big pores and smaller ones. Every time a coil passes through the detectors it will produce a peak.

Flow marker

Flow marker is an organic solvent (Toluene) that has:

- Low molar mass
- High solubility in the mobile phase at low concentration
- Long term stability
- Detectability by detectors
- Must not interact with the sample
- No co-elution with low molar mass of the sample component

It is used in order to avoid the shift of a specific signal over time during different analysis that make them non reproducible. The concentration of the flow marker must be always the same; the flow marker peak will be used as reference, and also to realign the peak of different test

Calibration

A calibration curve is required in order to assign different values of peak/time to a specific molecular weight. The calibration curve is generated by the elution of a series of monodisperse polymer standards of known molecular weight. These standards are 8-10 data points in order to have a good polynomial regression. (Esposti, Chromatographic Methods: GPC, 2021)

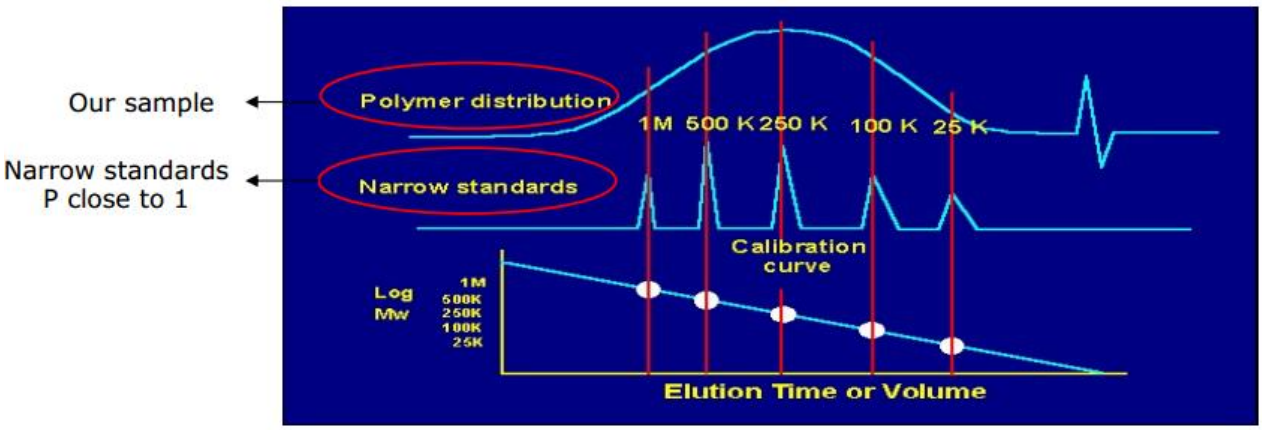

Figure 27 Example of a test and calibration curve cfr

GPC result

With the separation procedure it can be claimed that the content of additives was between the 5-10%. After this treatment, the polymer was detected in a XRD instrument, which gave the response. This response is Polyhydroxy-3butilate polymer with very low content of valerate. In order to detect the Molecular Weight and the Molecular Weight Distribution the pellets used for the preparation of the composites and the purified polymer are tested in a GPC machine to understand if and what it has been lost (oligomers/additives) during separation.

Instrument used

The instrument present in our lab is: Agilent 1260 Infinity instrument (G1322A 1260 Degasser, G1310B 1260 Isocratic Pump, G1316A 1260 TCC Thermostatted Column Compartment, G1362A 126 RID Reflective Index Detector, G1328C 126 Manual Injector); RID and column compartment were thermostatically controlled at 35 °C ± 0 .2 °C. The instrument was equipped with a PLgel MiniMIX-A column (20 µm particle size, 4.6 × 250 mm) coupled with a Tosoh TSKgel SuperMultipore HZM column (4 µm particle size, 4.6 × 150 mm); columns were preceded by a low dispersion in-line filter (frit porosity 0.2 µm) Data were processed with Agilent GPC/SEC software, version A.02.01 using a calibration curve obtained with monodispersed polystyrene standards (EasiCal PS-1 Agilent kit).

Calibration curve and flow marker

CHCl3 was used as mobile phase at a flow rate of 0.2 mL·min−1 and toluene was used as internal standard (0.2 µL·mL−1). The reference peak maximum for the Toluene flow marker was taken at 25.143 min (25 min and 8.6 s). For the calibration curve, two standards Spatulas of polystyrene (PS) have been analysed; the values of the different peaks were listed in Table 3 Spatulas A values.

Table 3 Spatulas A values

PEAK NUMBER	Light Scattering Mw [g/mol]	Mn [g/mol]	Mw [g/mol]	Mw/Mn	Mp [g/mol]
1	5’370’000	6’025’000	6’325’000	1.05	6’570’000
2	571’500	583’000	595’000	1.02	602’000
3	113’200	108’200	113’100	1.04	117’700
4	28’100	25’910	26’520	1.02	27’060
5	3’380	2’660	2’770	1.04	2’790

PEAK NUMBER	Light Scattering Mw [g/mol]	Mn [g/mol]	Mw [g/mol]	Mw/Mn	Mp [g/mol]
1	2’369’00	2’118’000	2’297’000	1.08	2’403’000
2	264’000	260’700	271’380	1.04	276’600
3	69’150	65’200	66’400	1.02	67’600
4	10’570	9’600	9’830	1.02	9’820
5	650	595	630	1.12	580

Table 4 Spatula B values

The analysis of the Reference samples reveals bad signals for both the peak at high molecular weight for the two spatulas, so it was decided to do an 8th point calibration curve with a polynomial of degree 3 with a regression :

$$R^2 = 0.9999494$$

To do this polynomial it is needed to assign each Mp for each peak signal, and this is the result:

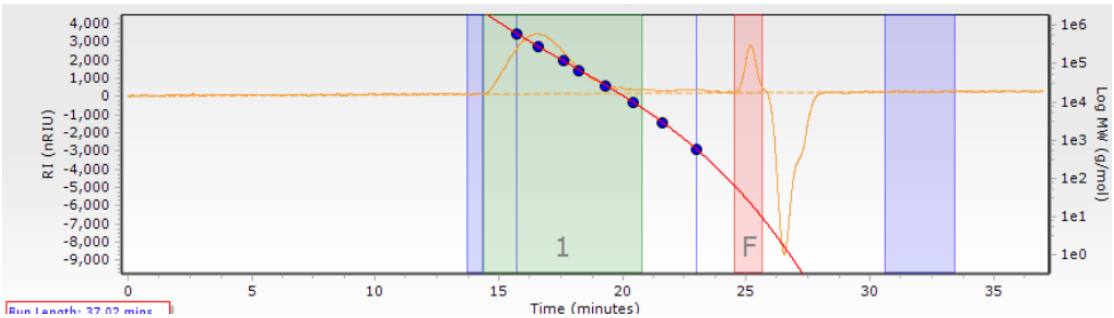

Figure 28 Calibration curve

Preparation of the sample

A solution of polymer with 2 ml of toluene in chloroform was prepared with:

- PHB pellets 10.8 mg stirred at ambient temperature
- PHB purified 10.4 mg in the same solution condition

The separated PHB solution of 180 µl is inserted in 125 µl of toluene in chloroform. The same procedure is done for the PHB pellets. Two filters of 0.45 and 0.20 micron, made of Teflon, are used to avoid the introduction of any contaminants. Then, with the help of a syringe, it is introduced in "load" 1 ml of the solution.

The concentration of the sample was:

- 3.082 mg/ml for PHB purified
- 5.2 mg/ml for PHB pellets

Result and conclusion

PHA pellets

For the analysis of the GPC data, it was selected the:

- Base line region: the extreme on the right and left side of the detection in order to fix the start and end of detection

Table 5 Base line region

Base line regions	Start [min]	End [min]
Base line region 1	13.30667	14.25000
Base line region 2	30.86333	34.47333

- Peak's region: the region where for detect the Molecular Weight and Molecular Weight distribution of the sample

Table 6 Peak detection

Peaks	Start [min]	End [min]	Peak Area
Peaks 1	14.38667	20.36000	574716
Peaks 2	21.85333	24.18667	193218.7

- Flowrate region: it does highlight the region related to the Flow marker that's Toluene (Peak at 25.143 min)

Table 7 Flow marker region

Flowrate region	Start [min]	End [min]
Flowrate marker region 1	24.55333	25.87000

PHA purified

In this analysis only one peak is present related to the molecular weight distribution:

Table 8 Base line region

Base line regions	Start [min]	End [min]
Base line region 1	13.73333	14.37000
Base line region 2	30.61000	34.47333

Table 9 Peak detection

Peaks	Start [min]	End [min]	Peak Area
Peaks 1	14.40333	20.81333	572778.5

Table 10 Flow marker region

Flowrate region	Start [min]	End [min]
Flowrate marker region 1	24.53667	25.69667

Graph and conclusion

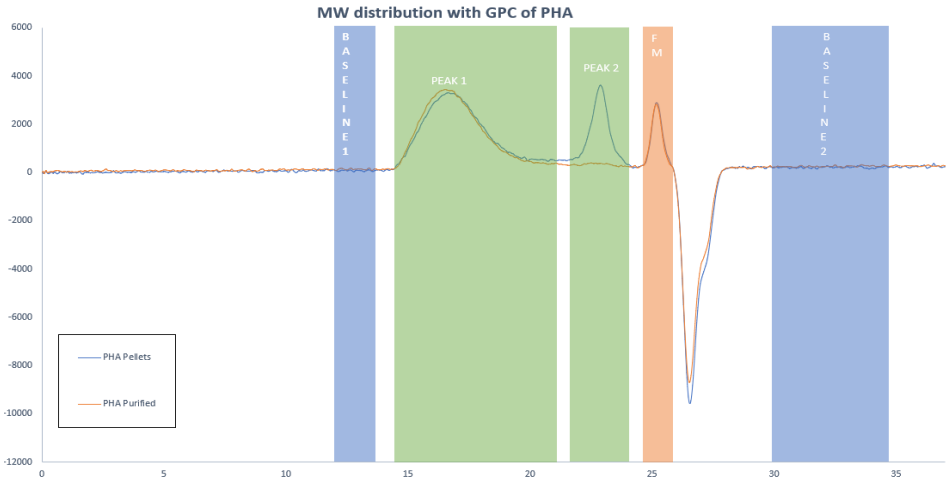

Figure 29 Graphical comparison

PHA Pellets

Table 11 Molecular weight of PHA pellets

Peaks	Mp [g/mol]	Mn [g/mol]	Mw [g/mol]	Mz [g/mol]	PD
Peaks 1	268900	106500	317400	627500	2.98
Peaks 2	700	600	800	1000	1.33

PHA Purified

Table 12 Molecular weight of PHA purified

Peaks	Mp [g/mol]	Mn [g/mol]	Mw [g/mol]	Mz [g/mol]	PD
Peak 1	294500	108200	329400	609100	3.04

Observing the final data obtain from GPC analysis, it can be noticed that:

- The purification process induces the loosing of low molecular weight molecules; this molecule has a maximum of 700 g/mol so it can be assumed that they could be oligomers of the polymer or additives like plasticizer; another interesting point of the second peak is a much lower polydispersity.
- The molecular weight distribution of the Purified PHA does have higher values of the different Molecular Weights, and also a higher Polydispersity. This might be related to the treatments that were done during the separation procedure.

SEM

Scanning electron microscopy use electron as “source of light”; electrons are accelerated with a high energy beam at high voltage, the wavelength created is much shorter than white light. The wavelength of an electron accelerated by an applying voltage is determined by the De Broglie formula:

$$\lambda_e = h/\sqrt{2m_0E\left(1+\frac{E}{2m_0c^2}\right)}$$

Where h is the Planck constant, m_0 the mass of the electron and E is the kinetic energy of the accelerated electron. When an electron is placed in contact with a matter, many different types of interaction may take place, creating different signals. So, depending on the type of detectors, it is possible to obtain different images of the detecting sample.

The scanning electron microscopy is constituted by:

- Electron gun that produces electrons from a tungsten (W) filament by heating
- Voltage generated by an anode; the higher will be the voltage the higher is the penetration under the surface of the sample
- Magnetic lenses that focused the fast moving electron
- Chamber where is mounted the sample; this chamber will be under vacuum, in order to avoid the contamination and oxidation on the specimen surfaces; also, to avoid electrical discharge and scattering that occurs for electron in gasses.

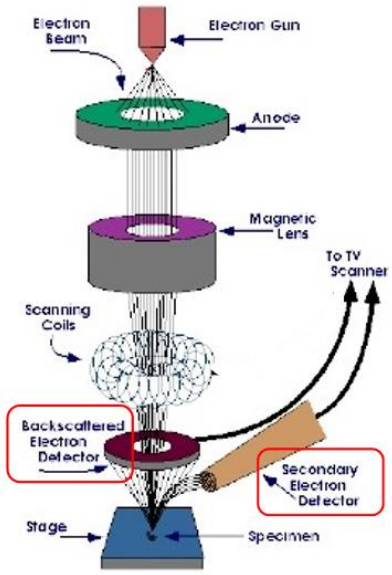

Figure 30 Scheme of SEM Microscopy

As it is seen in the above image, two main types of detectors are present: the backscattered electron detector and the secondary electron detector. The difference between them is described in the next section.

Backscattered electron

The beam of electrons, when hitting the surface of the sample, can interact with the nuclei of atoms deviating its trajectory. The incident electrons can be scattered back and merge on the surface of the sample preserving their high energy. Heavier elements, because of their bigger nuclei, can deflect incident electron stronger than lighter elements creating brighter signal. This signal is useful when it is needed to understand the composition of sample.

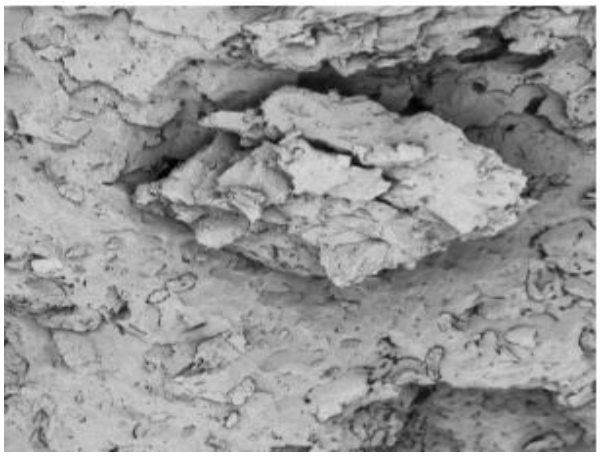

Figure 31 Example of a Backscattered image by SEM

Secondary electrons

They are generated from the surface or near the surface region of the sample. They are the result of inelastic interaction between primary electron beam and the sample. They have lower energy than the backscattered ones. Secondary electron is very useful for the inspection of the morphology of the sample's surface.

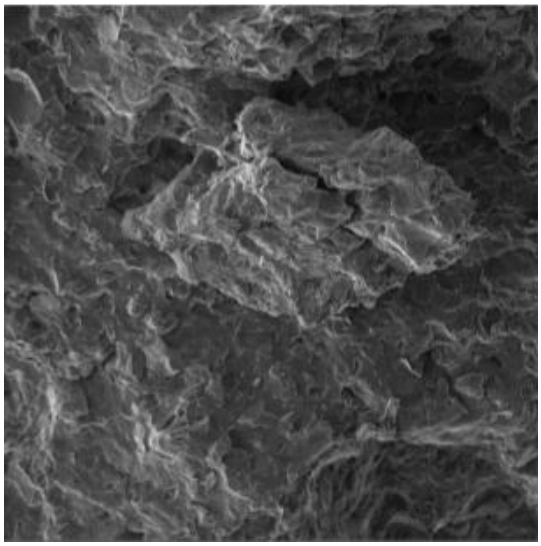

Figure 32 Example of a Secondary electron image by SEM

Sample preparation

In order to have a smooth and homogenous surface to detect, a brittle fracture is required. When the material is ductile for having a brittle fracture without any plastic deformation, the sample is immersed in liquid nitrogen and it breaks immediately after.

If we have nonconductive material, like the biocomposites under study, their surface acts like an electron trap charging it up, ruining the image forming extra white region. In order to avoid it, the sample is fine-grained coating with gold, silver or platinum with a sputter coater. With this coating, samples are becoming conductive. (Esposti, MICROSCOPIES: OPTICAL MICROSCOPY, SEM, TEM, AFM, CONFOCAL FLUORENCE MICROSCOPY, 2021)

In the case under study with a silver glue (SILVER CONDUCTIVE PAINT 503 1286-15, Electron Microscopy Science, Hatfield, PA) the test is stick in the sample holder, then, the glue is spread all around the holder in order to have a good contrast between the plate and the sample.

Figure 33 Stick of the test in the sample holder

The gold coating is done with the help of Quorum Q150R ES plus (Quorum, Laughton, East Sussex) where there is a foil of gold with a shelter right below that favour the creation of a thick layer of coating. High vacuum is applied (0.076 mbar) in argon atmosphere in order to avoid any oxidation that could be possible at that voltage; the electrical current is 16 mA the time is 120 s.

Figure 34 Gold coating

The SEM instrumentation is composed by:

- Field Emission Gun (FEG)
- Dissipation spectrometer (EDS)
- Detector for Electron Back Scatter Diffraction (EBSD)
- Vacuum pump
- Plasma cleaner

Vacuums impose for the electron scanning is $1.0\ e^{-02} Pa$

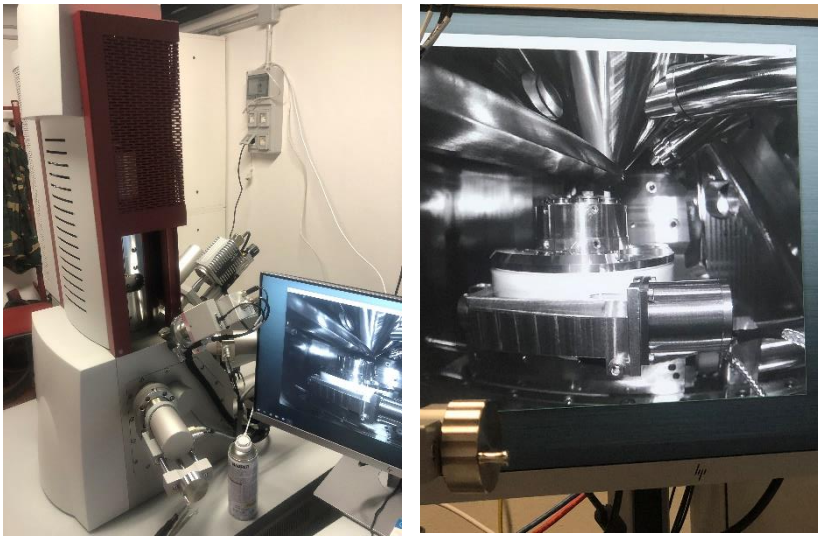

Figure 35 SEM Microscopy and chamber detail

TESTER PREPARATION

In order to test the melt blending biocomposites they must assume a shape that is possible to use in mechanical testing machine. Test requires a dog-bone's shapes tester; this kind of shape is described in the figure below:

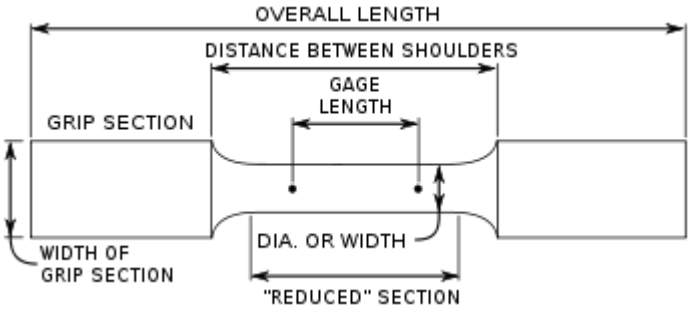

Figure 36 Shape of a dog bone tester

In order to obtain this shape, we firstly need to grind our composites with a CMG Series B30-50 (CMG Spa, Bologna, BO), then the grinded samples are placed in the oven at 70°C for PHA's matrix and 50°C for PLA's matrix for 24 h for dry them. Finally, with an injection moulding machine (Mega Tech H7/18-1, TECNICADUEBI srl, Fabriano, AN) it is possible to obtain the dog-bone tester.

Injection Moulding

In this type of processing there is an injection unit that acts like the screw of the extrusion technique, then, the melted polymer passes through a nozzle and goes to the clamping units where the mould of the required shape is placed. The mould is kept close with the applying of pressure. With the decrease of temperature, the melted polymer becomes solid.

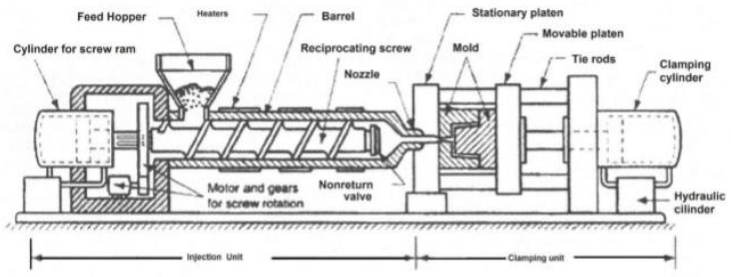

Figure 37 Example of an Injection Moulding

The temperature and pressure profile are fundamental in this process in order to melt and solidify the polymer in the right place and avoid detrimental behaviours like:

- Warpage that happens when we have high pressure at the end of processing that induce a relaxation of the molecules under the applying of a stress
- Sink Mark that is a surface shrinkage due to the imposition of lower pressure during processing (polymer will not completely fill the mould)
- Flash happens when high pressure is imposed during the initial part of processing that cause a leakage of the polymer out of the mould
- Free volume reduction in the mould by the decreasing of temperature that may lead to a shrinkage of the material that induce decay of the mechanical properties. (Saccani, 2021)

In the case under study, as it was said before, it is used a Mega Tech H7/18-1. In order to clean it from older polymer residue, the machine is filled with polypropylene (LyondellBasell,

Rotterdam) at 200°C. After this procedure we can set the parameters to print the composite as it can be seen in the figure below:

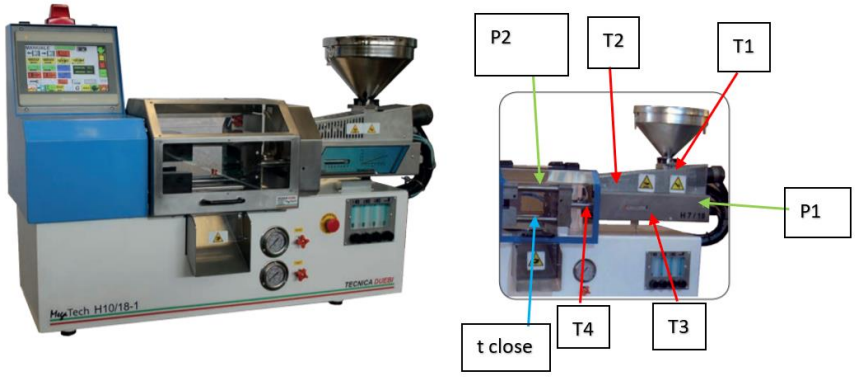

Figure 38 Setting parameters for printing

Where:

- P1 is the pressure inside the screw
- P2 is the pressure for keep the mould close
- T1 is the temperature before entering in the screw section
- T2 the temperature of the screw
- T3 the one of the valves
- T4 the temperature of the nozzle
- t close the time that the mould has to keep close

The mould is lubricated with WD40® in order to help the detach of the tester.

Figure 39 Example of PHB dog bone tester

PHA

PHA does have specific condition of pressure and temperature:

- T1: 140 °C
- T2: 165 °C
- T3: 165 °C
- T4: 160 °C
- P1: 100 bar
- P2: 60 bar
- t close: 10.5 s; 3 s for the filling of the mould and 7.5 s for cooling

PLA

For PLA the operative condition where:

- T1: 150 °C
- T2: 175 °C
- T3: 180 °C
- T4: 185 °C
- P1: 100 bar
- P2: 60 bar
- t close: 7.5 s

MECHANICAL TEST

The mechanical test is fundamental in order to detect the mechanical properties of the composites like:

- Young modulus
- Tensile stress

- Elongation at break
- Impact resistance
- Hardness

Before starting the mechanical test, it is required to wait for at least three weeks in order to allow the recrystallization of the PHA in the tester, the same time is waited for the PLA composites.

Tensile test

This is the most common mechanical stress-strain tests. The specimen is deformed till fracture with a constant speed of deformation. The tensile load is applied uniaxially along the long axis of the test. During testing, the deformation is located in the narrow middle region, the dog bone shape reduces the probability of fracture at the extremes of the specimen.

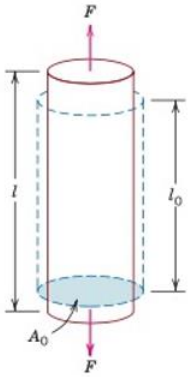

Figure 40 Deformation during the Tensile test, dashed lines represent the initial shape

The specimen is mounted by its ends into the holding grips of the apparatus; the sample, as said before, is elongated at a constant rate by the moving of the crossheads and measures the instantaneous applied load and the resulting elongation. The output of the tensile test is recorded on a computer that relates the load versus elongation in a graph; generally, these two values are normalized in order to give engineering stress and strain:

$$\sigma = \frac{F}{A_0}$$

$$\varepsilon = \frac{\Delta L}{L_0}$$

That is why it is required to fix the initial length (L_0) thickness and width ($A_0 = w * t$). By plotting this data it is possible to obtain the stress-strain curve; in this curve, there are present two different types of deformation:

- Elastic Deformation is a region where, until a certain load, the material is able to recover its original dimension after the removal of load. The deformation produced in the elastic region is proportional to the load, this is known as Hook's law:

  $$E = \frac{\sigma}{\varepsilon}$$

  Where E is the Young's modulus
- Plastic Deformation happens when the load exceeds the elastic limit, and the deformation is no longer recovered so the Hook's law will not be valid. The limit is determined by the elastic limit; where the curve deviates from linearity and increase until the value of Ultimate Tensile Stress (UTS) where it's started to decay. The fracture strain, or elongation at break, is the ratio between changed length and initial length after the breakage of the test specimen; is taken as the measure of ductility

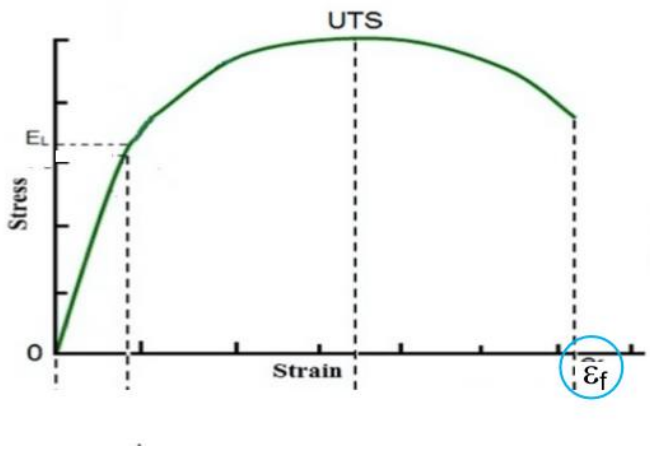

Figure 41 Typical Stress-strain curve

The types of fracture are essentially two:

- Ductile fracture: ductile material shows plastic deformation with high energy absorption before fracture
- Brittle fracture: little or no plastic deformation with low energy absorption. Fracture is sudden and catastrophic

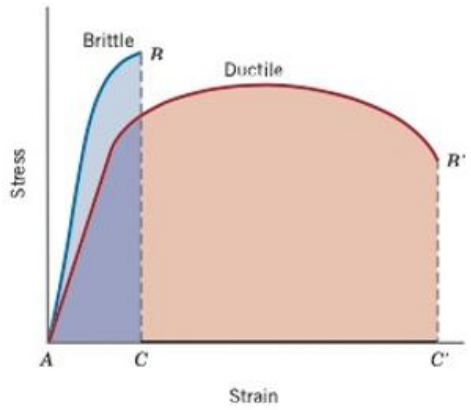

Figure 42 comparison between a Ductile and Brittle fracture

Ductile fracture is almost always preferred to brittle fracture: brittle fracture occurs suddenly and catastrophically without any warning as consequence of the rapid crack propagation. On the other hand, for ductile fracture, the presence of plastic deformation gives warning that failure is imminent, allowing preventive measures to be taken. (Esposti, Tensile test, 2021)

Test setting

The machine used for the tensile experiment is a Instrom 5966 (Norwood, Massachusetts, USA). That has a load of 10 kN; the testing ambient is fixed at 23°C and 65% of relative humidity. The testing machine is connected to a computer where a programme is able to detect the stress and strain curve during testing. A new "lot" is started, the polymer type is inserted, and a new interphase is opened. For every test, using a dog bone shape, it is required to insert the width and the thickness while the length is fixed:

- Thickness : 2.00 $\pm$0.05 mm
- Width : 5.00 $\pm$0.05 mm
- Length : 25 mm

The dog bone is initially set manually at a distance lower than 25 mm, around 0.3000 mm below, the tester is blocked manually with the help of two clamps, then it is brought back to the initial one in order to have a tester under a little tension before the start.

Due to the fact that we have PHB and PLA, the suggested speed of deformation is 10 mm/min.

Figure 43 Tension experiment setting

The result is then collected in an Excel file where it is possible to obtain:

- Stress at maximum load [MPa]
- Deformation at maximum load [%]
- Stress at break [MPa]
- Deformation at break [%]

The evaluation of the Young modulus by the test is not correct: the data were plotted, and by selecting a range of values that are linear, generally between 0.50 to 1.2 % of deformation, it is possible to linearly interpolate them in order to have a representative values of the modulus.

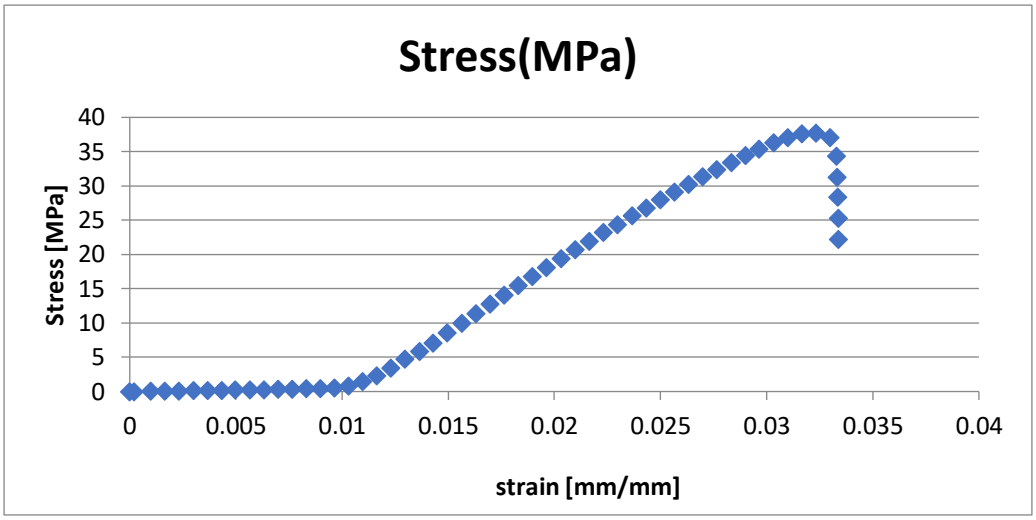

Graphic 1 Experimental values

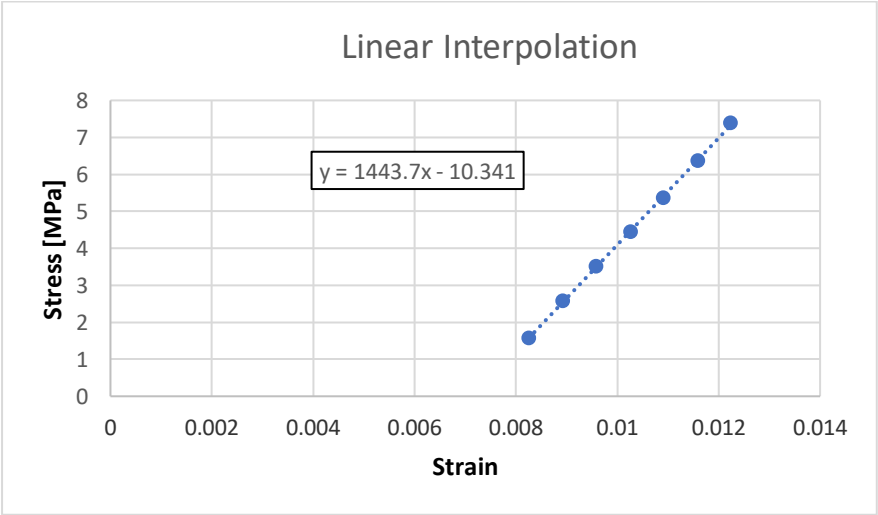

Graphic 2 Evaluation of the modulus with linear interpolation

For each type of biocomposite, a number of five tester is used in order to have a good estimation of the proprieties.

Impact

Impact test is done in order to determine the energy absorbed in fracturing a specimen at high velocity; typically, the test consists in placing the specimen in an impact tester and breaking the specimen with a swinging pendulum. The most know type of impact tester are Charpy and

Izod tests, that measure the impact energy. The main difference between the two is how the sample is placed and which type of hammer is used.

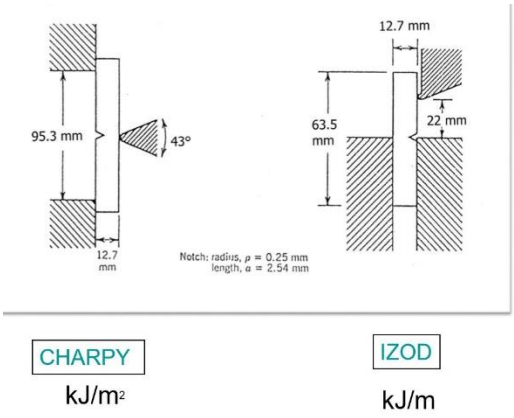

Figure 44 Difference between a Charpy and Izod test

Test setting

A weighted pendulum hammer is placed at a fixed height, while the tester is at the base of the system. With the release of the pendulum, the hammer strikes and fractures the specimen. After hitting the specimen, the pendulum continues its swing until a height lower than the initial ones. The energy absorbed by the material during fracture is calculated as the difference between the initial height and the final one. (Esposti, Impact test, 2021)

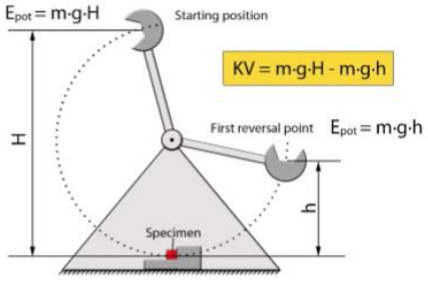

Figure 45 Working principle of an impact test

The machine used is a RESIL IMPACTOR CEAST Instron (Norwood, Massachusetts, USA) with a hammer of 5J with Charpy disposition. The first measure is done without placing the sample in order to detect the value of the air friction and it is equal to:

$$air_{friction} = 0.013\ J$$

Before placing the tester, it is required to measure the width and thickness of it in order to calculate the impact energy as follow:

$$E_{impact} = \frac{\llbracket E_{measure} - air_{friction}\rbrace}{w\ t} * 1000 = [\frac{kJ}{m^2}]$$

Where w is the thickness and t is the thickness measured in [mm]. Every test is repeated three times.

Hardness

In order to understand the hardness of a material there are many kinds of test; the most used for measuring the hardness of plastics is the Shore hardness test.

Shore hardness test uses a durometer scale defined by Albert Ferdinand Shore; this device does have a calibrated spring that applies a specific pressure to an indenter foot with a specific shape. The indenter measures the maximum penetration depth at the applied load, the determination of the hardness is achieved by visually reading the dial in the durometer.

Shore hardness does have two scale values depending on the type of indenter:

- Shore A where the durometer has a truncated conical shape
- Shore D with a conical indenter

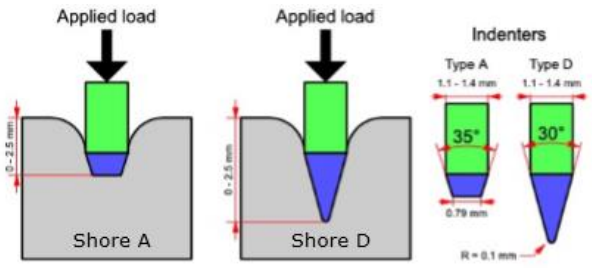

Figure 46 Indenter for Shore hardness

The use of Shore A or D indenter depends on the type of plastic tested; for soft ones, Shore A is used, while for harder ones, Shore D is the correct ones.

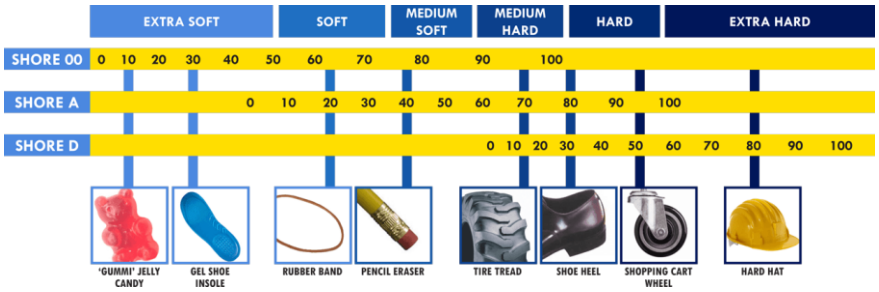

Figure 47 Shore scales

Test setting

The durometer used is a Shore D W Testor AMSLER ISO R 868 (GmbH, Germany) for every specimen the test is done 5 times and it's firstly recorded the instantaneous hardness than after 10s.

Figure 48 Measurement of Shore Hardness

RESULT AND DISCUSSION

In this section are analysed the result of each test done on the different composites in order to understand how different types of shell fillers, with different concentrations and grain sizes, influence the properties of the material.

Wettability angle

The value of the angle was the average between the experiments done and also its standard deviation, the results were plotted in a column chart.

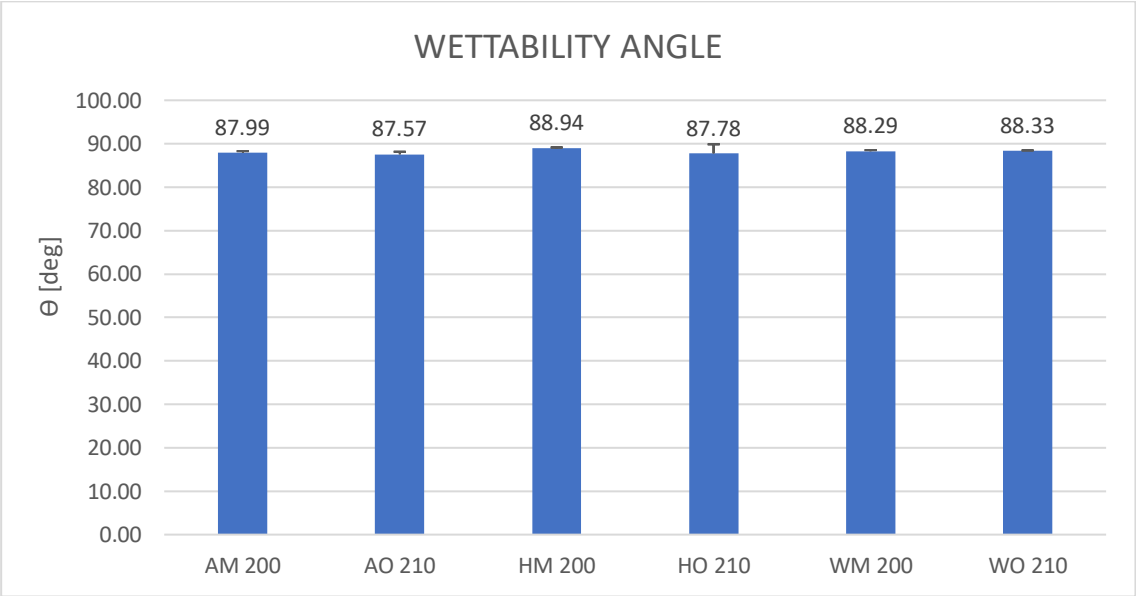

Graphic 3 Wettability of the shell powders

By looking to the values obtained, it is possible to say that there is not a big difference between the different shells, and that the grain size does not influences the wettability angle: all of them are between 87 and 89 [deg], so they are in the range of “partial wetting”.

Torque evaluation

During the melt blending, the equilibration torque was collected at 6 min (PHB-PLA/FILLER COMPOSITES PREPARATION) in order to have an evaluation of how the rheology could change with the increasing of the filler content; the result were plot in a graphical way:

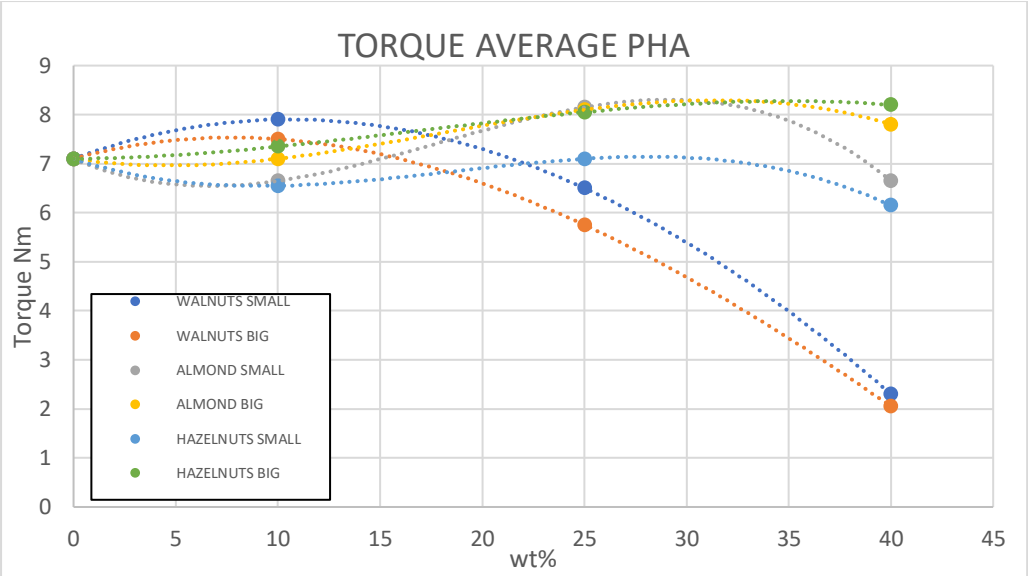

Graphic 4 Torque evaluation in PHB composite

As we can see, the torque fluctuates between 6 and 8 Nm. Fillers with higher grain size does have higher values of the equilibration torque than the smaller ones. The most interesting data are the ones related to the walnuts, where we have a big decay of the torque. This is probably due to the fact that, at high temperature (175 °C), we could have the release of substances that degrades the polymer's chains of PHA.

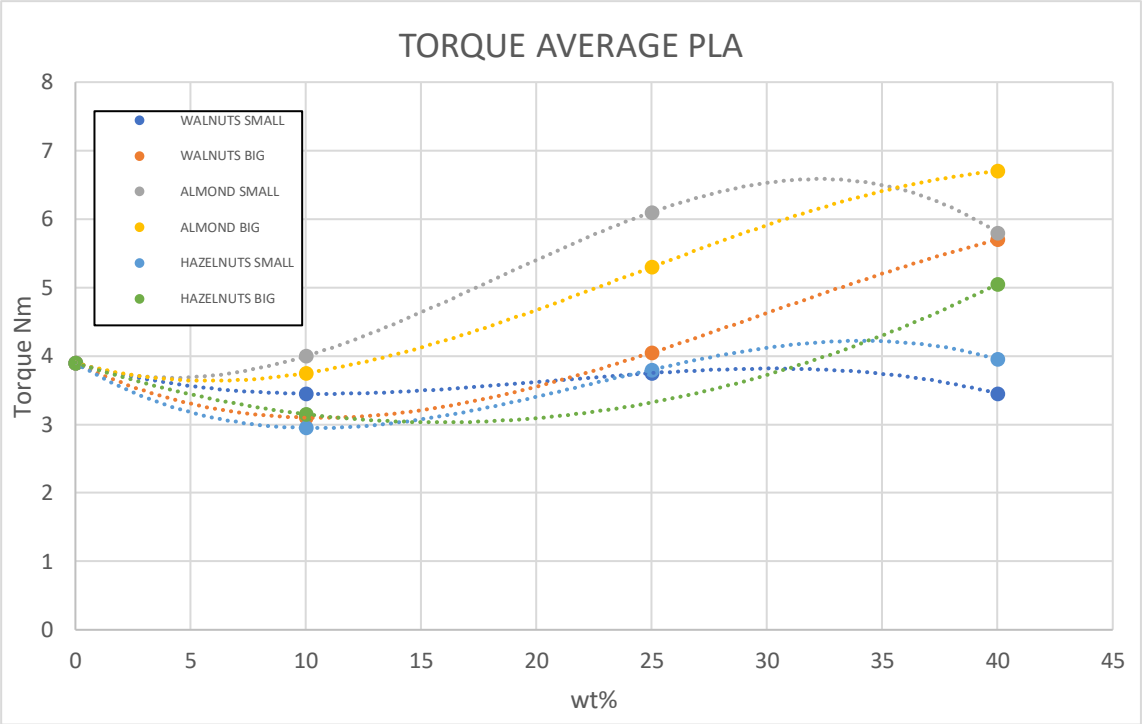

Graphic 5 Torque evaluation in PLA composites

By looking at the equilibration torque for PLA's composites, we have a clearer increase of the value with the increase of the composite concentration; they firstly decrease a little, due to a less presence of the polymer, then the friction of the filler becomes predominant. In this case, we do not have any decay of the value with the presence of the walnut's filler.

Thermal properties

The thermal properties are detected with the usage of the "DSC, Method," the properties are evaluated at the second heating scan; the first ones are used for deleting all the past history of the composite:

- PHA: it is possible to detect the melting temperature and the degree of crystallinity with the use of the linear integration of the melting peak and with the usage of the following formula:

$$X_c[\%]: \frac{\Delta H_m}{\Delta H_m^0 (1 - w_{filler})} * 100$$

Where ΔH_m is the melting enthalpy of the polymer matrix, w_{filler} is the weight fraction of the shell's fillers and ΔH_m^0 is the melting enthalpy of 100% crystalline PHB that is equal to 146 [J/g].

- PLA: the polylactic acid used (MATERIALS) with the help of the pure polymer DSC analysis it is completely amorphous, so it is possible only to detect the Glass transition temperature (T_g) and the entropy ($\Delta S_g = [\frac{J}{g\,°C}]$)

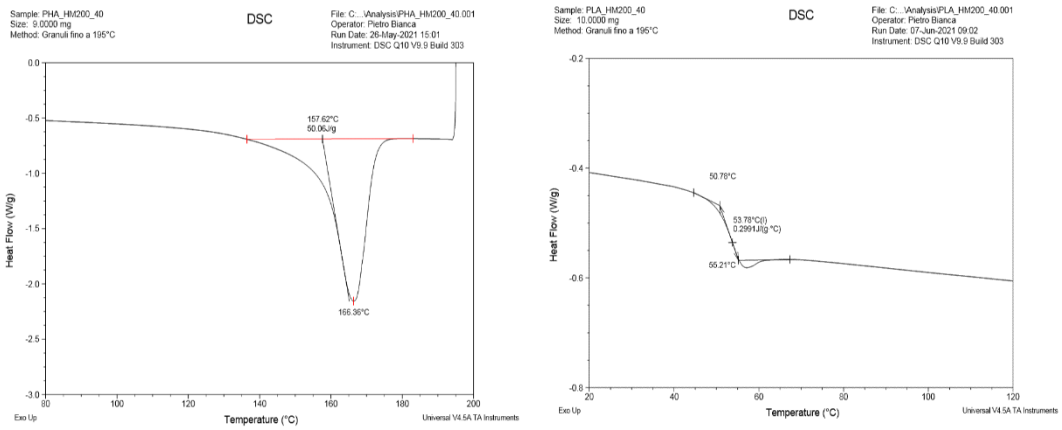

Figure 49 Comparison between PHB and PLA matrix with same amount of filler

In order to be as clear as possible, the result is split in table and divided by each type of polymer matrix and filler.

PHA

Table 13 Thermal properties of PHB pure

ID	Tm [°C]	ΔHm [J/g]	Xc [%]	Tc [°C]
PHA_Pure	171.2	96.1	65.8	115.6

Almonds

Table 14 Thermal properties of PHB almond's fillers composites

ID	Filler content [wt%]	Grain size (µm)	Tm [°C]	ΔHm [J/g]	Xc [%]	Tc
PHA_AM200_10	10	0-200	171	77	58.6	114.4
PHA_AM200_25	25	0-200	169.2	68	62.1	106.2
PHA_AM200_40	40	0-200	168.7	48.9	60.1	109.6
PHA_AO210_10	10	200-1000	172.5	69.6	53	114.5
PHA_AO210_25	25	200-1000	170.9	67.4	61.6	114.2
PHA_AO210_40	40	200-1000	168.5	44.1	50.3	113.2

In order to better understand how the proprieties change with the amount and grain size of the filler, the degree of crystallization and the melting temperature are plotted with the amount of filler:

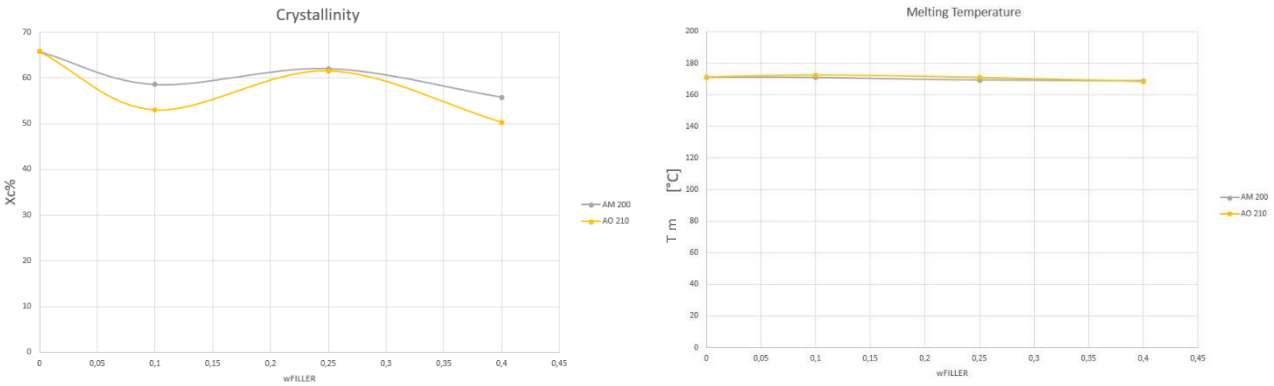

Graphic 6 Degree of crystallinity and melting temperature Almond's fillers composite

It is possible to see that there is not a great decrease of the two properties by increasing the amount of filler, and that the trend is mostly similar for smaller and higher grain size. The degree of crystallization is lower for filler with grain size 200-1000 µm, while the melting temperature is assumed equal to the pure.

Hazelnuts

Table 15 Thermal properties of PHB hazelnut's fillers composites

ID	Filler content [wt%]	Grain size (µm)	Tm [°C]	ΔHm [J/g]	Xc [%]	Tc
PHA_HM200_10	10	0-200	170.6	80.2	61.0	113.3
PHA_HM200_25	25	0-200	169.5	76.3	70	113.8
PHA_HM200_40	40	0-200	166.4	50.1	57.2	108.3
PHA_HO210_10	10	200-1000	173	75.1	57.2	114.4
PHA_HO210_25	25	200-1000	170	64.9	59.2	114.4
PHA_HO210_40	40	200-1000	170.5	33.5	43.9	111.1

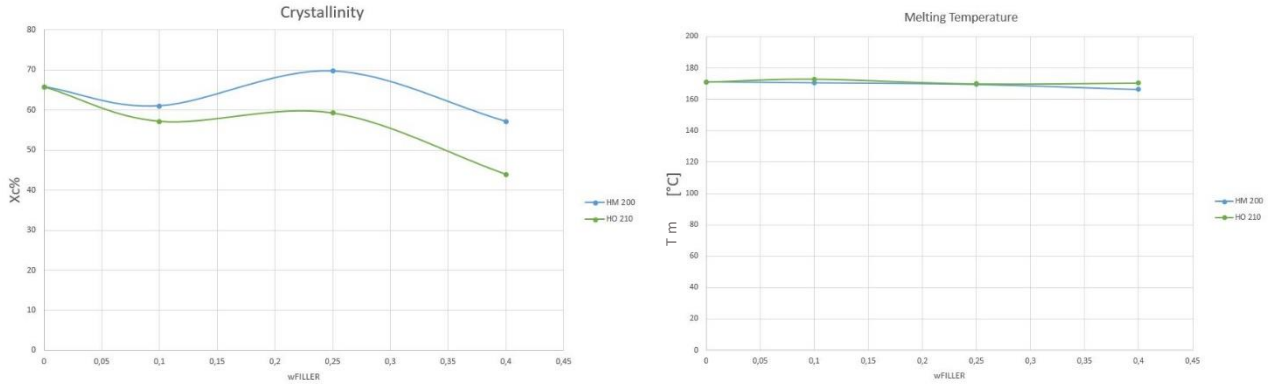

Graphic 7 Degree of crystallinity and melting temperature Hazelnut's fillers composite

The trends are similar to the ones of Almond; the most interesting point is the one at 25%

small grain size, where there is a higher degree of crystallinity than pure PHA.

Walnuts

Table 16 Thermal properties of PHB Walnut's fillers composite

ID	Filler content [wt%]	Grain size (µm)	Tm [°C]	ΔHm [J/g]	Xc [%]	Tc
PHA_WM200_10	10	0-200	171.9	75.4	57.3	112.1
PHA_WM200_25	25	0-200	173.7	52.9	48.3	107.6
PHA_WM200_40	40	0-200	166.4	49.5	56.5	108.6
PHA_WO210_10	10	200-1000	169.9	77	65.2	113.3
PHA_WO210_25	25	200-1000	170.7	57.9	52.9	106.2
PHA_WO210_40	40	200-1000	169.34	52.61	60.06	107.6

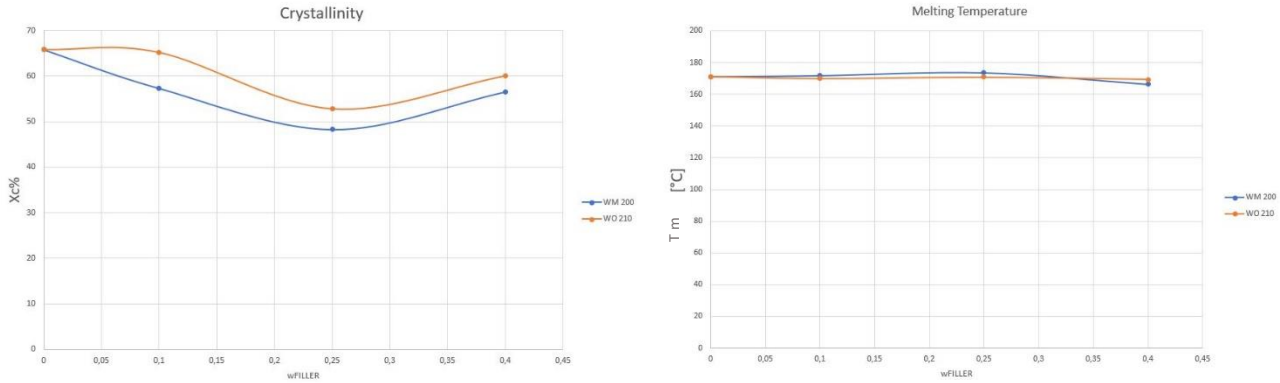

Graphic 8 Degree of crystallinity and melting temperature Walnut's fillers composite

Walnuts does have different behaviour than the other two filler:

- The degree of crystallinity is higher for bigger grain size than smaller ones, a k-data is the one at 10% where the degree of crystallinity is higher than the pure PHA
- The melting temperature does have a higher increase at 25% of filler with bigger grain size.

PLA

Table 17 Thermal properties of PLA pure

ID	Tg [°C]	ΔSg [J/°Cg]
PLA_Pure	58.2	0.52

Almond

Table 18 thermal properties of PLA Almond's fillers composite

ID	*Filler content [wt%]*	*Grain size (µm)*	*Tg [°C]*	*ΔSg [J/°Cg]*
PLA_AM200_10	*10*	*0-200*	57.4	0.46
PLA_AM200_25	*25*	*0-200*	56	0.35
PLA_AM200_40	*40*	*0-200*	58.4	0.27
PLA_AO210_10	*10*	*200-1000*	57.7	0.40
PLA_AO210_25	*25*	*200-1000*	57.7	0.37
PLA_AO210_40	*40*	*200-1000*	57	0.28

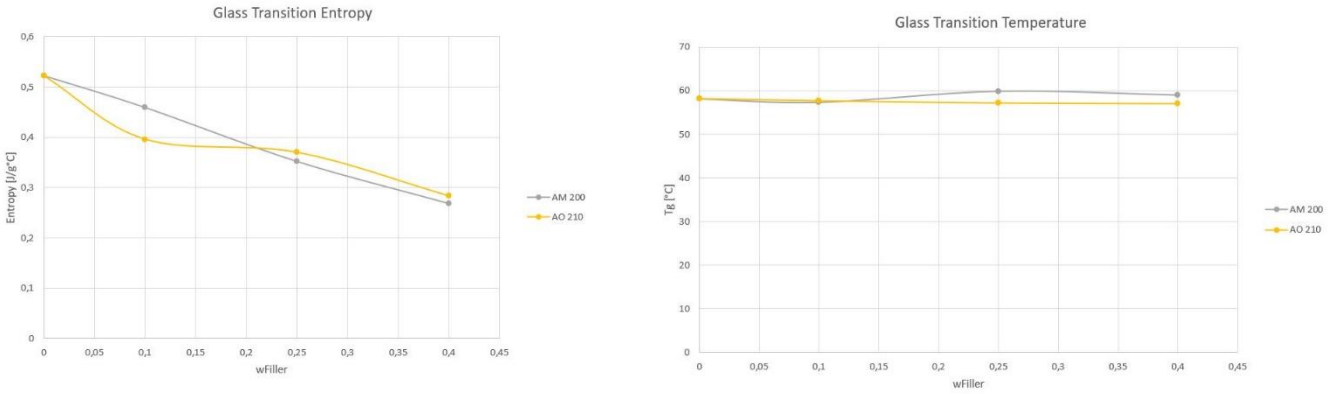

Graphic 9 Glass transition temperature and entropy Almond's fillers composite

For smaller grain size it has a mostly linear decrease of the Glass transition entropy, while with the increase of the filler content, the glass transition temperature increases.

For big filler, the entropy is lower than small once at 10%, then it becomes slightly higher at concentration higher than 25%; by looking at the glass transition temperature, the value is mostly stable but higher than pure PLA.

Hazelnuts

Table 19 Thermal properties of PLA Hazelnut's fillers composite

ID	*Filler content [wt%]*	*Grain size (µm)*	*Tg [°C]*	*ΔSg [J/°Cg]*
PLA_HM200_10	*10*	*0-200*	56.7	0.38
PLA_HM200_25	*25*	*0-200*	54.6	0.34
PLA_HM200_40	*40*	*0-200*	53.8	0.2991
PLA_HO210_10	*10*	*200-1000*	57.5	0.45
PLA_HO210_25	*25*	*200-1000*	58.3	0.40
PLA_HO210_40	*40*	*200-1000*	56.2	0.23

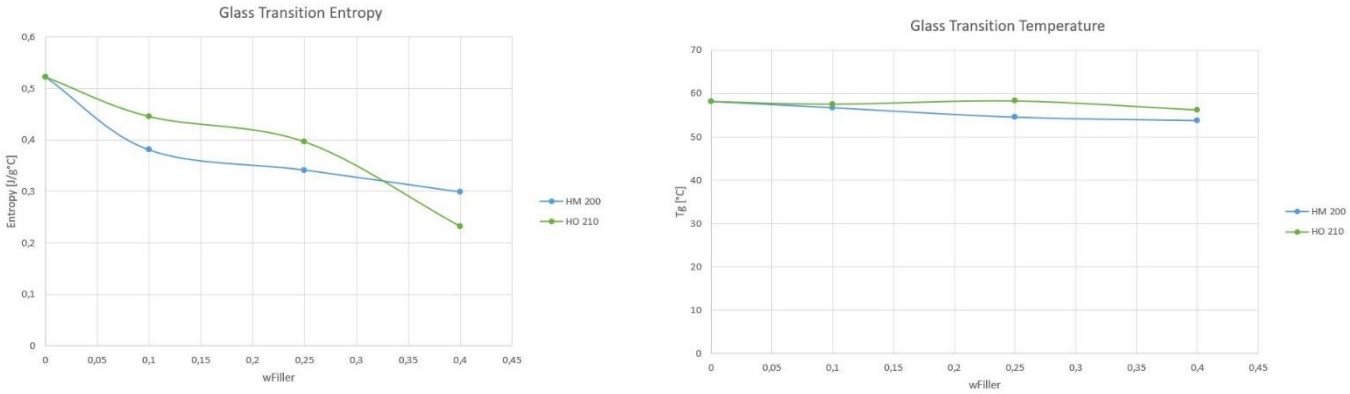

Graphic 10 Glass transition temperature and entropy Hazelnut's fillers composite

For Hazelnuts, the trend is different than that of the Almonds; bigger grain size fillers do have lower glass transition entropy than smaller ones; the only exception is for weight fraction of 40%; the glass transition temperature remain stable with big grain size, while for smaller decreases even if the change between pure PLA and PLA's hazelnuts composites is low.

Walnuts

Table 20 Thermal properties of PLA Walnut's fillers composite

ID	*Filler content [wt%]*	*Grain size (µm)*	*Tg [°C]*	*ΔSg [J/°Cg]*
PLA_WM200_10	*10*	*0-200*	55.6	0.43
PLA_WM200_25	*25*	*0-200*	53.8	0.36
PLA_WM200_40	*40*	*0-200*	53.8	0.26
PLA_WO210_10	*10*	*200-1000*	60	0.33
PLA_WO210_25	*25*	*200-1000*	56	0.30
PLA_WO210_40	*40*	*200-1000*	58.4	0.25

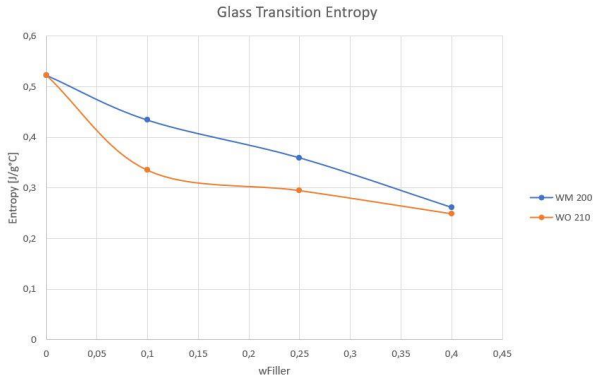

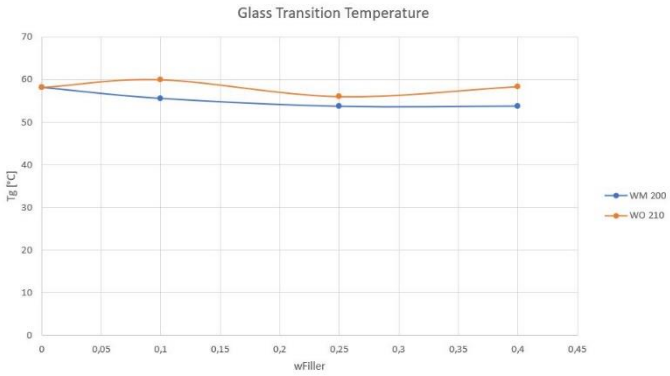

Also, walnuts behave differently; the glass transition entropy is higher for composites with smaller grain; the difference between the two decreases till the 40% where they are mostly similar.

Looking at the glass transition temperature, bigger grain size does have higher temperature of glass transition, a significant data is the one at 10% where the glass transition temperature is more than 1°C higher than pure PLA.

Injection moulding operative problem

During the creation of the dog-bone tester some composites were impossible to be formed: regarding PHA matrix, the ones with the hazelnut's filler with big grain size at 25 and 40% block the screw so the injection was enabled. This is probably due to a friction between the fillers, present at high concentration and high size, and the wall of the screw. For composite with the PLA matrix the creation of the tester was difficult; the only dog-bones produced were the ones with concentration of filler of 10% and small grain size (PLA_AM200_10; PLA_HM200_10; PLA_WM200_10). By increasing the one or both of the characteristics implies a clog of the nozzle inhibiting the filling of the mould. Due to this fact, it is possible to assume that the injection moulding type of processing is not a suitable way for producing biocomposite with PLA matrix and shell's fillers.

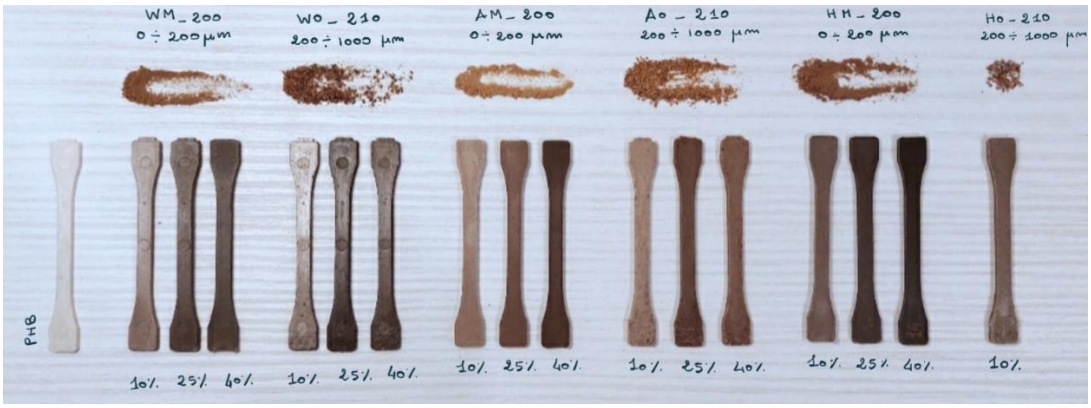

Figure 50 PHA biocomposite Dog bone tester final shape and shades

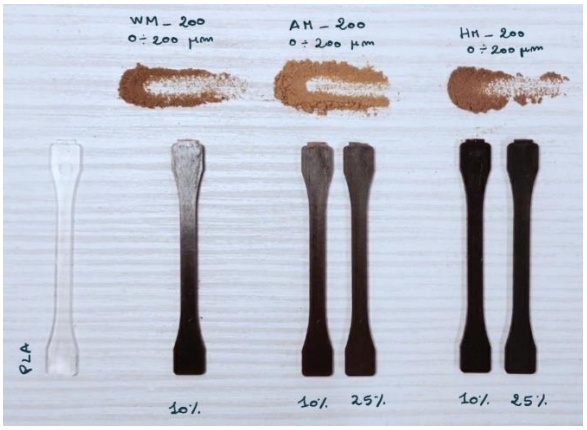

Figure 51 PLA biocomposite Dog bone tester final shape and shades

Scanning electron microscopy

PHA

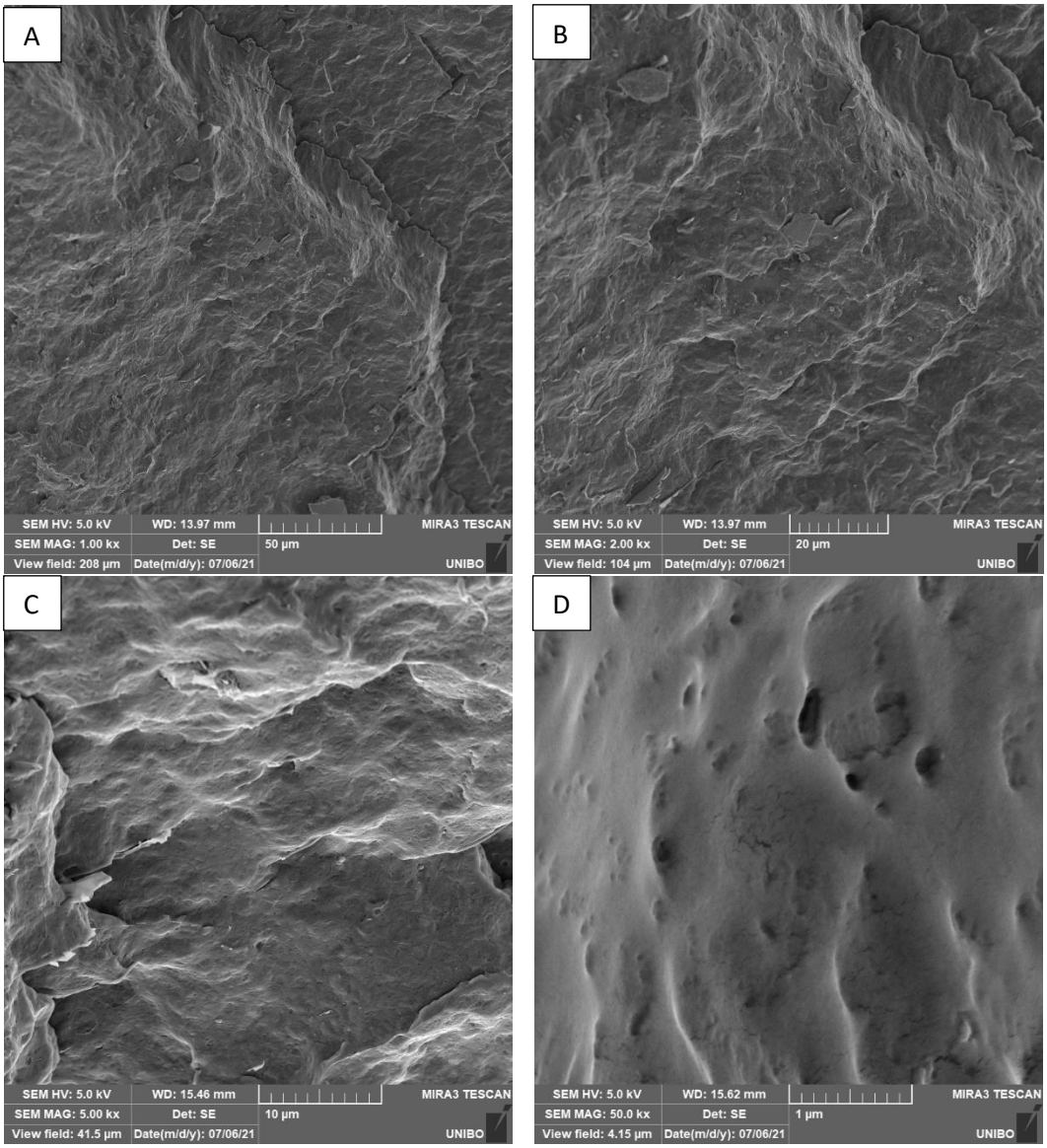

Figure 52 Pure PHA with different enlargement: A) enlargement 1.00 kx, B) enlargement 2.00 kx, C) enlargement 5.00 kx, D) enlargement 50.0 kx

By looking at the Pure PHA it is possible to see a quite rough surface with the presence of some pores (Figure 52 Pure PHA with different enlargement, D).

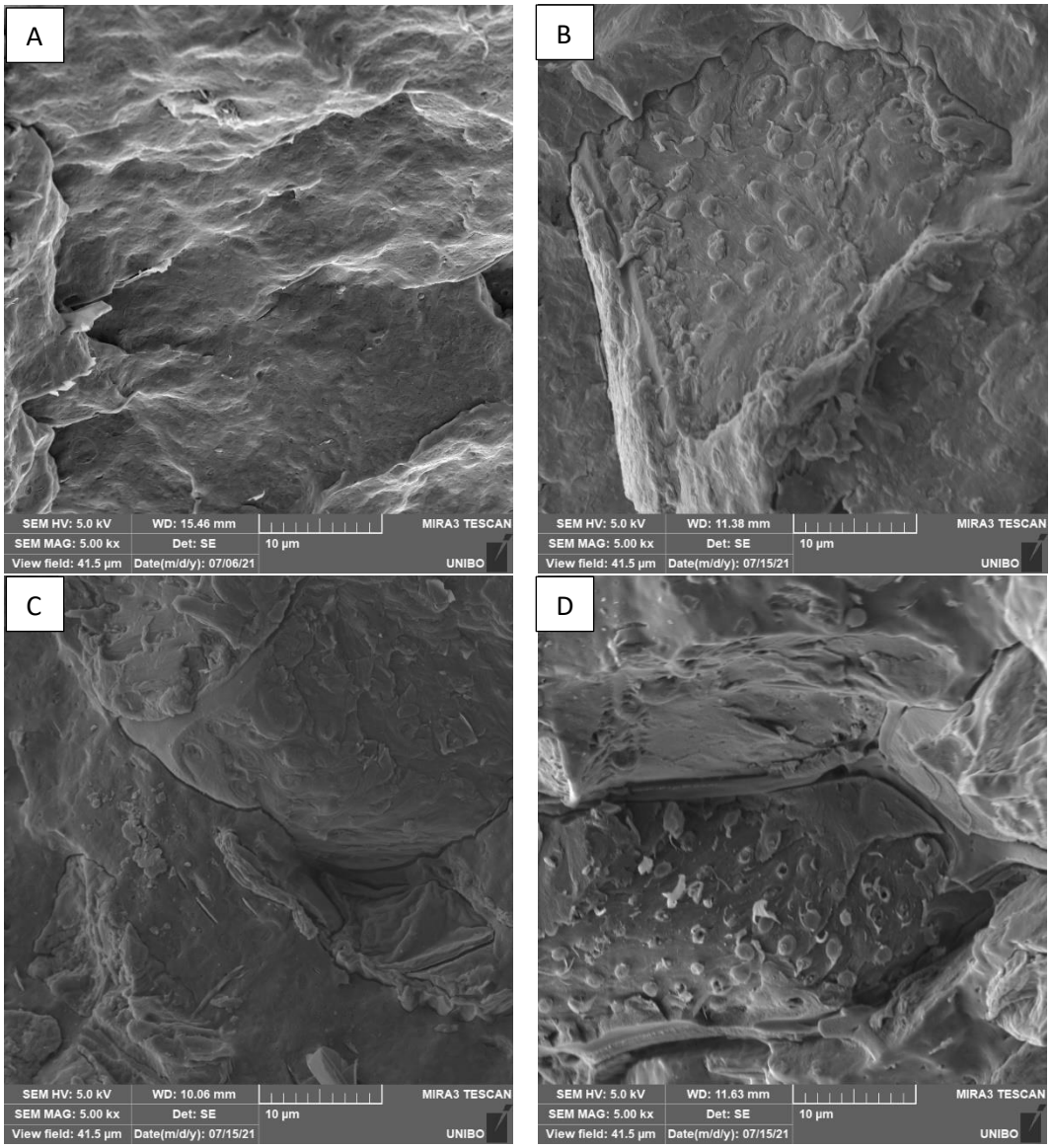

Figure 53 PHA + AM 200 at different concentration with a resolution of 5'000 x where: A) pure PHA, B) PHA_ AM200_10, C) PHA_AM200_25, D) PHA_AM200_40

With the introduction of the Almond filler with small grain size, it is possible to see a good interaction between the two, the interphase is very small and this might induce good mechanical properties even at high concentration of the filler.

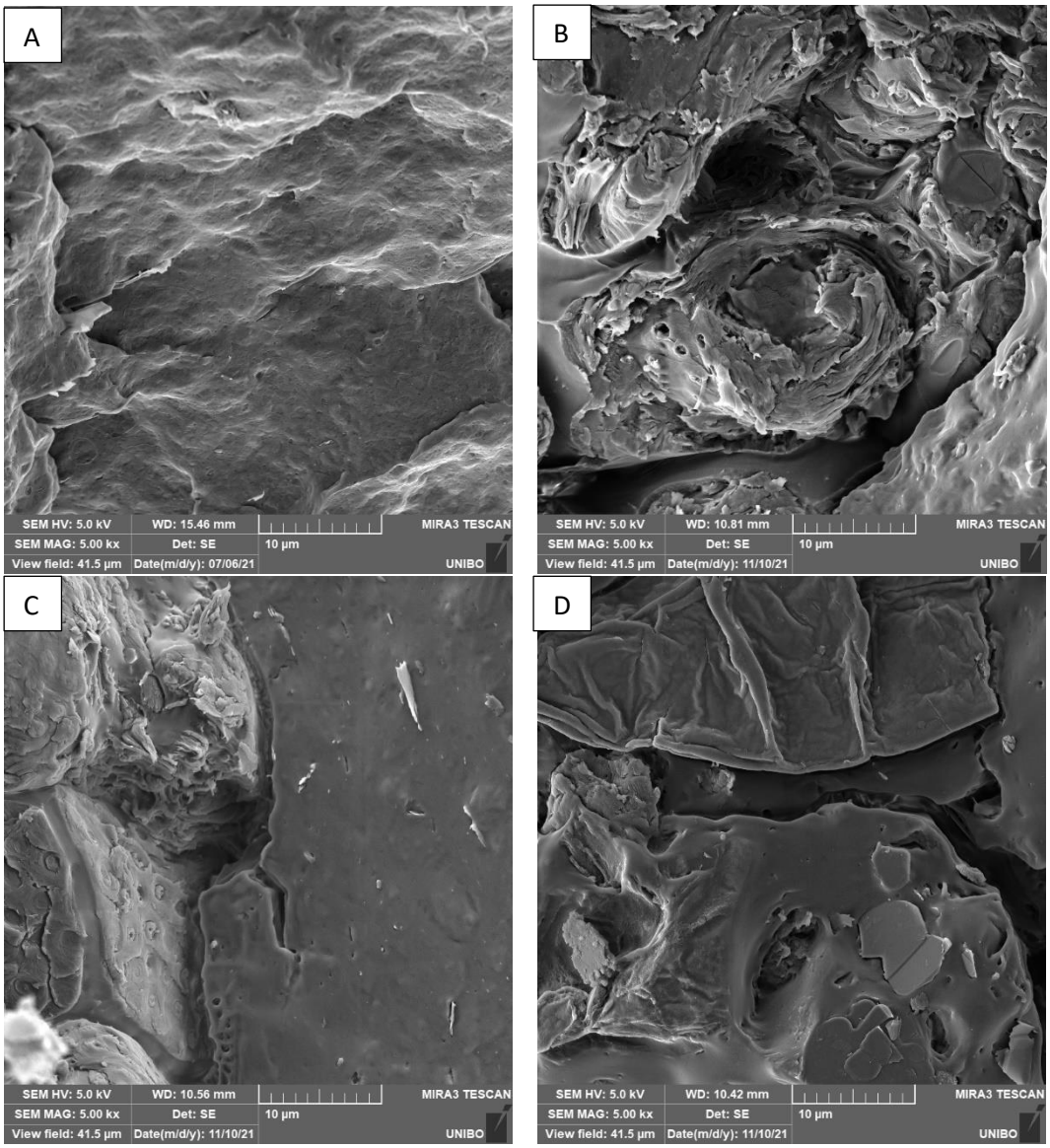

Figure 54 PHA + AO 210 at different concentration with a resolution of 5'000 x where: A) pure PHA, B) PHA_ AO210_10, C) PHA_AO210_25, D) PHA_AO210_40

Almond's filler at bigger grain size shows a less good interaction with the polymer matrix that could induce lower mechanical properties respect to the smaller grain size.

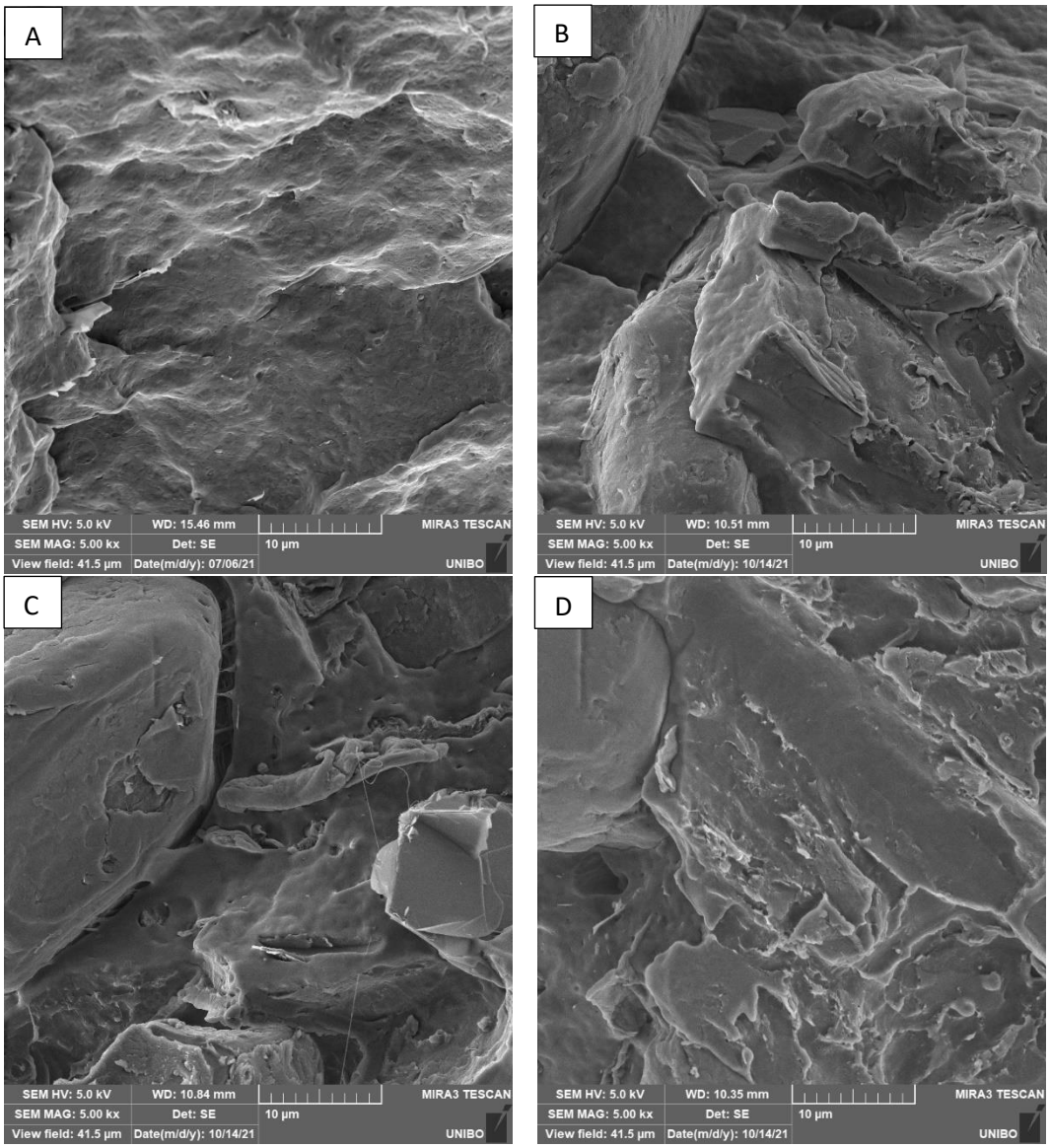

Figure 55 PHA + HM 200 at different concentration with a resolution of 5'000 x where: A) pure PHA, B) PHA_ HM200_10, C) PHA_HM200_25, D) PHA_HM200_40

Hazelnut's filler, small grain size, does also show a quite good interphase, one of the most peculiar images is the Figure 55 C) where it is possible to see clearly the interaction at the interphase between the filler and the matrix.

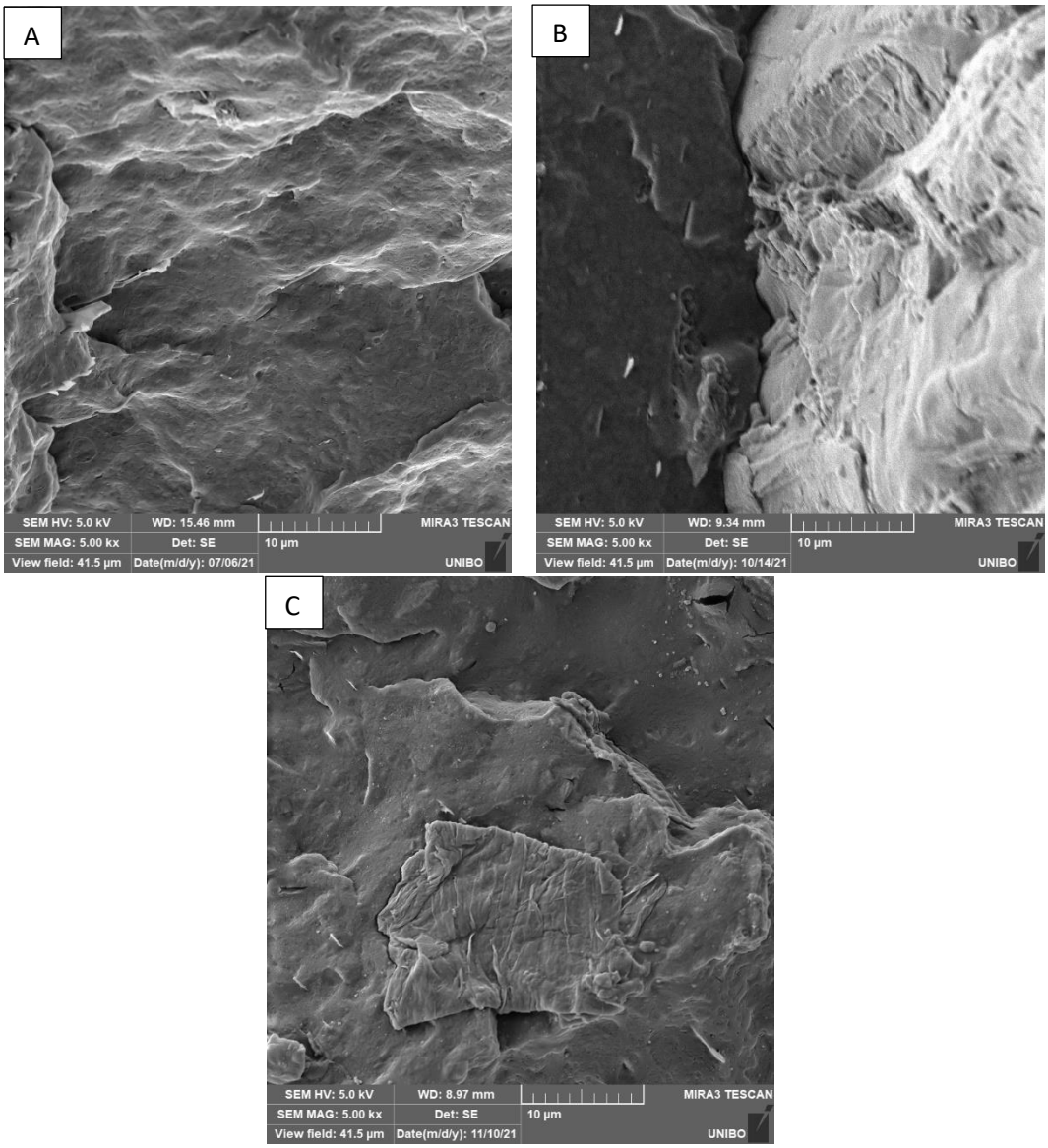

Figure 56 PHA + HO 210 at different concentration with a resolution of 5'000 x where: A) pure PHA, B) PHA_ HO210_10, C) PHA_HO210_25

Hazelnut's big grain size does show an interphase that seems less good than the ones with smaller grain size, but better than the ones made by the almonds with the same grain size.

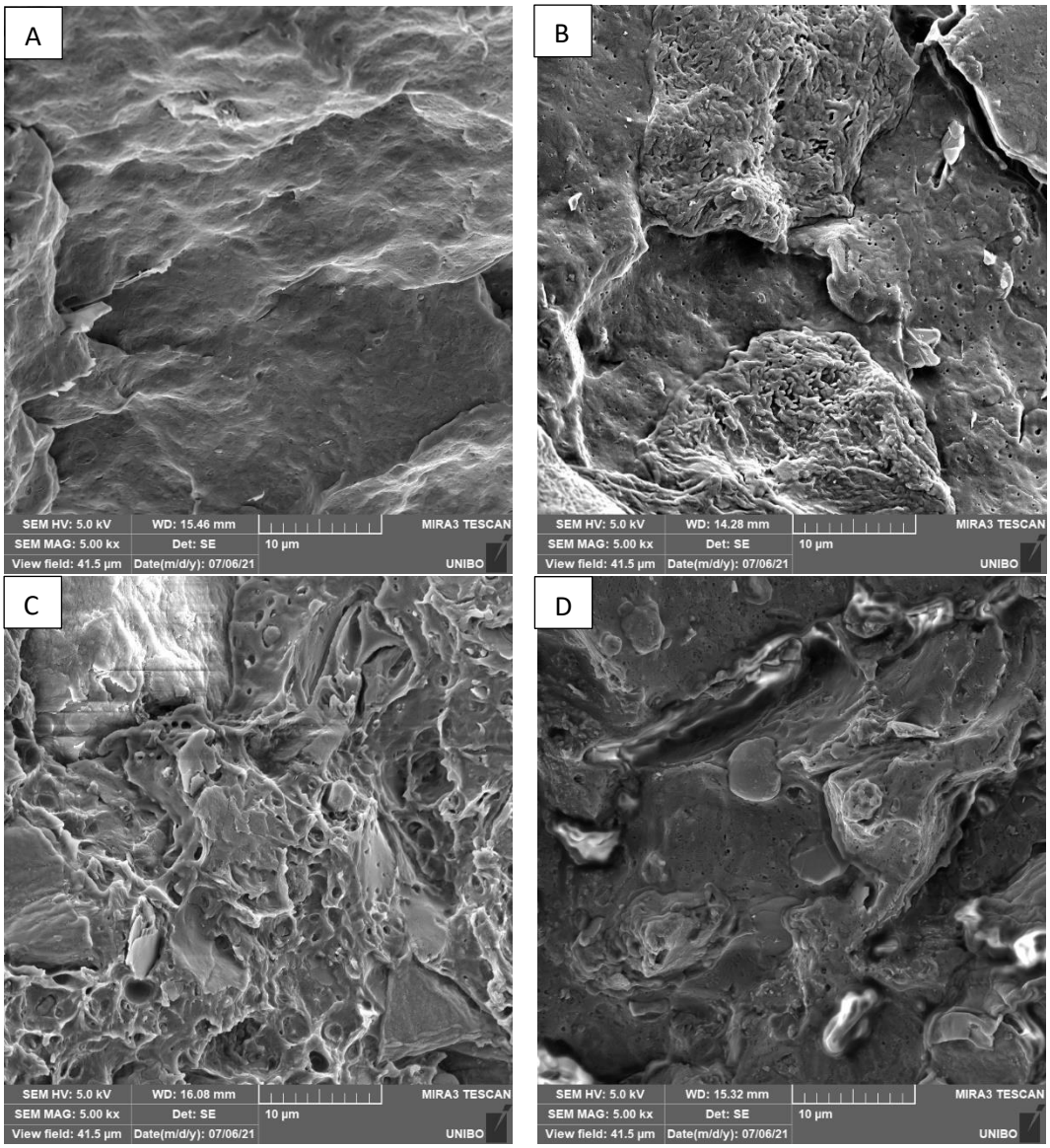

Figure 57 PHA + WM 200 at different concentration with a resolution of 5'000 x where: A) pure PHA, B) PHA_ WM200_10, C) PHA_WM200_25, D) PHA_WM200_40

Walnuts, small grain size, like the other two detected before, shows a good interphase, the fillers seem to be well intercalated in the polymer matrix.

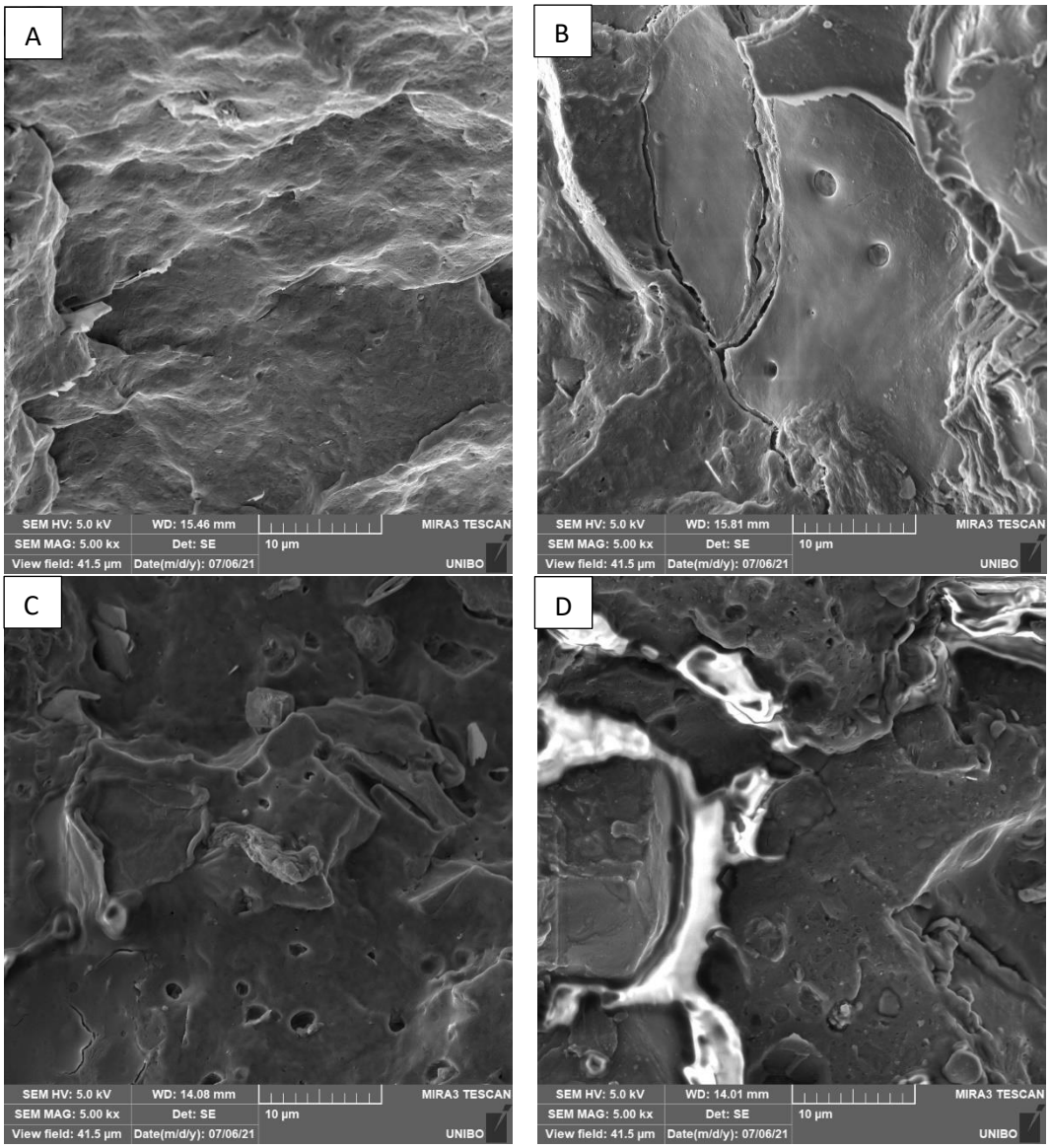

Figure 58 PHA + WO 210 at different concentration with a resolution of 5'000 x where: A) pure PHA, B) PHA_ WO210_10, C) PHA_WO210_25, D) PHA_WO210_40

Big grain size Walnut's filler shows, like the others, a less good interaction between the filler and the matrix, the most significative image is Figure 58 B) where the interphase is quite thick between filler and matrix.

PLA

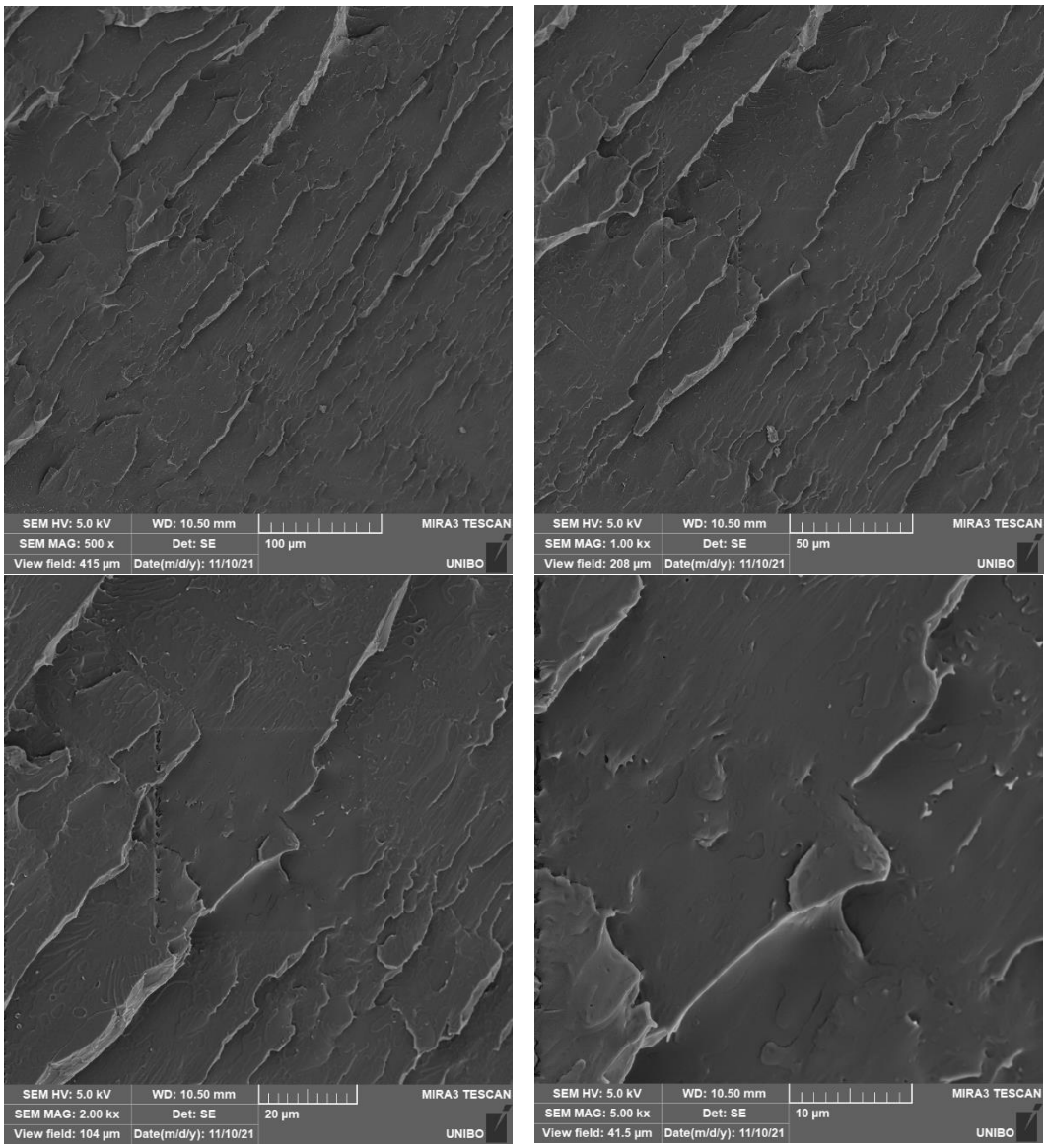

Figure 59 Pure PLA with different enlargement A) enlargement 500 x, B) enlargement 1.00 kx, C) enlargement 2.00 kx, D) enlargement 5.00 kx

PLA shows a smoother and denser surface, this could induce a different behaviour of the properties with the introduction of filler respect to the ones with PHA.

Tension

Tension experiment, described in “Test setting”, will be divided in type of matrixes and, then, in type of filler and grain size. In this kind of composite, generally, the Young Modulus increases with the increase of the filler, while the tensile stress and elongation have the tendency to decrease.

PHA

Pure PHA does have the listed properties:

- Young Modulus: 2096 [MPa]
- Tensile stress: 36.38 [MPa]
- Elongation: 2.26 [%]
- Tensile stress at break: 35.82 [MPa]
- Elongation at break: 2.31 [%]

Almond

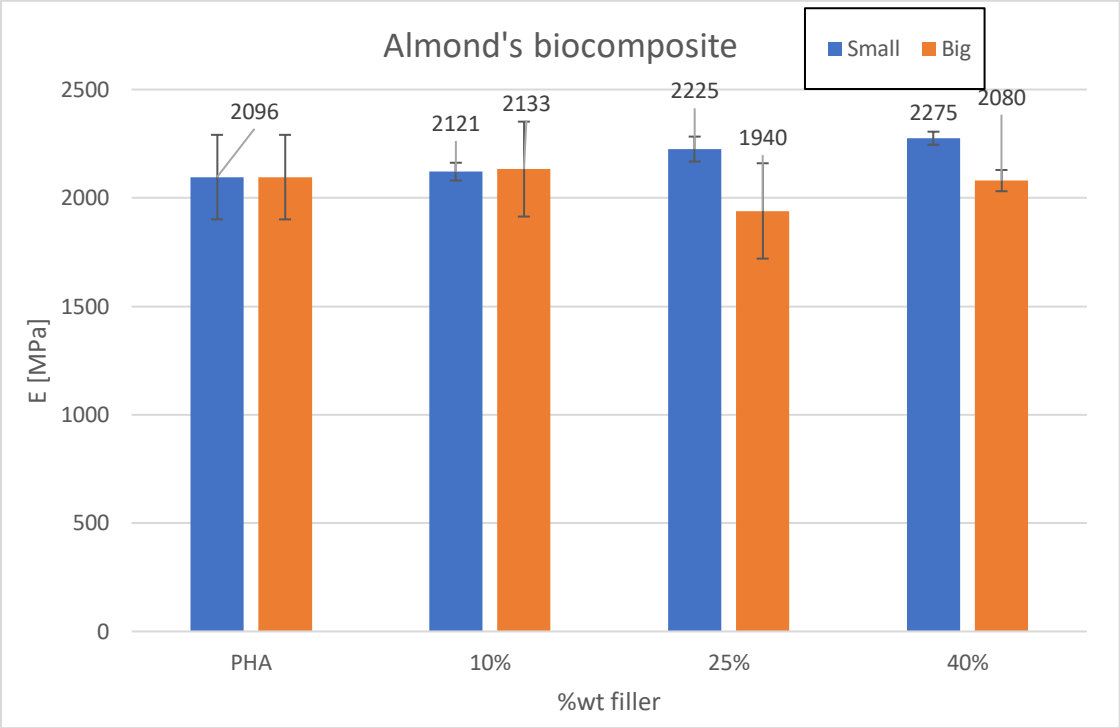

Graphic 11 Young Modulus for PHA + Almonds composite

The Young modulus has the tendency to increase with the addition of Almond's filler at small grain size, while, with bigger grain size, we have an increase at 10%, then a decrease, but the value did not change too much.

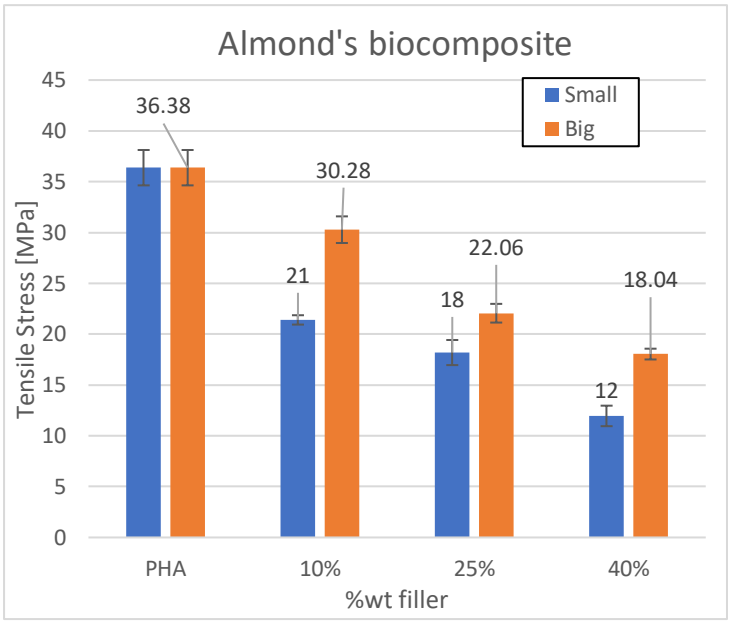

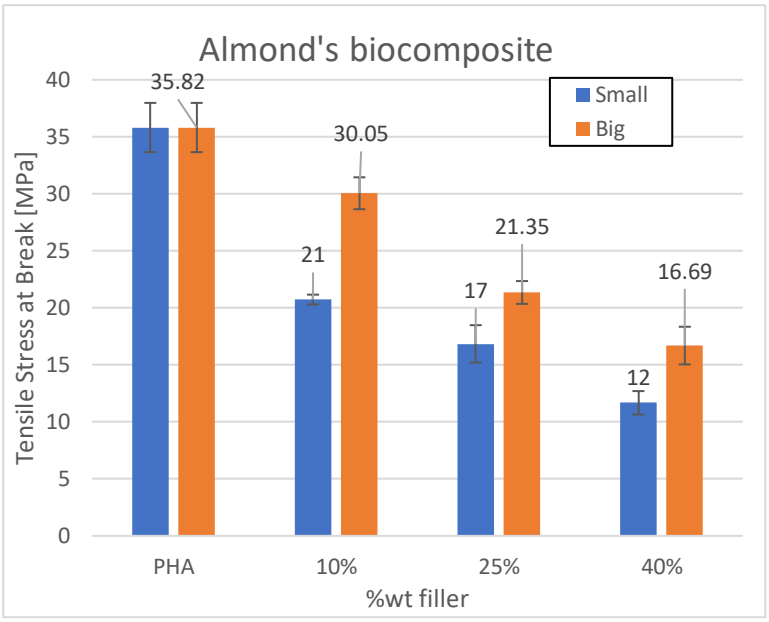

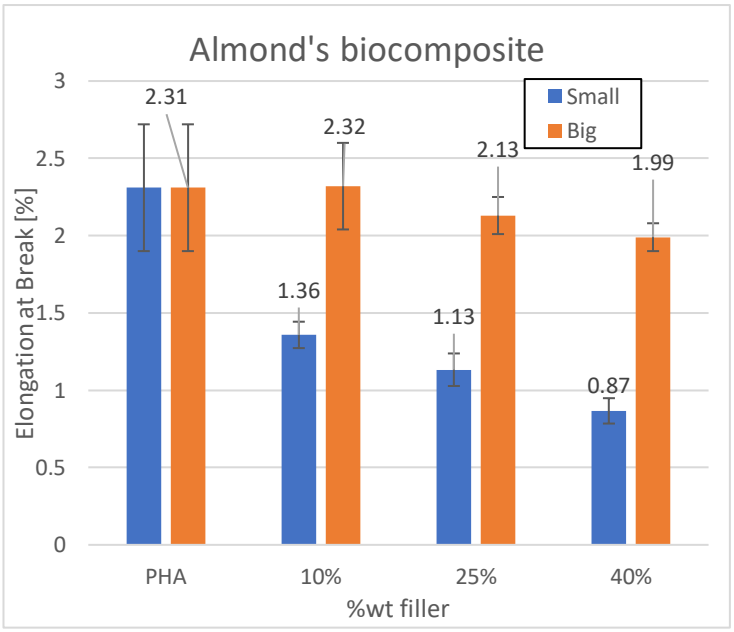

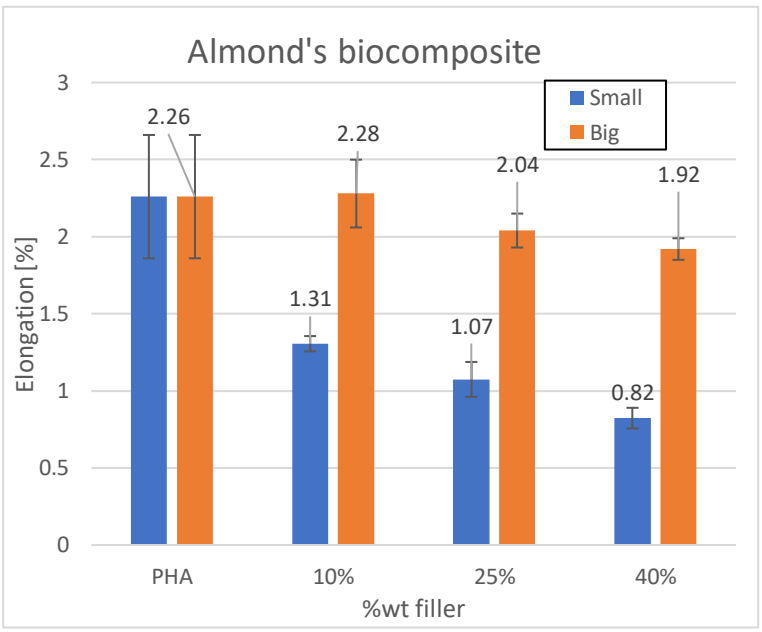

Graphic 12 Tensile stress and elongation for PHA +Almonds composite

The tensile stress and the elongation at break with the increase of the filler content tend to decrease, but the biocomposites with big grain size decrease less strongly than the smaller ones.

Hazelnut

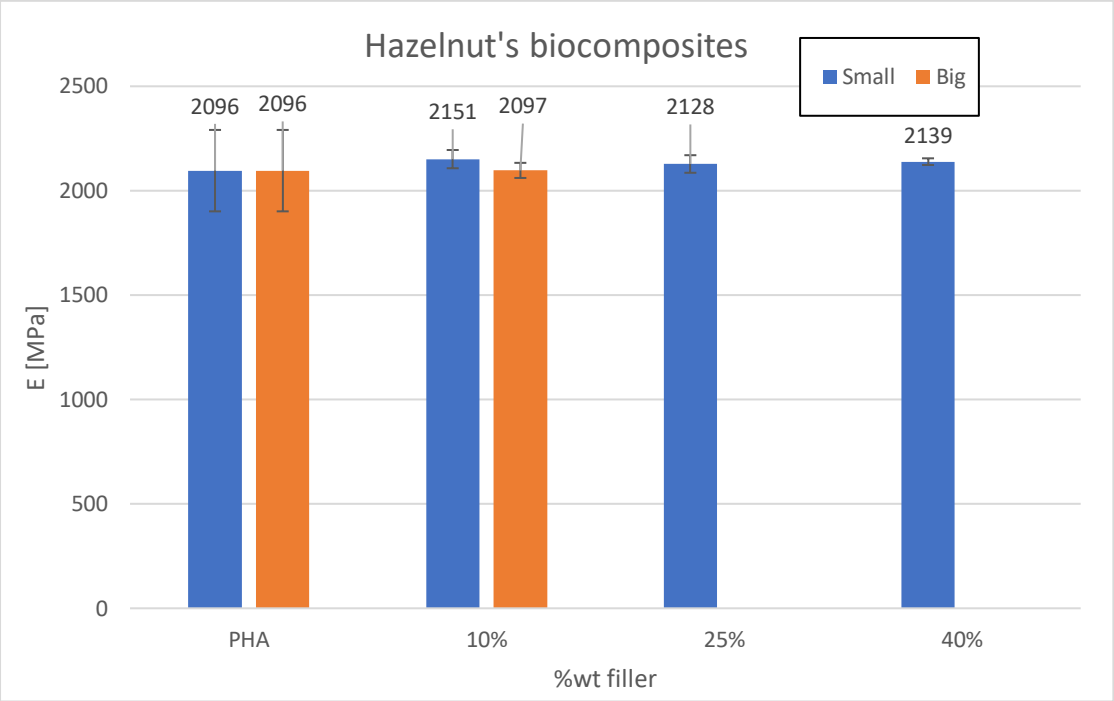

Graphic 13 Young Modulus for PHA + Hazelnuts composite

In this case, due to the problems regarding the injection moulding we are able to detect well only the composites with small grain size and, regarding the Young Modulus, there is not great difference between pure PHA and the biocomposites with hazelnuts, they are generally less than 100's MPa higher.

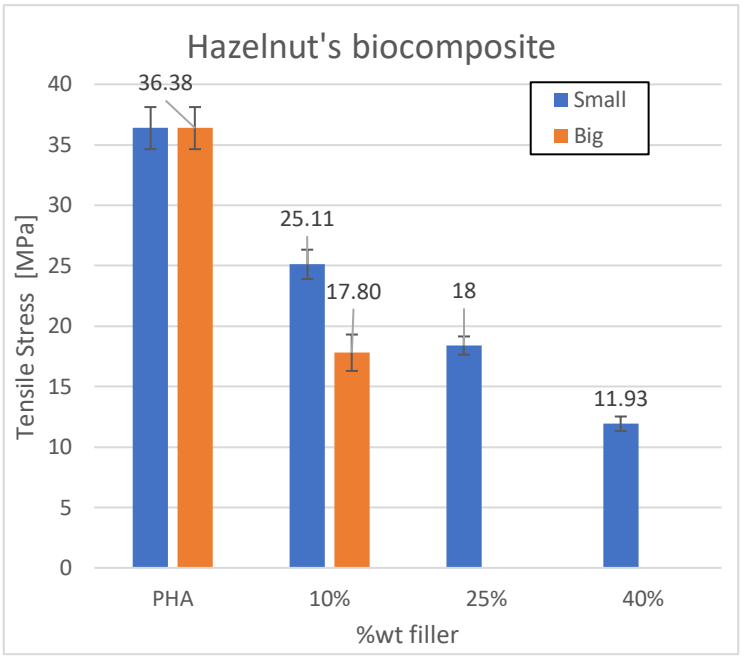

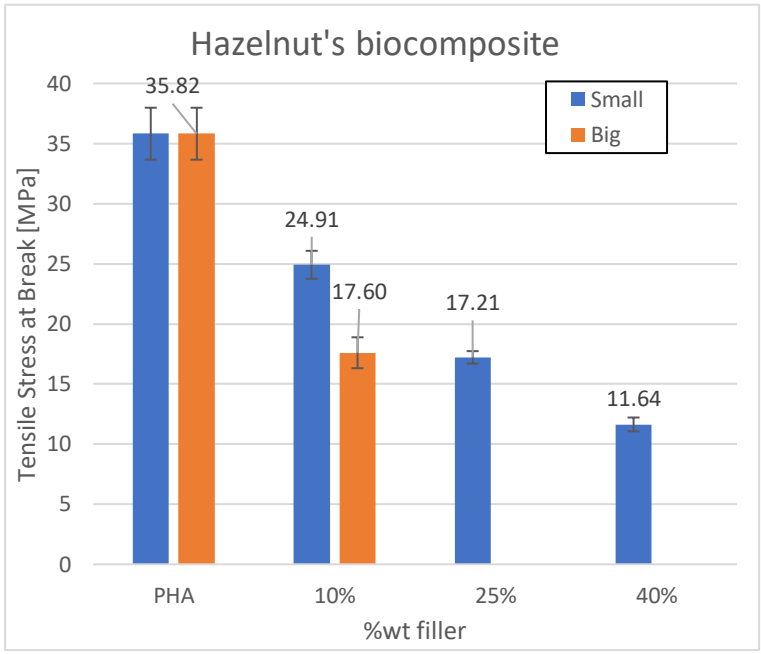

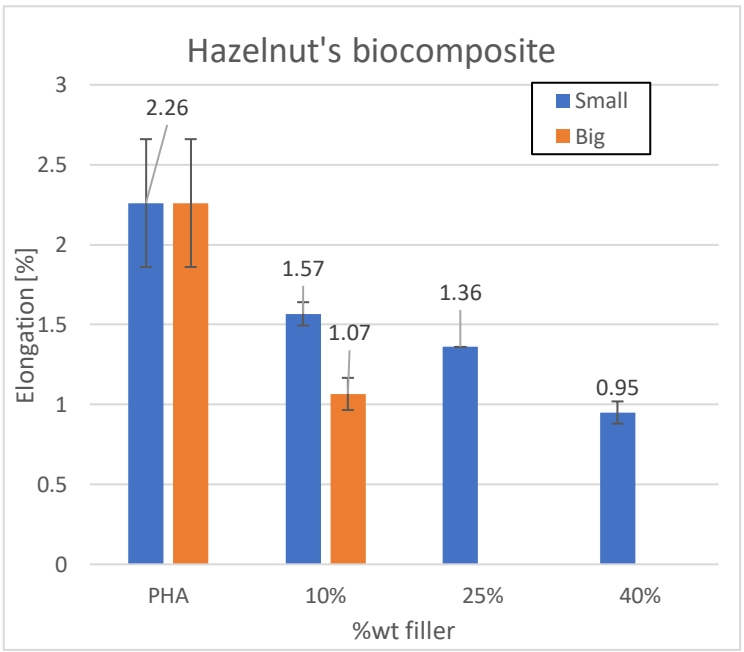

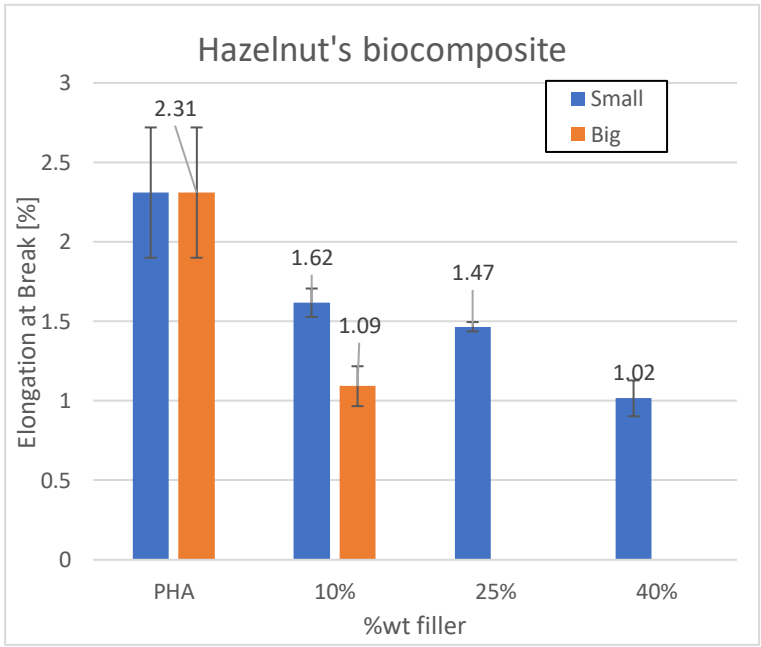

Graphic 14 Tensile stress and elongation for PHA +Hazelnuts composite

By looking to the tensile stress and the elongation the trend is mostly similar to the composites with almonds, but, in this case, the values are higher than the ones detected above.

Walnut

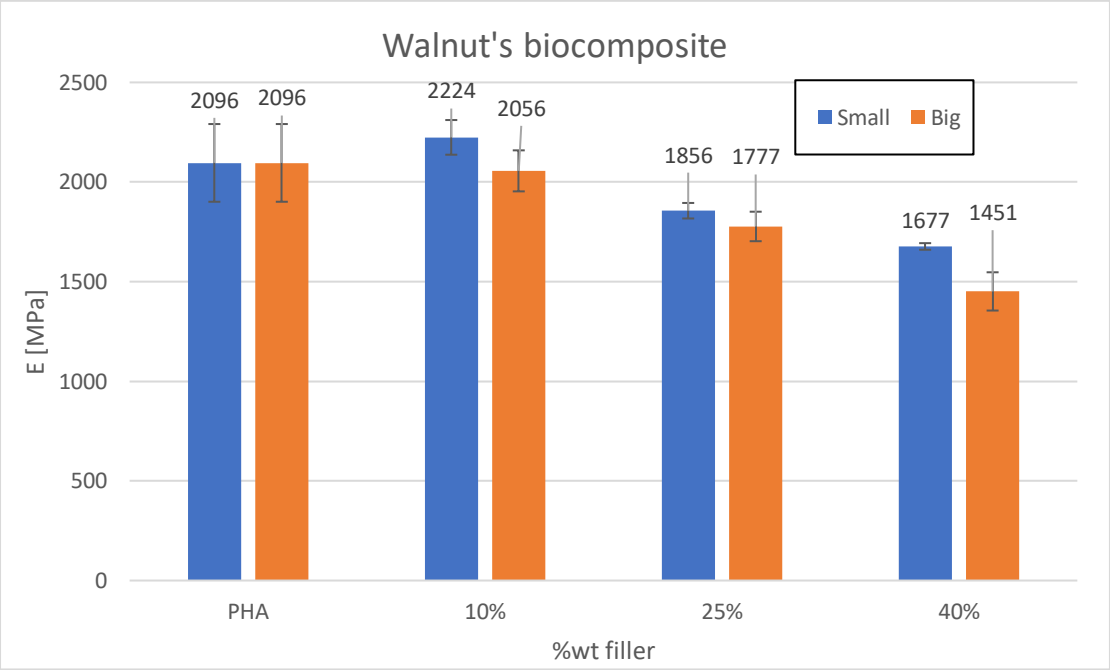

Graphic 15 Young Modulus for PHA + Walnuts composite

For Walnut's biocomposite with PHA the Young modulus tend to decrease with the increasing of the filler content for both big and small grain size; the values are incredibly low for the composites with 40% of filler.

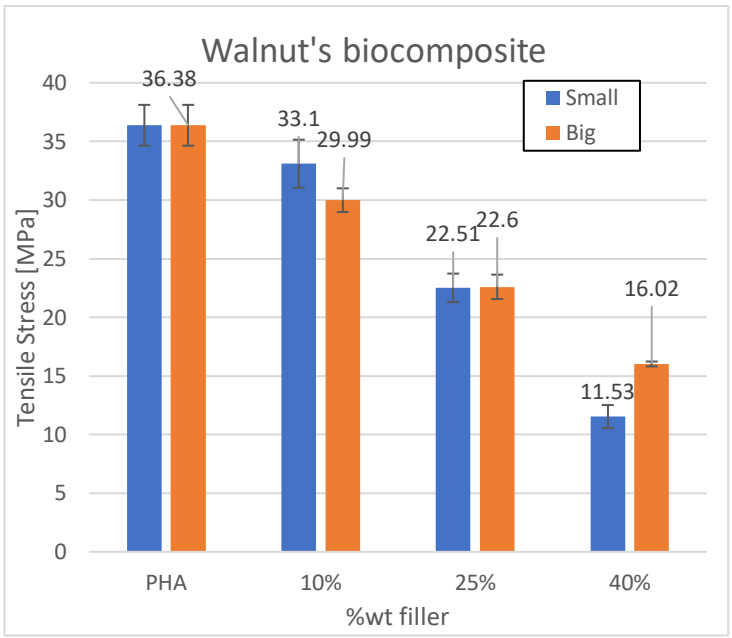

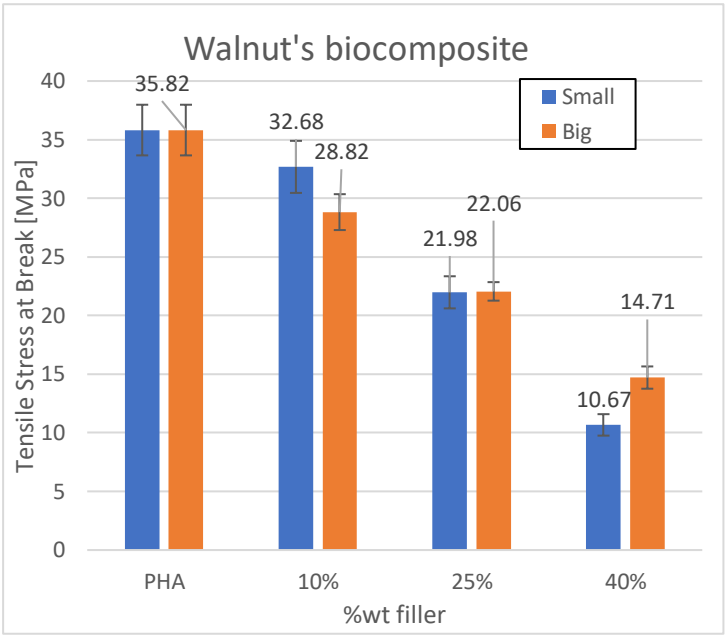

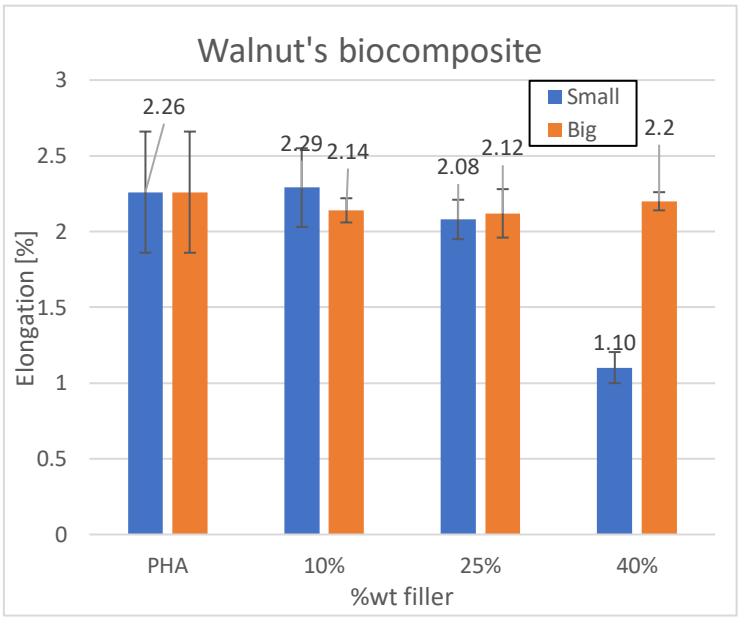

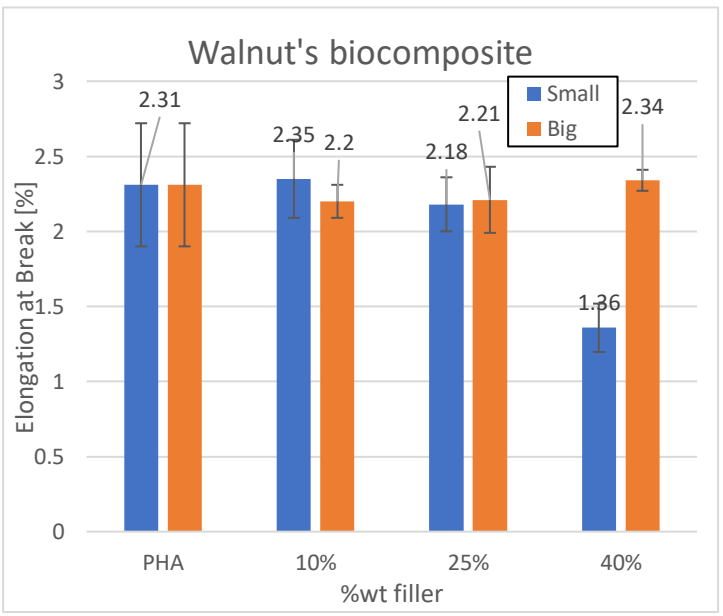

Graphic 16 Tensile stress and elongation for PHA +Walnuts composite

Walnuts does show similar behaviours than Almonds and Hazelnuts PHA's biocomposite, but the tensile stress and tensile stress at break show a much higher values than the other two. By looking at the elongation at break, the values are nearer to the pure PHA respect to the other composites; the only exception is the one with small grain size with a filler load of 40%.

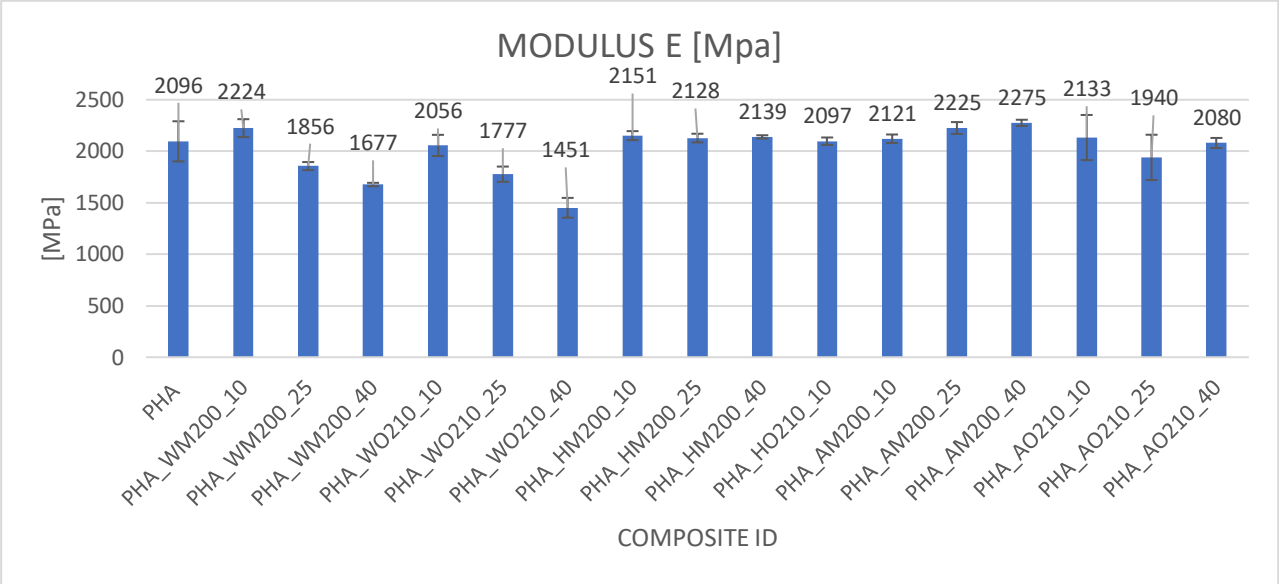

Graphic 18 Resume of the Young Modulus in PHA's biocomposite

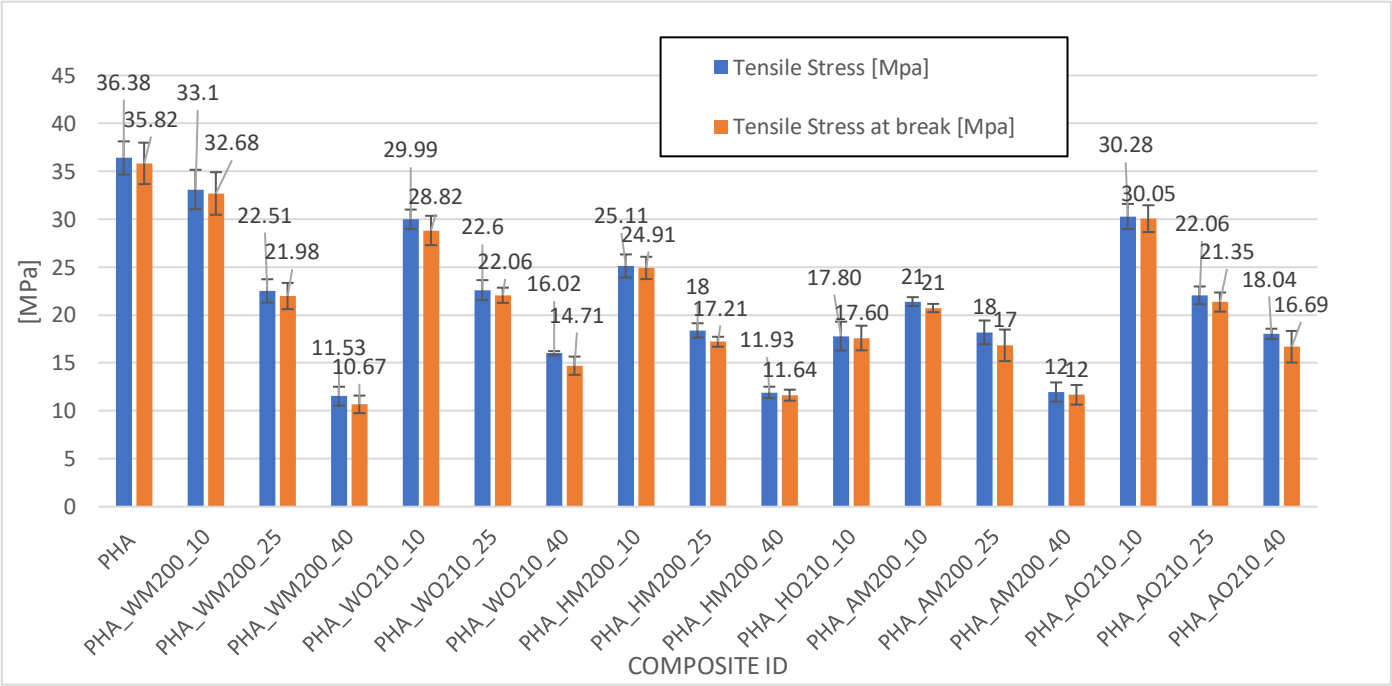

Graphic 17 Resume of the Tensile stress and Tensile stress at break in PHA's biocomposite

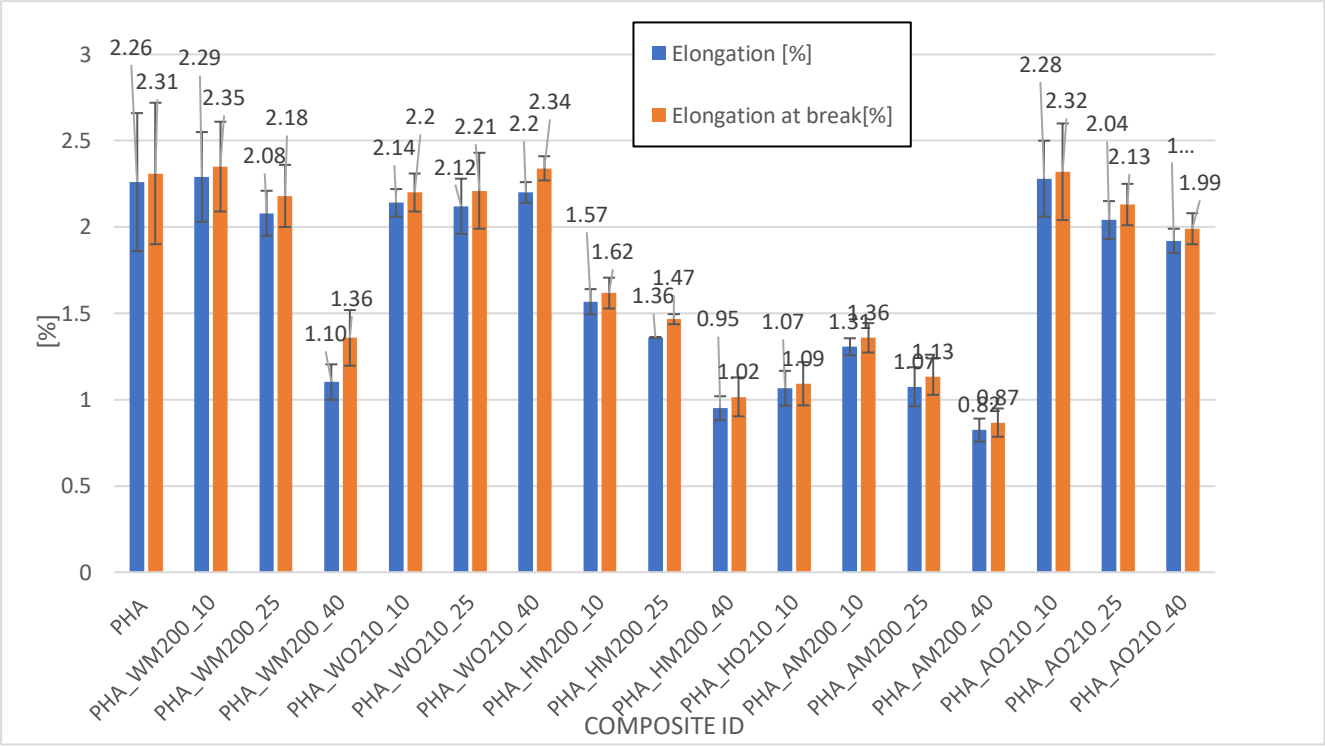

Graphic 19 Resume of the Elongation and Elongation at break for PHA's biocomposite

PLA

As said before, in “Injection moulding operative problem” the only PLA biocomposites present are the ones with small grain size and filler content of 10%, so, all the data are compared with the same composites done with PHA matrix in order to evaluate how the filler participates to the properties in the two matrixes. This procedure is going to be the same for all the mechanical properties.

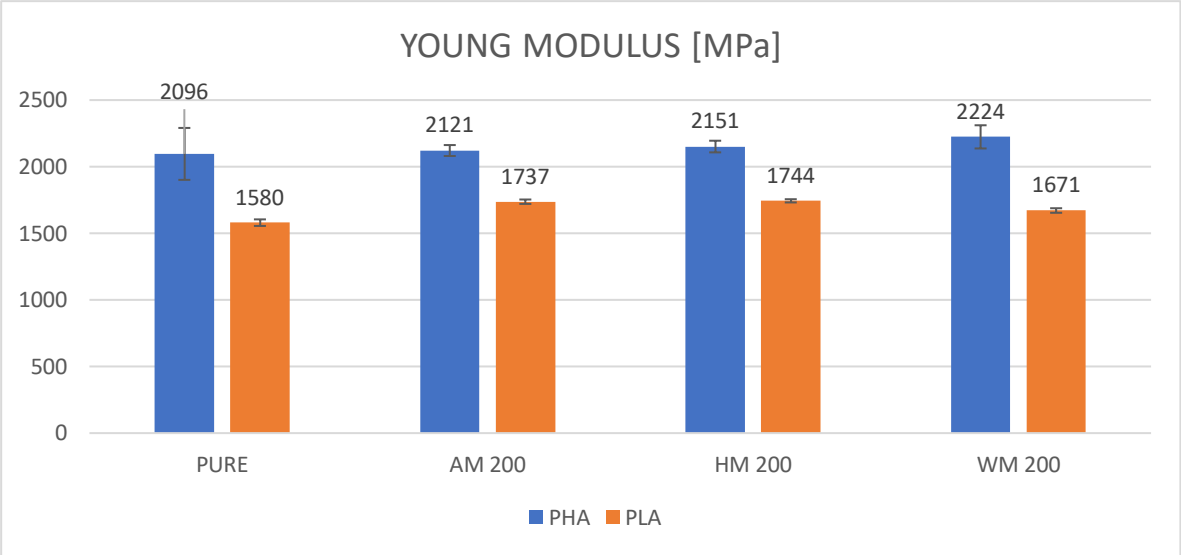

Graphic 20 Comparison between PHA's and PLA's biocomposite of the Young modulus

The Young modulus for PLA is smaller than the one of PHA, but both have the tendency to increase with the introduction of 10% of small grain size filler. The increase is higher for biocomposite with PLA, this can be seen in the next table.

Table 21 Change of the Young modulus for the two type of biocomposite

	MODULUS			
	PHA		PLA	
	VALUE [Mpa]	CHANGE [%]	VALUE [Mpa]	CHANGE [%]
PURE	2096		1579,76	
AM 200	2121	1,20%	1737,103333	9,96%
HM 200	2151	2,64%	1743,66	10,37%
WM 200	2224	6,11%	1671,041429	5,78%

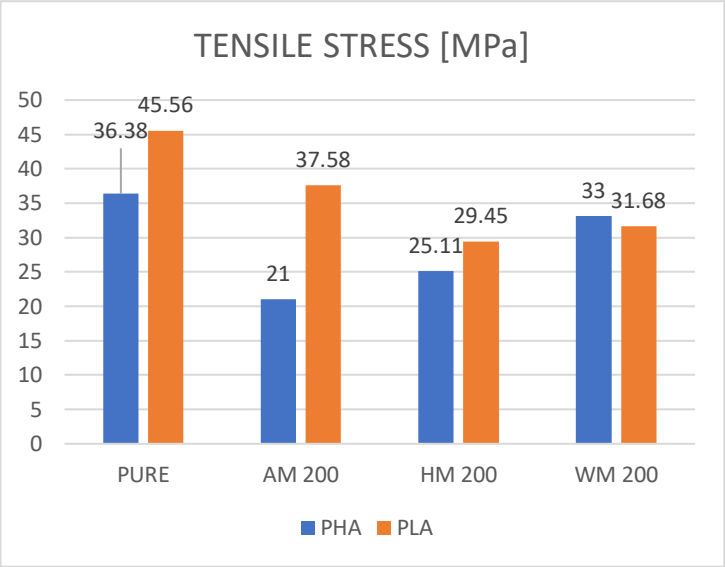

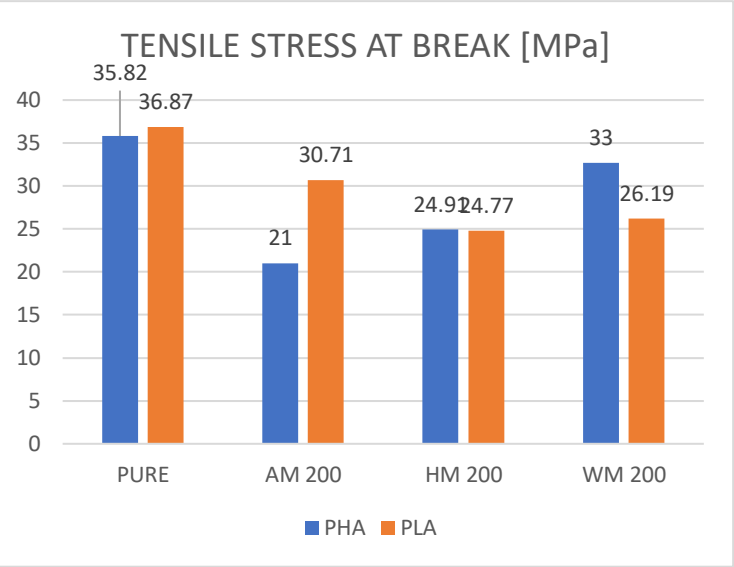

Graphic 21 Comparison between PHA's and PLA's biocomposite of the Tensile stress

Regarding the tensile stress, the value of PLA's composite is higher than PHA and it does decrease with the introduction of filler; the ones with almonds show a lower decrease than the others. An interesting set of data is the tensile stress at break that is significantly lower, this is due to the fact that PLA shows a more ductile fracture than PHA that is more brittle.

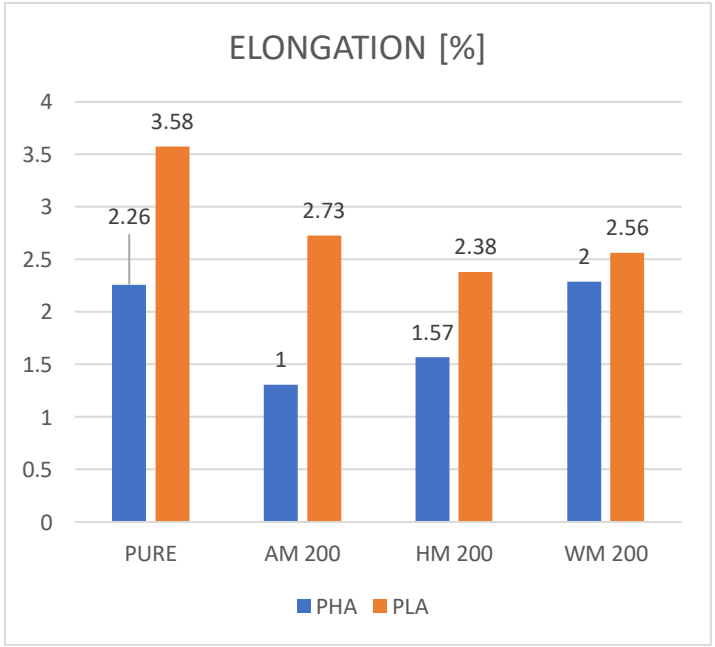

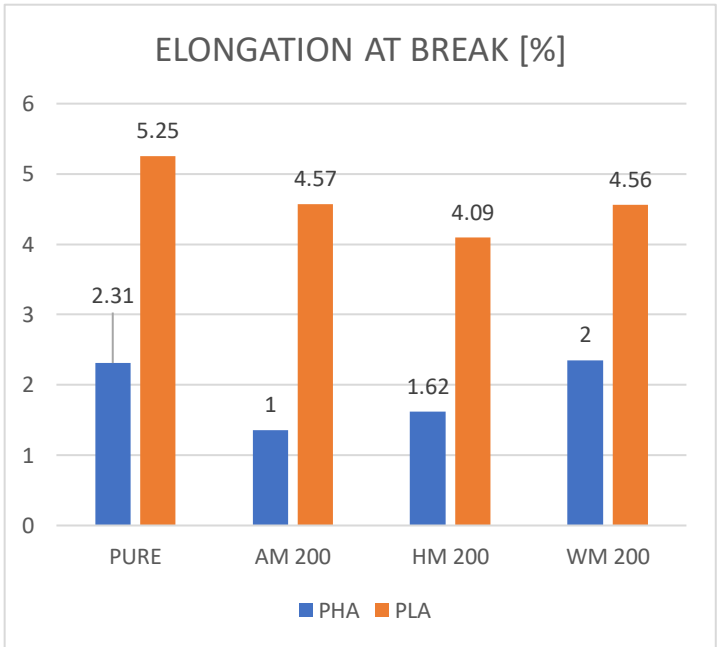

Graphic 22 Comparison between PHA's and PLA's biocomposite of the Elongation

Elongation, like the Tensile stress, shows similar behaviour, the elongation at break is much higher due to the fact that there is a ductile fracture. As for the Tensile stress, the best behaviour seems to take place for almonds biocomposite.

Impact

The procedure to detect the Impact energy was described before in “Test setting”; the results are plotted in bar charts divided by the type of polymer matrix.

PHA

The first biocomposites analysed are the ones with PHA matrix at increasing concentration of filler divided by type of filler and grain size

Almond

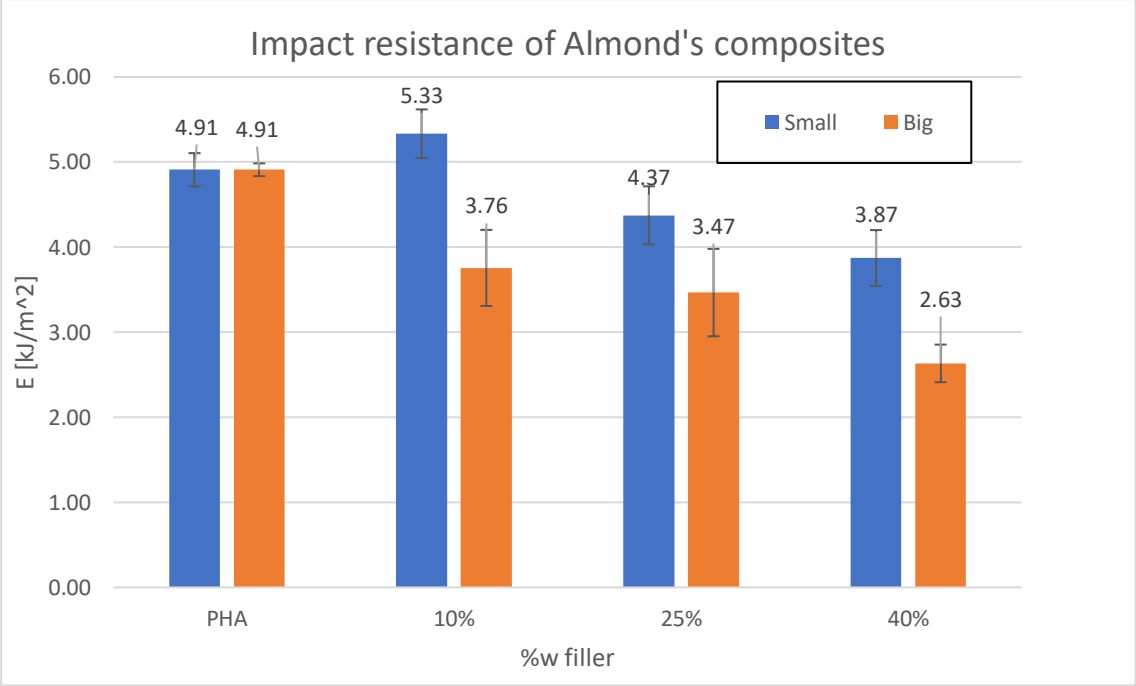

Graphic 23 Impact resistance of biocomposites with almond fillers

By looking at this chart it is possible to see that biocomposites with smaller grain size behave better than bigger ones; generally, the impact resistance tends to decrease with the increasing of the filler content. An interesting data is the one with the 10% of filler, small grain size (PHA_AM200_10) that has an higher impact resistance than pure PHA.

Hazelnut

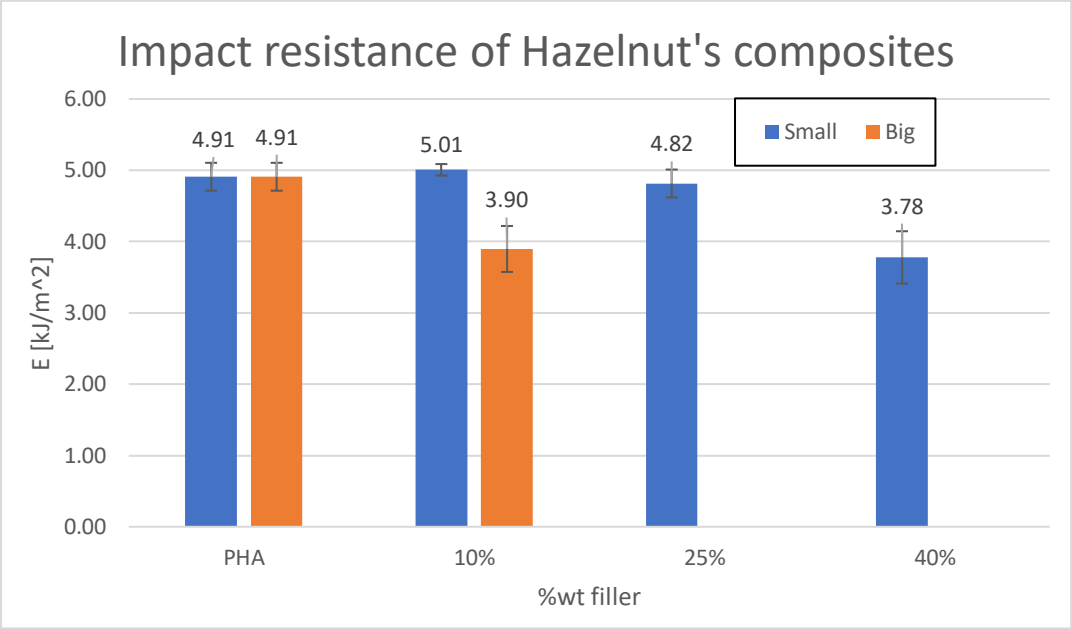

Graphic 24 Impact resistance of biocomposites with hazelnut fillers

As it was said in "Injection moulding operative problem" it was impossible to have tester of PHA with big grain size at concentration higher than 10% (PHA_HO210_25; PHA_HO210_40). However, the trend is mostly the same of almonds with some differences. The composite charged with 10%wt of filler does have higher impact resistance (lower values than the one with almonds) than the pure ones and decrease with the increasing of the filler concentration; by comparing hazelnut's fillers with the ones done with almonds, the composite at 25%wt of filler does have higher impact resistance, while at 40%wt almonds is lower.

Walnuts

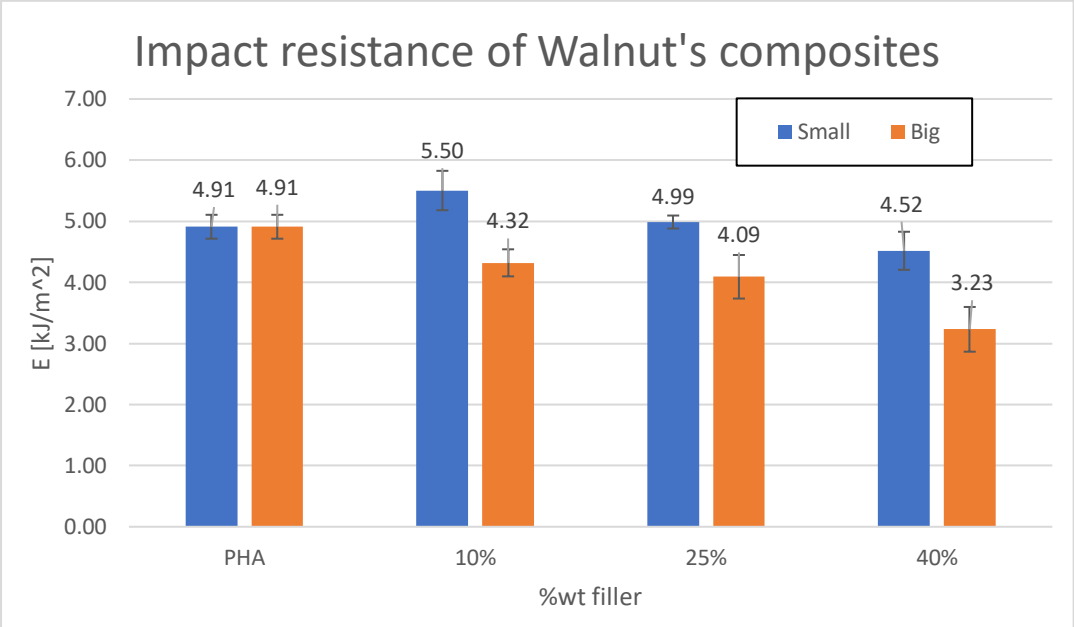

Graphic 25 Impact resistance of biocomposites with walnuts fillers

Biocomposites with walnut's fillers have the best behaviour in terms of impact resistance; even the composite with a charge of 25%wt small grain size does have impact resistance higher than pure PHA. Also, the composites with big grain size filler behaves better than the others with values significantly higher than almonds and hazelnuts at the same charge (PHA_WO210_25 > PHA_AO210_10> PHA_HO210_10).

Resume

In the next two charts are summarized all the values of Impact resistance of the all composites with PHA matrix; they are divided in small and big grain size.

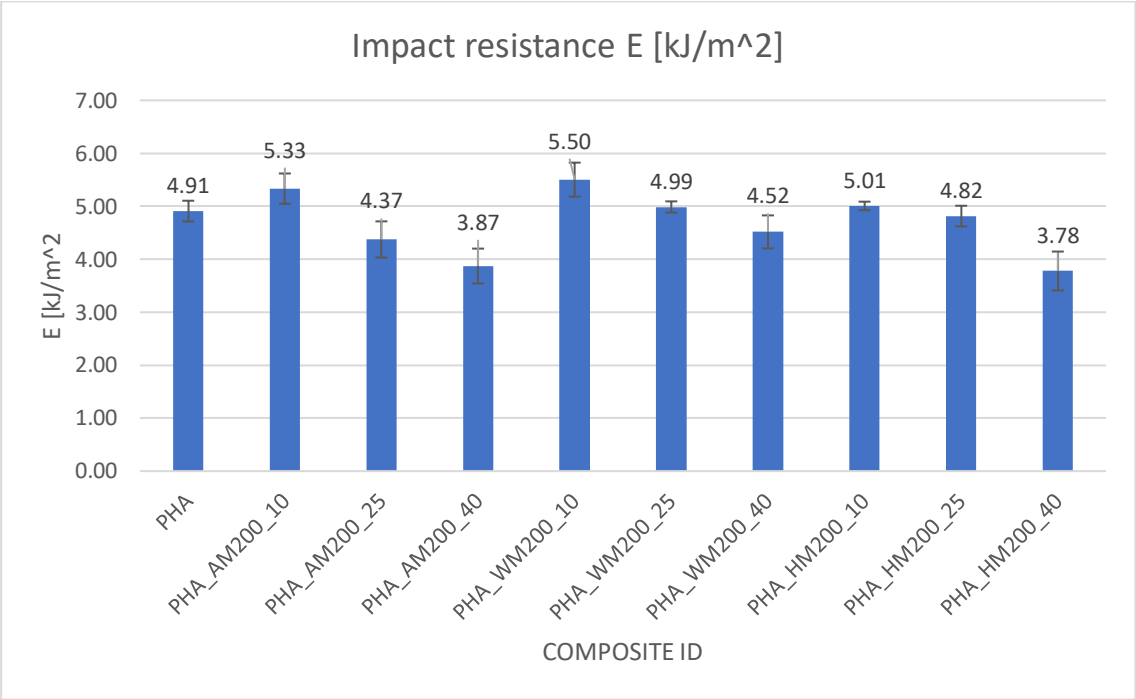

Graphic 26 Impact resistance for biocomposite with small grain size at increasing concentration of the filler

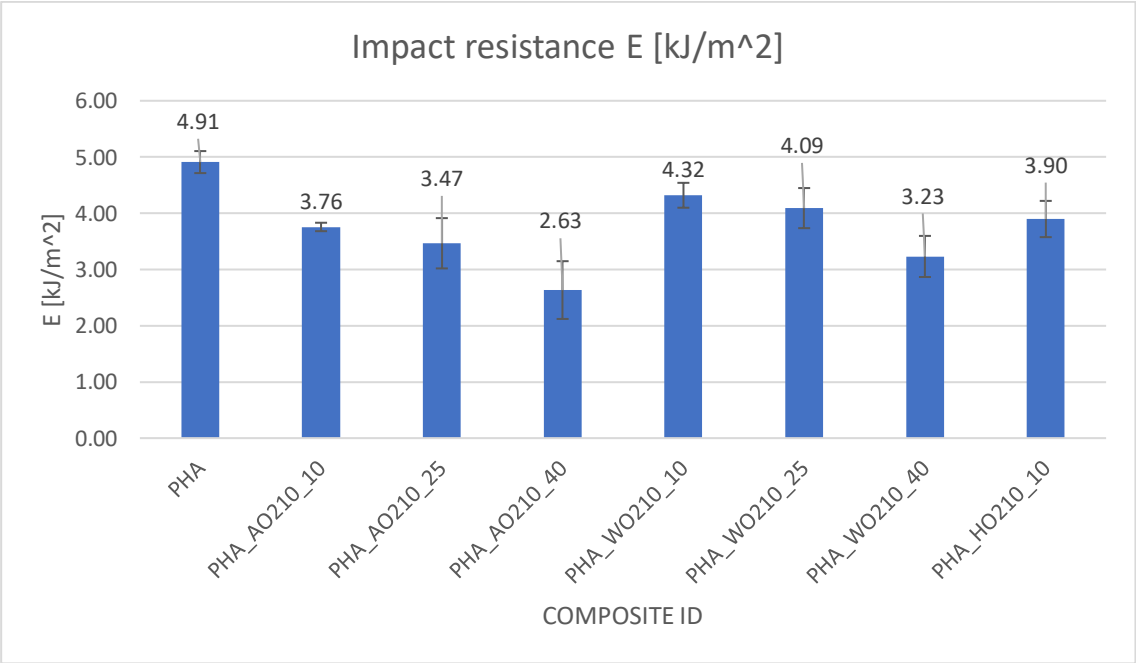

Graphic 27 Impact resistance for biocomposite with big grain size at increasing concentration of filler

PLA

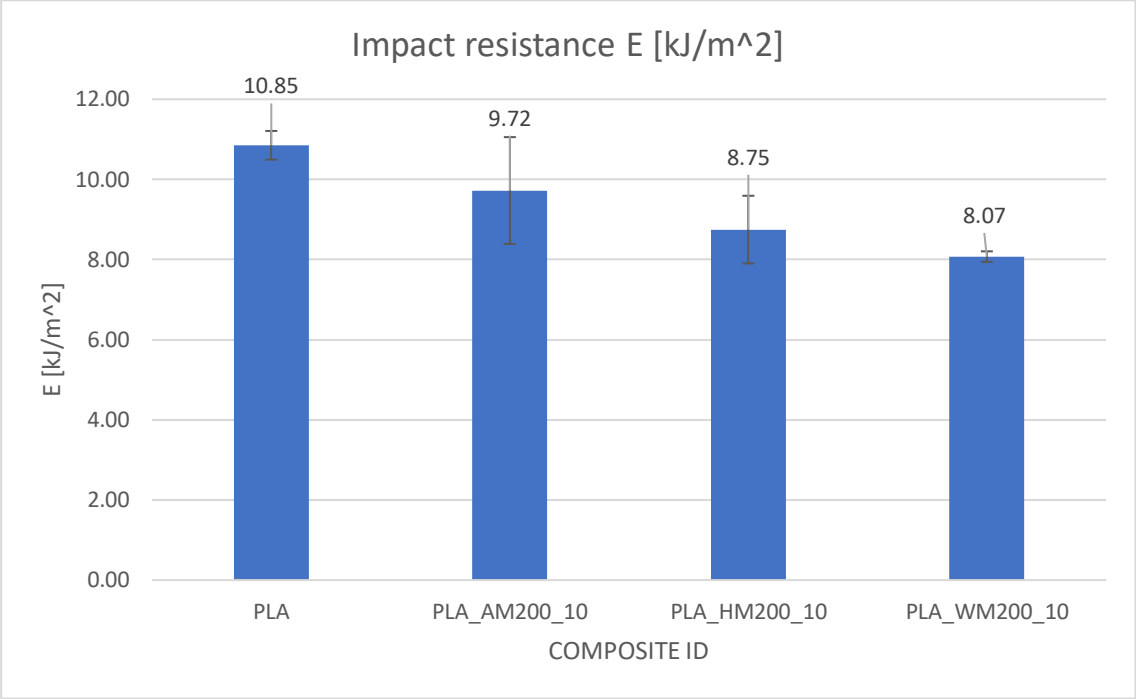

Graphic 28 Impact Resistance in PLA matrix with filler content of 10% and small grain size

The impact resistance in PLA matrix has the tendency to decrease with the introduction of the filler; with almonds it decreases less while for walnuts it decreases more.

Comparison between PLA and PHA

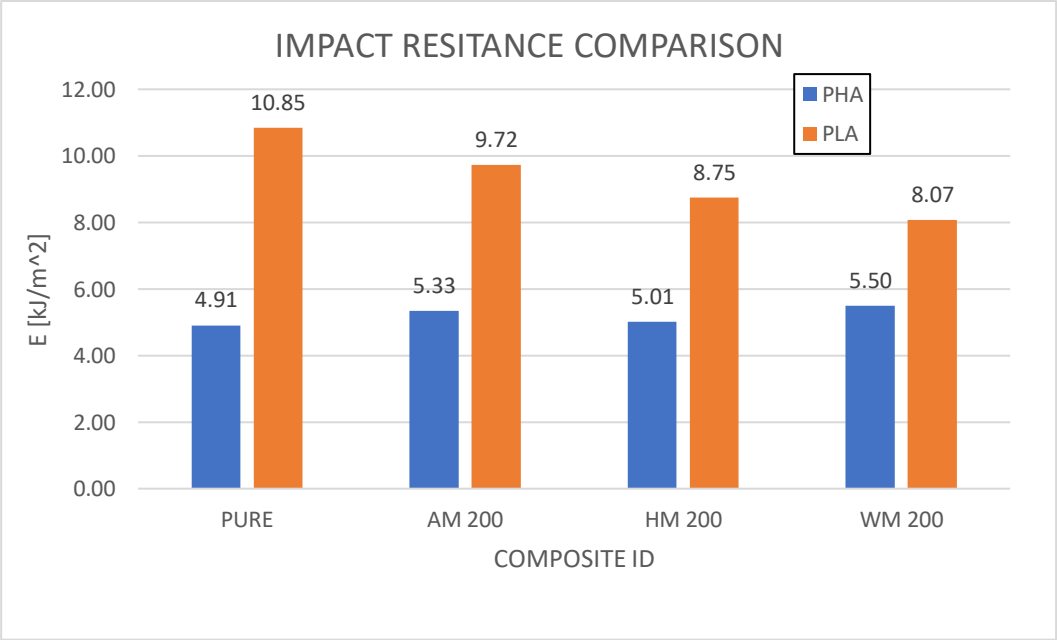

Graphic 29 Impact resistance with different polymer matrix same fillers

PLA has an higher impact resistance than PHA, but, by adding the filler it decreases, while for PHA there is an increase. By looking at the table below it is possible to notice that PLA change more than PHA with the addition of filler; for both the change is higher with the introduction of walnuts (in PHA increase and in PLA decrease).

Table 22 Change of the Impact resistance with the concentration of filler in the two matrixes

	PHA		PLA	
	VALUE [kJ/m^2]	CHANGE	VALUE [kJ/m^2]	CHANGE
PURE	4,91		10,85	
AM 200	5,33	8,63%	9,72	-10,41%
HM 200	5,01	1,98%	8,75	-19,38%
WM 200	5,50	12,08%	8,07	-25,60%

Hardness

Hardness test procedure was described in “Test setting”, the results are divided in type of filler and type of hardness, instantaneous or after 10 s, clearly the values after 10 s are smaller than the instantaneous ones.

PHA

The first set of data is the biocomposite with PHA as matrix; the results are divided by the type of filler.

Almond

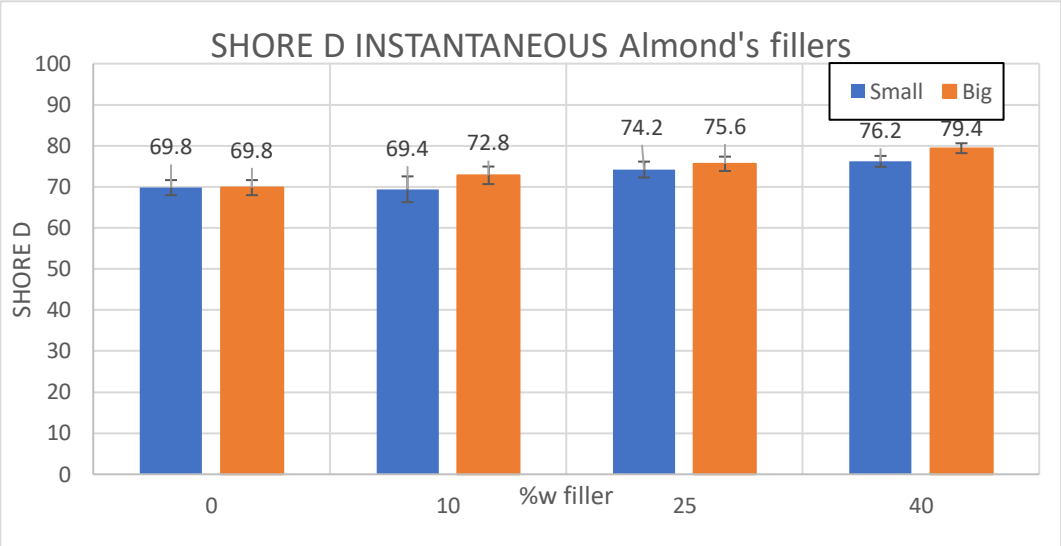

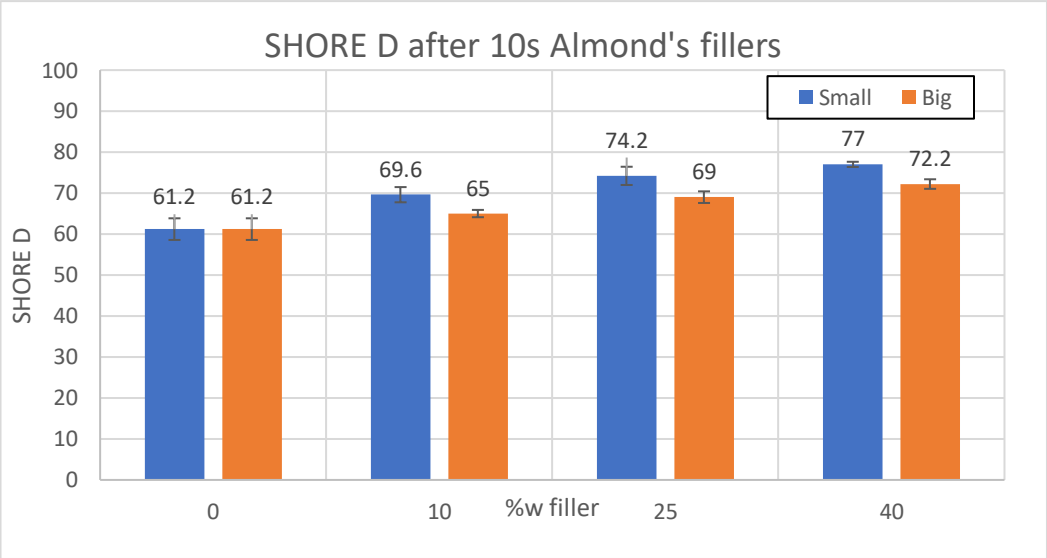

Graphic 30 Comparison of SHORE D hardness between instantaneous and after 10 s

In the instantaneous hardness, the charts show a higher increase for composite with big grain size at the increasing of the filler content respect to the smaller ones while, for the SHORE D measured after 10 s, this trend is inverted; smaller grain size increases more strongly than bigger grain size.

Hazelnut

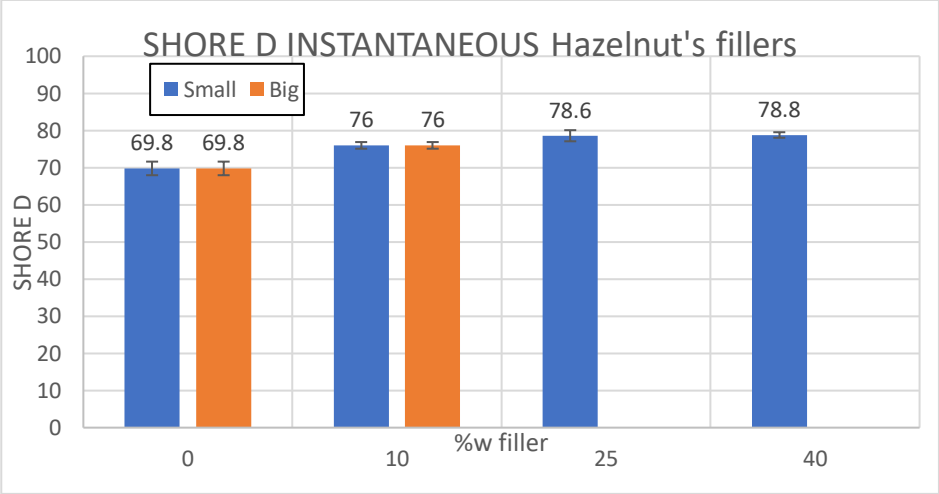

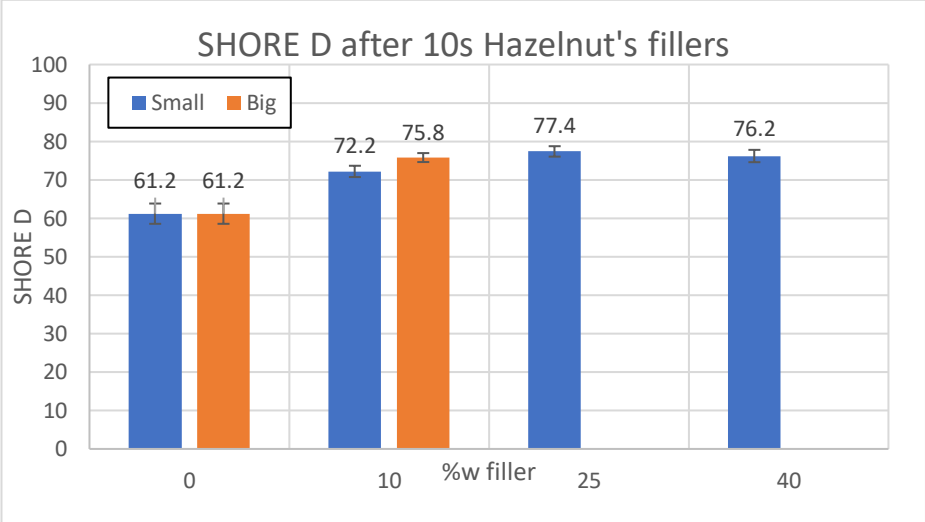

Graphic 31 Comparison of SHORE D hardness between instantaneous and after 10 s

Biocomposites with hazelnuts show similar behaviour of the ones with almonds; due to the fact that we only have one composite with big grain size (PHA_HO210_10), it is not possible to have a complete analysis.

Walnut

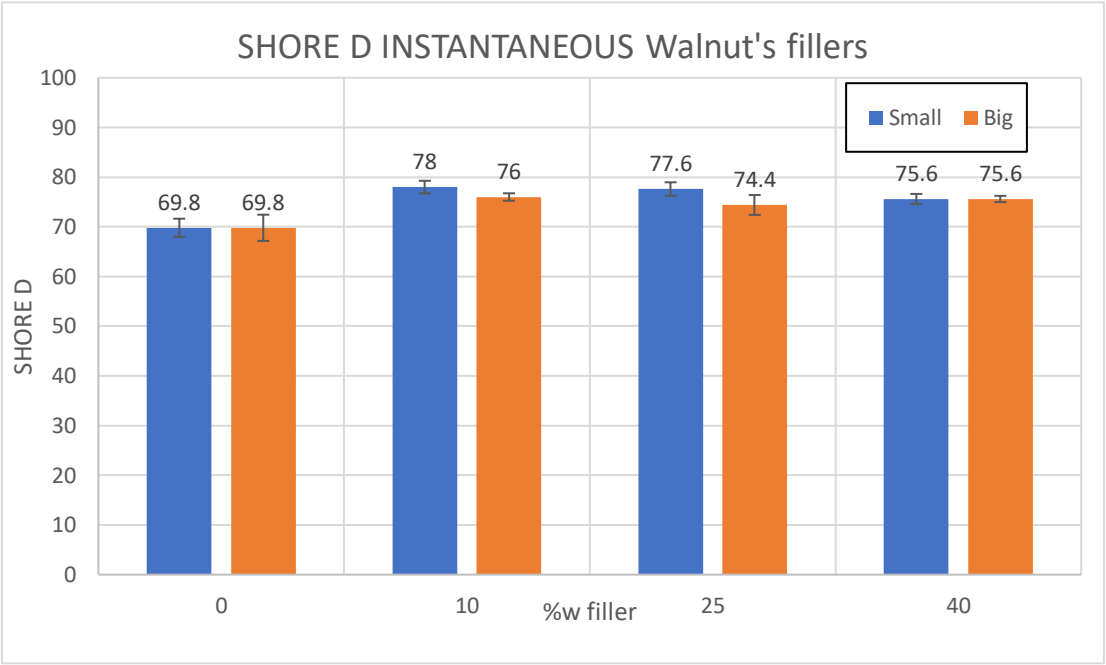

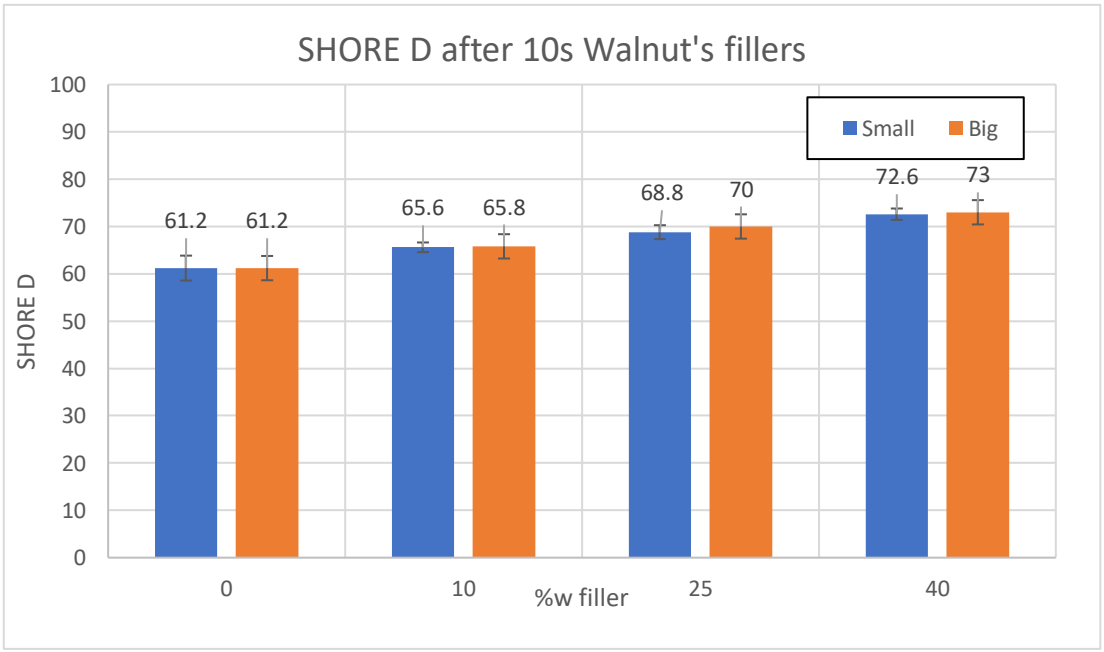

Graphic 32 Comparison of SHORE D hardness between instantaneous and after 10 s

The behaviour for walnut's composite is different; it does have less higher values of hardness for bigger grain size in the instantaneous hardness, while is mostly the same for the SHORE D after 10 s where bigger and smaller grain size behaves mostly similarly.

Resume

In order to resume the different values and trend of the hardness, the whole data are show in the graph below:

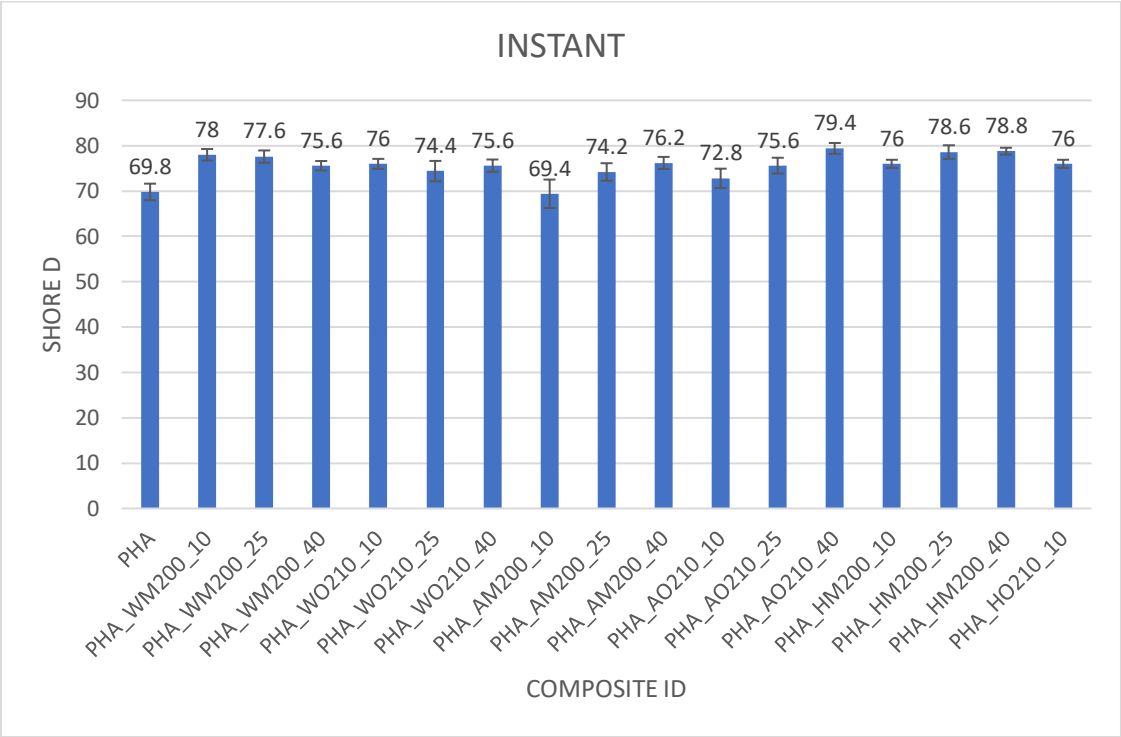

Graphic 33 Resume of the Instantaneous hardness values of the different composite

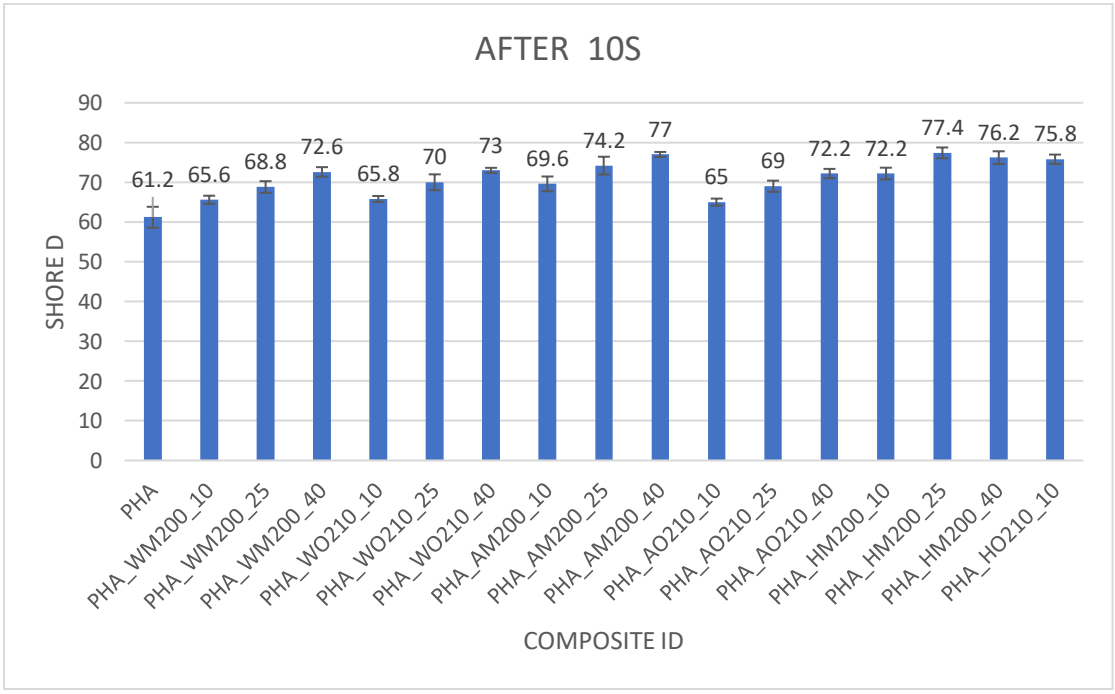

Graphic 34 Resume of the hardness after 10 s of the different composite

PLA

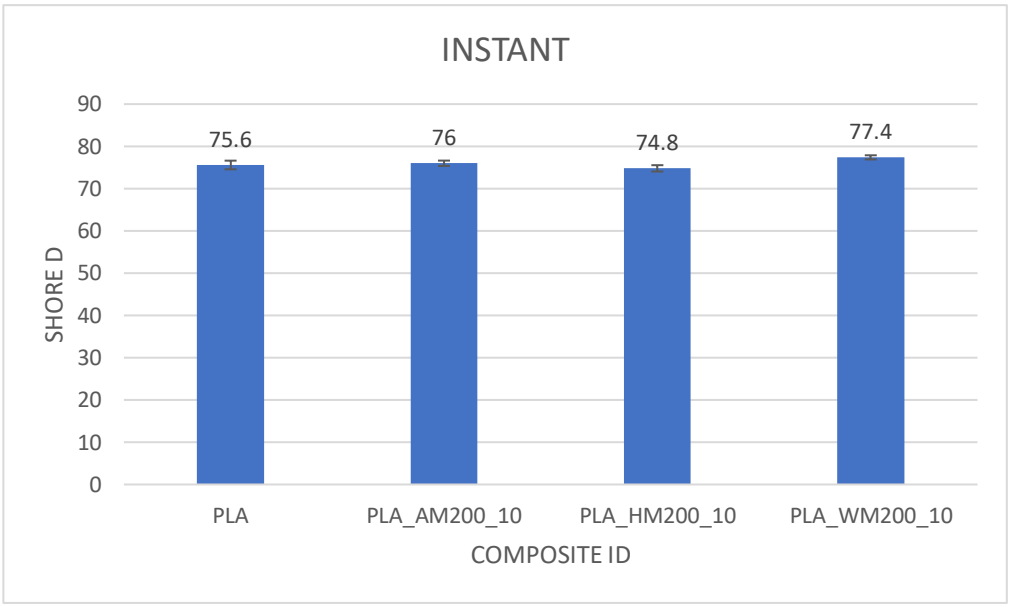

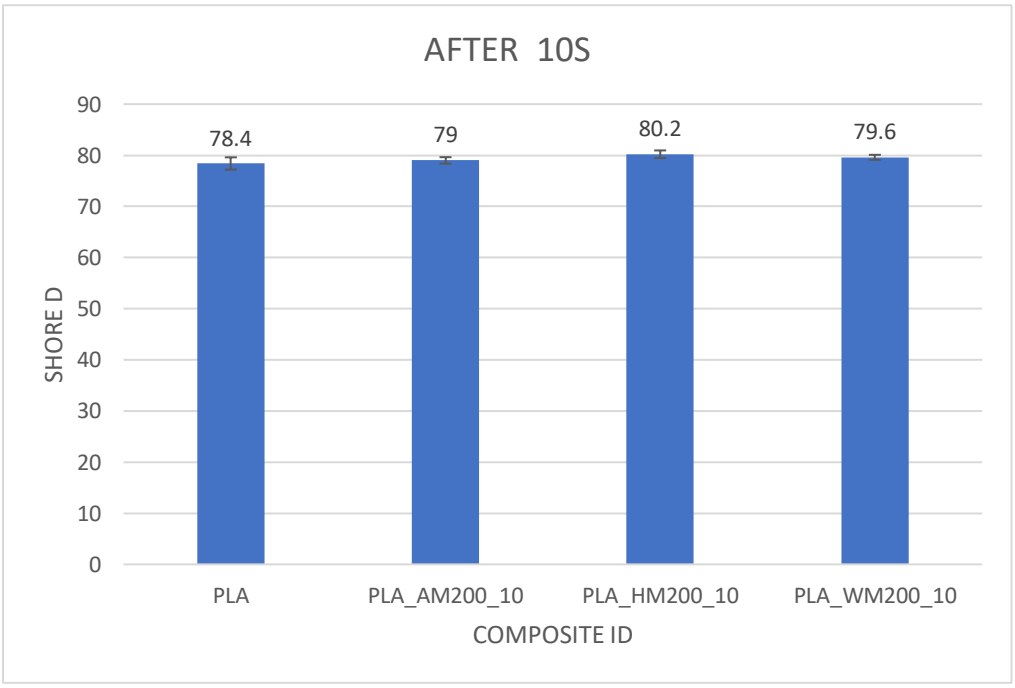

Graphic 35 SHORE D Hardness in PLA matrix with filler content of 10% and small grain size

Also, with PLA matrix the hardness tends to increase, the only exception is the “Instant Hardness” for the composite with Hazelnuts, but it is a small difference in respect to the pure ones.

Comparison between PLA and PHA

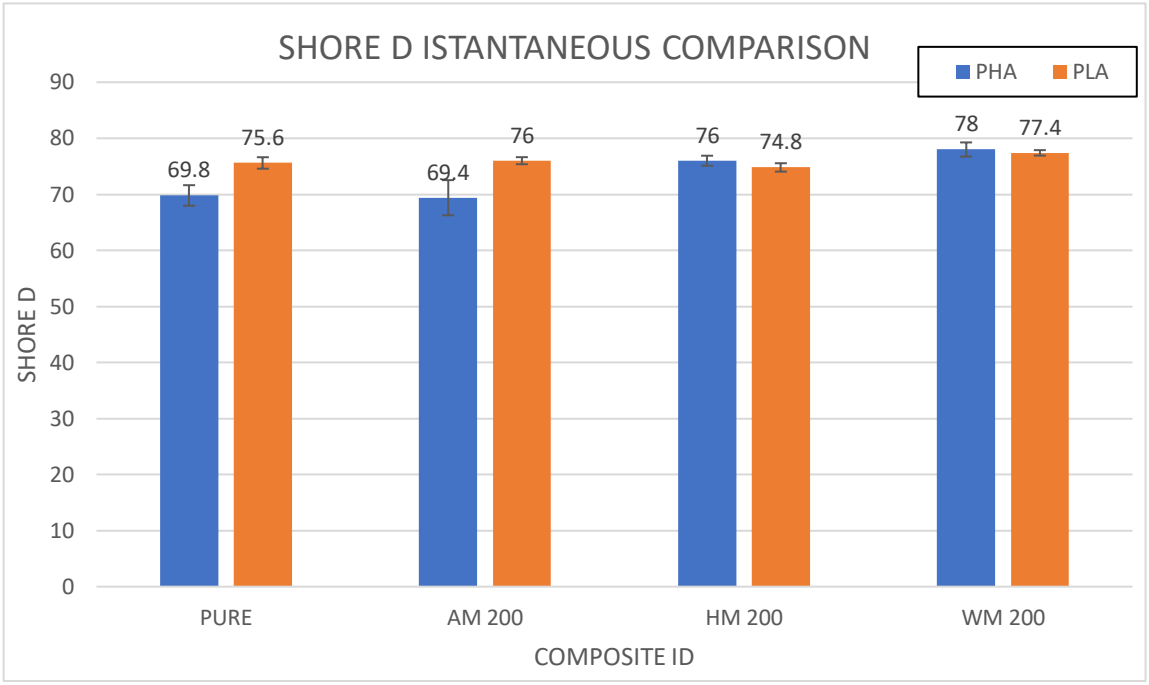

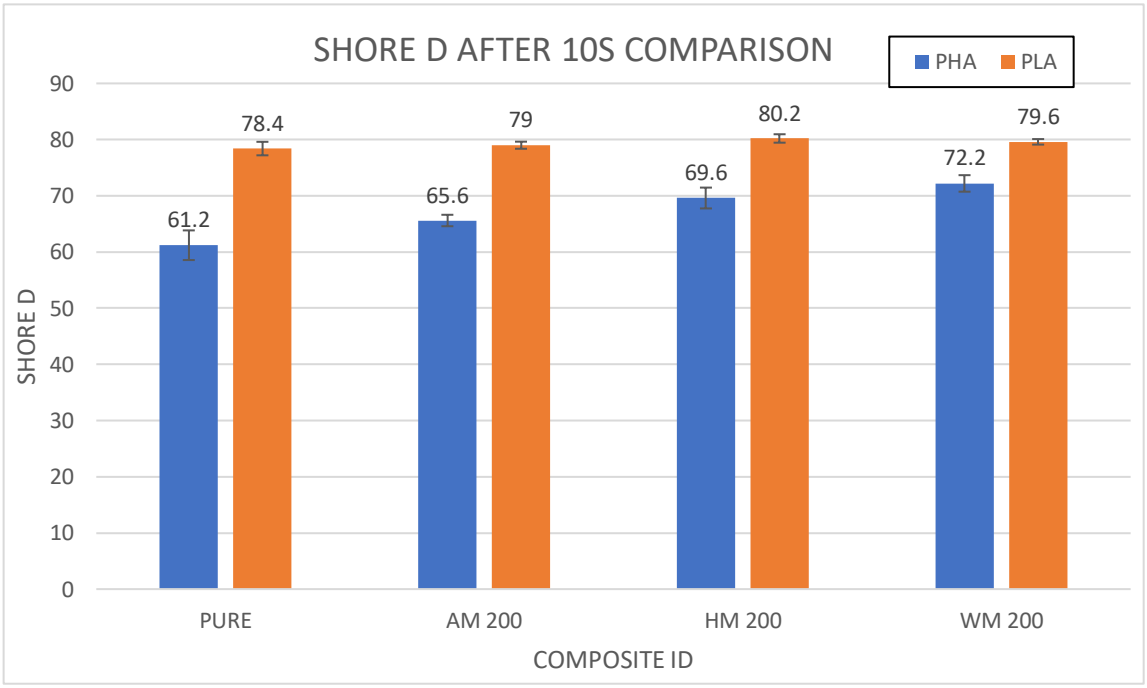

Graphic 36 Hardness in different polymer matrix with same filler

By looking at the instantaneous hardness, both the matrix has the tendency to increase with the addition of filler, and the values are quite similar. Instead, for the "after 10 s", the PLA hardness is higher than the instantaneous one and there's mostly no change between pure PLA and PLA's biocomposite. The tables show high changes in the Hardness for PHA's composite, while, the PLA's one does not.

Table 23 Change of the Instant SHORE D Hardness resistance with the concentration of filler in the two matrixes

INSTANT	PHA		PLA	
SHORE D	VALUE	CHANGE [%]	VALUE	CHANGE [%]
PURE	69,8		75,6	
AM 200	69,4	-0,57%	76	0,53%
HM 200	76	8,88%	74,8	-1,06%
WM 200	78	11,75%	77,4	2,38%

Table 24 Change of the after 10 s SHORE D Hardness resistance with the concentration of filler in the two matrixes

AFTER 10 S	PHA		PLA	
SHORE D	VALUE	CHANGE [%]	VALUE	CHANGE [%]
PURE	61,2		78,4	
AM 200	65,6	7,19%	79	0,77%
HM 200	69,6	13,73%	80,2	2,30%
WM 200	72,2	17,97%	79,6	1,53%

CONCLUSION

In this last section all the properties collected will be summarized and discussed in order to understand how the different fillers change the properties of the biopolymer matrix. The analysis, as usual, is going to be divided by the type of biopolymer and, then, the type of filler.

PHA

The type of Polyhydroxyalkanoate used (MATERIALS) does shows the following properties:

- Thermal:
  1) Melting Temperature: $T_m = 117.2\ °C$
  2) Degree of crystallinity: $X_c = 65.8\ \%$
- Mechanical Tension:
  1) Young Modulus: $E = 2096\ MPa$
  2) Tensile Stress: $\sigma = 36.38\ MPa$
  3) Tensile Stress at break: $\sigma_{BREAK} = 35.82\ MPa$
  4) Elongation: $\varepsilon = 2.26\ \%$
  5) Elongation at break: $\varepsilon_{BREAK} = 2.31\ \%$
- Mechanical Hardness (SHORE D):
  1) Instantaneous : 69.8
  2) After 10s : 61.2
- Mechanical Impact Resistance : $E_{IMPACT} = 4.91\ kJ/m^2$

Almond

Regarding the thermal properties, there is not a great change of the melting temperature, that seems not to be directly correlated to the degree of concentration of the filler. The degree of crystallization tends to decrease with the presence of the filler, one of the most interesting points is that at 25% of the filler concentration, both grain size decrease less than the ones at 10%, while the ones at 40% decrease more than the ones at 10%.

Table 25 Thermal properties of Almonds biocomposite with PHA matrix

	Thermal			
ID	Tm [°C]		Xc [%]	
	Value	Change [%]	Value	Change [%]
PHA	171,2		65,8	
PHA_AM200_10	171	-0,11%	58,6	-10,53%
PHA_AM200_25	169,2	-1,13%	62,1	-5,70%
PHA_AM200_40	168,7	-1,42%	55,8	-15,20%
PHA_AO210_10	172,4	0,74%	53	-19,50%
PHA_AO210_25	170,9	-0,18%	61,6	-6,43%
PHA_AO210_40	168,5	-1,59%	50,3	-23,57%

Regarding the mechanical properties, we have an increase of the Hardness with the increase of the filler content with both grain size, but the increase is higher with the smaller ones.

Table 26 Hardness and Impact resistance of Almonds biocomposite with PHA matrix

	Hardness				Impact resistance	
ID	Instantaneous [SHORE D]		After 10 s [SHORE D]		E [kJ/m^2]	
	Average	Change [%]	Average	Change [%]	Average	Change [%]
PHA	69,8		61,2		4,91	
PHA_AM200_10	69,4	-0,57%	69,6	13,73%	5,33	8,55%
PHA_AM200_25	74,2	6,30%	74,2	21,24%	4,37	-11,00%
PHA_AM200_40	76,2	9,17%	77	25,82%	3,87	-21,18%
PHA_AO210_10	72,8	4,30%	65	6,21%	3,76	-23,42%
PHA_AO210_25	75,6	8,31%	69	12,75%	3,47	-29,33%
PHA_AO210_40	79,4	13,75%	72,2	17,97%	2,63	-46,44%

By looking at the impact resistance, the tendency is the decrease of the properties with the increase of the filler content

Table 27 Tensile properties of Almonds biocomposite with PHA matrix

	Tension									
ID	Young Modulus [Mpa]		Tensile Stress [Mpa]		Tensile stress at Break [Mpa]		Elongation [%]		Elongation at break [%]	
	Average	Change [%]	Average	Change [%]	Average	Change [%]	Average	Change [%]	Average	Change [%]
PHA	2096		36,38		35,82		2,26		2,31	
PHA_AM200_10	2121	1,19%	21	-42,28%	21	-41,37%	1,31	-42,04%	1,36	-41,13%
PHA_AM200_25	2225	6,15%	18	-50,52%	17	-52,54%	1,07	-52,65%	1,13	-51,08%
PHA_AM200_40	2275	8,54%	12	-67,01%	12	-66,50%	0,82	-63,72%	0,87	-62,34%
PHA_AO210_10	2133	1,77%	30,28	-16,77%	30,05	-16,11%	2,28	0,88%	2,32	0,43%
PHA_AO210_25	1940	-7,44%	22,06	-39,36%	21,35	-40,40%	2,04	-9,73%	2,13	-7,79%
PHA_AO210_40	2080	-0,76%	18,04	-50,41%	16,69	-53,41%	1,92	-15,04%	1,99	-13,85%

The tensile properties of almonds filler PHA's matrix composite does show:

- Increase of the Young modulus with the increase of the filler content for small grain size while bigger ones decrease a little.
- Decrease of the Tensile stress and Tensile stress at break with the increase of the filler content, but the biocomposites made with bigger grain size decrease less than the ones with smaller filler.
- The Elongation and Elongation at break does show the same trend; bigger grain size decrease less than smaller grain size.

Hazelnut

Table 28 Thermal properties of Hazelnuts biocomposite with PHA matrix

	Thermal			
ID	Tm [°C]		Xc [%]	
	Value	Change [%]	Value	Change [%]
PHA	171,2		65,8	
PHA_HM200_10	170,6	-0,36%	61	-7,29%
PHA_HM200_25	169,5	-0,96%	70	5,91%
PHA_HM200_40	166,4	-2,81%	57,2	-13,15%
PHA_HO210_10	173	1,05%	57,2	-13,15%
PHA_HO210_25	170	-0,70%	59,2	-9,98%
PHA_HO210_40	170,48	-0,40%	43,89	-33,30%

Like the Almonds biocomposite, Hazelnuts do not show great change in the Melting temperature, and the degree of crystallization shows a decrease with the increase of the filler content. Also, here the ones at 25% in weight concentration of filler shows a lower decrease or an increase in the degree of crystallization.

Table 29 Hardness and Impact resistance of Hazelnuts biocomposite with PHA matrix

	Hardness				Impact resistance	
ID	Instantaneous [SHORE D]		After 10 s [SHORE D]		E [kJ/m^2]	
	Average	Change [%]	Average	Change [%]	Average	Change [%]
PHA	69,8		61,2		4,91	
PHA_HM200_10	76	8,88%	72,2	17,97%	5,01	2,04%
PHA_HM200_25	78,6	12,61%	77,4	26,47%	4,82	-1,83%
PHA_HM200_40	78,8	12,89%	76,2	24,51%	3,78	-23,01%
PHA_HO210_10	76	8,88%	75,8	23,86%	3,9	-20,57%

Hazelnuts, like almonds, show an increase in the Hardness with the increase of the filler content but there is not great change between the composites made with 25% and the ones with 40%. The Impact resistance increases with filler content of 10% and small grain size, then it decrease less strongly than the ones made with almonds.

Table 30 Tensile properties of Hazelnuts biocomposite with PHA matrix

	Tension									
ID	Young Modulus [MPa]		Tensile Stress [MPa]		Tensile stress at Break [MPa]		Elongation [%]		Elongation at break [%]	
	Average	Change [%]	Average	Change [%]	Average	Change [%]	Average	Change [%]	Average	Change [%]
PHA	2096		36,38		35,82		2,26		2,31	
PHA_HM200_10	2151	2,62%	25,11	-30,98%	24,91	-30,46%	1,57	-30,53%	1,62	-29,87%
PHA_HM200_25	2128	1,53%	18	-50,52%	17,21	-51,95%	1,36	-39,82%	1,47	-36,36%
PHA_HM200_40	2139	2,05%	11,93	-67,21%	11,64	-67,50%	0,95	-57,96%	1,02	-55,84%
PHA_HO210_10	2097	0,05%	17,8	-51,07%	17,6	-50,87%	1,07	-52,65%	1,09	-52,81%

Regarding the tensile properties, Young modulus increase with the increase of the filler content, but it is not so significant. Tensile stress and Tensile stress at break decrease with the increase of the filler content; but lesser than the ones with almonds; same behaviour with the Elongation. The composite made with Hazelnuts filler with big grain size at 10% wt shows worst properties than the one made with almonds with the same characteristics.

Walnut

Table 31 Thermal properties of Walnuts biocomposite with PHA matrix

	Thermal			
ID	Tm [°C]		Xc [%]	
	Value	Change [%]	Value	Change [%]
PHA	171,2		65,8	
PHA_WM200_10	171,9	0,40%	57,3	-12,86%
PHA_WM200_25	173,7	1,45%	48,3	-26,58%
PHA_WM200_40	166,4	-2,81%	56,5	-14,07%
PHA_WO210_10	169,9	-0,77%	65,2	-0,94%
PHA_WO210_25	170,7	-0,25%	52,9	-19,64%
PHA_WO210_40	169,3	-1,07%	60,1	-8,72%

Walnuts biocomposite show, like the others, not a great change in the Melting temperature, while the degree of crystallization decreases with the increase of the filler content and there is not a change in the behaviour when the biocomposite are made with the 25% of filler.

Table 32 Hardness and Impact resistance of Walnuts biocomposite with PHA matrix

	Hardness				Impact resistance	
ID	Instantaneous [SHORE D]		After 10 s [SHORE D]		E [kJ/m^2]	
	Average	Change [%]	Average	Change [%]	Average	Change [%]
PHA	69,8		61,2		4,91	
PHA_WM200_10	78	11,75%	65,6	7,19%	5,5	12,02%
PHA_WM200_25	77,6	11,17%	68,8	12,42%	4,99	1,63%
PHA_WM200_40	75,6	8,31%	72,6	18,63%	4,52	-7,94%
PHA_WO210_10	76	8,88%	65,8	7,52%	4,32	-12,02%
PHA_WO210_25	74,4	6,59%	70	14,38%	4,09	-16,70%
PHA_WO210_40	75,6	8,31%	73	19,28%	3,23	-34,22%

Hardness increases with the increase of the filler content; this increase is slightly higher than in the other two biocomposites; the Impact resistance shows an increase in with filler with small grain size and concentration of 10% while the one at 25% has the same behaviour of the pure one; while the one made with bigger grain size does have same behaviour of the others made with almonds or hazelnuts.

Table 33 Tensile properties of Walnuts biocomposite with PHA matrix

	Tension									
ID	Young Modulus [MPa]		Tensile Stress [MPa]		Tensile stress at Break [MPa]		Elongation [%]		Elongation at break [%]	
	Average	Change [%]	Average	Change [%]	Average	Change [%]	Average	Change [%]	Average	Change [%]
PHA	2096		36,38		35,82		2,26		2,31	
PHA_WM200_10	2224	6,11%	33,1	-9,02%	32,68	-8,77%	2,29	1,33%	2,35	1,73%
PHA_WM200_25	1856	-11,45%	22,51	-38,13%	21,98	-38,64%	2,08	-7,96%	2,18	-5,63%
PHA_WM200_40	1677	-19,99%	11,53	-68,31%	10,67	-70,21%	1,1	-51,33%	1,36	-41,13%
PHA_WO210_10	2056	-1,91%	29,99	-17,56%	28,82	-19,54%	2,14	-5,31%	2,2	-4,76%
PHA_WO210_25	1777	-15,22%	22,6	-37,88%	22,06	-38,41%	2,12	-6,19%	2,21	-4,33%
PHA_WO210_40	1451	-30,77%	16,02	-55,96%	14,71	-58,93%	2,2	-2,65%	2,34	1,30%

Walnuts influenced the polymer matrix with a decrease of the Young modulus with the increase of the filler content. The Tensile stress decreases significantly with the increase of the

filler, while the elongation decreases less than the biocomposite made with the others two filler.

PLA

The analysis of the properties of PLA's matrix biocomposites will be done differently; it starts with the Thermal properties of all the composites, while the mechanical properties will be done only for the composites with filler content of 10% small grain size.

Thermal

Table 34 Glass transition temperature of PHA's matrix biocomposites

Thermal	Tg [°C]	
	Value	Change [%]
PLA	58,2	
PLA_AM200_10	57,4	-1,31%
PLA_AM200_25	59,9	2,92%
PLA_AM200_40	59	1,48%
PLA_AO210_10	57,7	-0,83%
PLA_AO210_25	57,2	-1,69%
PLA_AO210_40	57	-1,93%
PLA_HM200_10	56,7	-2,48%
PLA_HM200_25	54,6	-6,17%
PLA_HM200_40	53,8	-7,52%
PLA_HO210_10	57,5	-1,08%
PLA_HO210_25	58,3	0,22%
PLA_HO210_40	56,2	-3,44%
PLA_WM200_10	55,6	-4,37%
PLA_WM200_25	53,8	-7,53%
PLA_WM200_40	53,8	-7,46%
PLA_WO210_10	60	3,10%
PLA_WO210_25	56	-3,65%
PLA_WO210_40	58,4	0,34%

Glass transition temperature did not change a lot with the introduction of the filler; the most interesting data are the Hazelnuts and Walnuts biocomposite with filler of small grain size and concentration of 40% where there is a change of around the 7%; generally, the change is higher than the Melting temperature in the PHA's biocomposite.

Mechanical

Table 35 Hardness and Impact resistance of biocomposites with PLA matrix

	Hardness				Impact resistance	
	Instantaneous [SHORE D]		After 10 s [SHORE D]		E [kJ/m^2]	
	Average	Change [%]	Average	Change [%]	Average	Change [%]
PLA	75,6		78,4		10,85	
PLA_AM200_10	76	0,53%	79	0,77%	9,72	-10,41%
PLA_HM200_10	74,8	-1,06%	80,2	2,30%	8,75	-19,35%
PLA_WM200_10	77,4	2,38%	79,6	1,53%	8,07	-25,62%

The Hardness does not show great difference between pure PLA and PLA's biocomposite, while the impact resistance shows higher decrease than the ones with the same amount of filler and PHA's matrix; the most significant ones are Hazelnuts and Walnuts biocomposite.

Table 36 Tensile properties of biocomposite with PLA matrix

	Tension									
	Young Modulus [Mpa]		Tensile Stress [Mpa]		Tensile stress at Break [Mpa]		Elongation [%]		Elongation at break [%]	
	Avarage	Change [%]	Avarage	Change [%]	Avarage	Change [%]	Avarage	Change [%]	Avarage	Change [%]
PLA	1580		45,56		36,87		3,58		5,25	
PLA_AM200_10	1737	9,94%	37,58	-17,52%	30,71	-16,71%	2,73	-23,74%	4,57	-12,95%
PLA_HM200_10	1744	10,38%	29,45	-35,36%	24,77	-32,82%	2,38	-33,52%	4,09	-22,10%
PLA_WM200_10	1671	5,76%	31,68	-30,47%	26,19	-28,97%	2,56	-28,49%	4,56	-13,14%

Tensile properties in PLA's matrix biocomposites show an increase of the Young Modulus; the most significant one is the one made with Hazelnuts. The Tensile stress and elongation do decrease more in the Hazelnuts and Walnuts; the best biocomposite seems to be the one made with Almonds, but if we compare it with the one done with PHA's matrix the decrease is significantly higher.

FINAL STATEMENT

As it was said in “FILLER”, the development of biocomposite with shell fillers derived from the food industry is crucial in terms of sustainability and circular economy due to the high cost of the biopolymer matrixes and the increase of production of nuts in the last years.

All the properties detected in this work does show small differences between small (0-200 µm) and big (200-1000 µm) depending on the properties. This is good regarding pre-treatment of the shells in terms of granulometry. On the other side, big grain size induce problem in terms of injection moulding where big grain size may occlude the nozzle lowering the processability.

Thermal properties like Melting temperature (PHA matrix) and glass transition temperature (PLA matrix) are not influenced by the introduction of filler in both matrixes. The degree of crystallization changes with the concentration of filler but there is not an intrinsic correlation between the two.

Mechanical properties are bad influenced by the introduction of high percentage of filler; composite becomes more brittle and less resistant to stress. Those results were expected due to the non-polar characteristic of the Biopolymer and the quite polar behaviour of the fillers, that induces the formation of a bad interphase in the composite. Another big problem is the high content of filler. When present in high quantities, fillers have the tendency to interact more between each other than with the matrix that causes clots with the creation of regions matrix rich and regions matrix poor. Those regions produce a non-homogeneous distribution of the stresses lowering the mechanical properties.

Despite those relevant problems, an high interest is present in the development of these kind of composites. The work done in this thesis helps the creation of a catalogue done for “Arianna

Fibers srl", start-up placed in Pistoia (Italy), done by Irene Tedesco for her master degree. That work included the composites done with PHA matrix for the creation of packaging for cosmetic products. Seven different containers were created in order to contain creams, shampoos and solid cosmetics like lipsticks. The geometry was very simple, mostly parallelepipeds, in order to have an easy processability like blow moulding or injection moulding. The dispensers were supposed to be done in pure PHA due to the fact that they require low thickness and high mechanical properties, characteristics that are not present in these composites. The k-aspects of those products were, obviously, the green characteristics like a completely bio based composite, waste reduction and biodegradability. Another aspect, suggested by Irene Tedesco, that can increase the market's interest, is the possibility to customize the packaging by choosing the type of filler and concentration (colour) and the grain size (texture). This will create special personal packaging for every type of cosmetic product (Tedesco, 2021).

Figure 60 Homepage

Figure 61 Possible packaging solution with PHA composites

Bibliography

al., E. L.-S. (2018). Biocomposites of different lignocellulosic wastes for sustainable food packaging applications. *ELSEVIER*.

Calcagni, G. (2019). *Situazione internazionale prospettive e potenzialità della Nocicultura.* Napoli.

Calcagni, R. (2020). *Meeting ortofrutta Italia Germania.* Fruchthandel Magazine .

Conrad, J. (2009). *The rheology, degradation, processing and characterization of renewable resource polymers.* Clemson University.

Davis, R. (2013). Conversion of grass biomass into fermentable sugars and its utilization. In R. Davis, *Bioresource Technology* (pp. 202-209). Dublin: School of Biomolecular and Biomedical.

E. Bugnicourt, P. C. (2014). *Polyhydroxyalkanoate (PHA): Review of synthesis, characteristics, processing and potential application.* eXPRESS Polymer Letters Vol.8, No.11.

Esposti, M. D. (2021). Chromatographic Methods: GPC. *Material Characterisation* (pp. 1-37). Bologna: Alma Mater Studiorum.

Esposti, M. D. (2021). Impact test. *MECHANICAL TESTING: HARDNESS, TENSILE, FLEXURAL, COMPRESSION AND IMPACT TESTING, INTRODUCTION TO FRACTURE AND FATIGUE* (pp. 45-53). Bologna: DICAM ALMA MATER STUDIORUM UNIVERSITA' DI BOLOGNA.

Esposti, M. D. (2021). MICROSCOPIES: OPTICAL MICROSCOPY, SEM, TEM, AFM, CONFOCAL FLUORENCE MICROSCOPY. *Material Characterization* (pp. 10-34). Bologna: DICAM ALMA MATER STUDIORUM UNIVERSITA' DI BOLOGNA.

Esposti, M. D. (2021). Tensile test. *MECHANICAL TESTING: HARDNESS, TENSILE, FLEXURAL, COMPRESSION AND IMPACT TESTING, INTRODUCTION TO FRACTURE AND FATIGUE* (pp. 14-39). Bologna: DICAM ALMA MATER STUDIORUM UNIVERSITA' DU BOLOGNA.

Esposti, M. D. (2021). THERMAL ANALYSIS: TGA DSC. *Material Characterization* (pp. 17-51). Bologna: DICAM ALMA MATER STUDIORUM UNIVERSITA' DI BOLOGNA.

Estefanía Lidón Sánchez-Safonta, A. A.-P. (2018). *Biocomposites of different lignocellulosic wastes for sustainable food packaging applications.*

Europe, P. (2020). *Plastics- the Facts 2020* .

(n.d.). *https://www.landini.it/produzione-mondiale-noci/.*

Marius Murariu, P. D. (2016). *PLA composites: From production to properties.* Belgium: Center of Innovation and Research in Materials and Polymers (CIRMAP), Laboratory of Polymeric and Composite Materials (LPCM), University of Mons & Materia Nova Research Centre,.

Pelegalli, M. (2021). *Mandorle, nel 2020 il raccolto cresce di oltre il 4%.* AgroNotizie.

Reusch, R. N. (2012). *Biogenesis and functions of model integral outer membrane proteins: Escherichia coli OmpA Pseudomonas aeruginosa OprF.* East Lansing, MI, USA: Department of Microbiology and Molecular Genetics, Michigan State University.

S. Ferrándiz-Bou, A.-G. A.-G. (2020). *Influence of Almond Shell Content and Particle Size on Mechanical Properties of Starch-Based Biocomposites.* Springer Nature 2021.

Saccani, A. (2021). Processing. *Polymer Science and Technology* (pp. 23-29). Bologna: ALMA MATER STUDIORUM UNIVERSITA' DI BOLOGNA.

Shahbandeh, M. (2020). *Almond production worldwide 2019/20, by country.*

(n.d.). *Sigma700/701 Operation Manual Force Tensiometer Revision 2.7.* Biolin Scientific.

Soressi, M. (2020). *Boom delle mandorle, se ne vendono in un anno 8,5 milioni di kg per 130 milioni di euro.* Rome : Sole 24 ore.

(2011). *Technical Data Sheet & Processing Guide.* ENMAT.

Tedesco, I. (2021). *Karà bio-cosmetics: il packaging cosmetico sostenibile.* Bologna: Laurea Magistrale in Advanced Design.

(2021). *Universal Sector.* SpecialChem.

Xue Li, L. G. (2007). Chamical Treatments of Natural Fiber for Use in Natural-Reinforced Composites: A Review. *Springer Science+Business Media, LLC 2006*.